RMIT UNIVERSITY

Synthesis of Novel Small Molecules for use in Bulk Heterojunction Solar Cells

A thesis submitted in fulfilment of the requirements for the degree of Doctor of Philosophy

Aaron Michael Raynor

B.Sc (Honours)

School of Applied Science

College of Science, Engineering and Health

RMIT University

May 2016

Declaration

I certify that except where due acknowledgement has been made, the work is that of the author alone; the work has not been submitted previously, in whole or in part, to qualify for any other academic award; the content of this thesis is the result of work which has been carried out since the official commencement date of the approved research program; any editorial work, paid or unpaid, carried out by a third party is acknowledged; and, ethics procedures and guidelines have been followed.

Aaron Raynor

10-6-2016

Acknowledgments:

I would firstly like to thank RMIT for the support throughout my candidature. I would also like to thank my supervisors Sheshanath Bhosale and Trevor Rook for their unconditional and priceless support. Shesh, if it wasn't for you I don't know what I would have done with my time at RMIT, you're a fantastic supervisor and a great friend. I owe most if not all of my success to your guidance and support. Trevor, your support throughout my time as a student will never be forgotten, you're an amazing educator and one of my closest friends.

I would also like to thank my group members, Sam Jackson, Hemlata Patil, Anushri Rananaware, Melissa Kelson, Anurhada and La Duoc Dong for their support and kindness throughout my time in the lab and office, I blame Sam for most of the distractions though.

To all the people I have met and had fun with along the way, Dr. Spit, Steve Privér, Jos Campbel, Andrew Basil, Vivian Li, Emma Goethales, Andrew Pearson and many many more that I'm sure to have forgotten, thank you all.

To all the academic staff who have helped me while at RMIT, in particular Julie Niere, Oliver Jones, Jeff Hughes, Andrew Smith, and Helmut Hügel, you're support has been a constant reminder that good people exist in this world! Thanks too to the technical staff that have helped me on numerous occasions Robert Brkjazka, sorry for not understanding things at times and Frank Antolastic thanks for the chats, help and advice.

Bartronica, don't ever change, thanks for having a Donkey Kong machine! It made some of those long nights bearable.

To Scott McMaster and Chris Plummer. Without you two I don't know what I would have done, your friendship, constructive criticism and abuse has made me

a better person. Plum, I promise to get you that 88 page document as soon as you need it and Panks always remember dry tinder starts the best fires.

To my family: Mum thanks for not killing me, you're the best person I know, thank you for all the support and encouragement you have given me over the years. John I appreciate that you still put up with me, I really don't know how you do it to be honest, thanks for all your advice and support. To Andrew and Kimmie without your tireless support and encouragement I wouldn't be were I am today. To the rest of you that I haven't mentioned by name know that I love you all, except you Kirean, you I can't stand!

Kris and Jess, you two have no idea how much you mean to me. You're friendship, company, determination and strength knows no bounds and has given me strength in times where I thought I had none left. I love you two.

Taidgh and Jack, one day you'll probably read this, when you do know that I will always love you, remember that everything in life I do, I do for you two. I love nothing more than you two and always will.

Jade, words cannot express my gratitude for everything you have done and continue to do for me. You are an amazing person, capable of incredible empathy and compassion. You're an inspiration to me everyday and you give me the strength to do all that I do. I love you.

To anyone else that I may have missed I apologise. I promise to buy you a beer if you say to me "hey, remember that time you left me out of your acknowledgements?"

Dedication:

This thesis is dedicated to the memory of my father Micheal Raynor. It's a shame we never had the chance to have a beer, an argument or a laugh together. Such is life.

“In the beginning the Universe was created. This made a lot of people very angry and has been widely regarded as a bad move”

- Douglas Adams

Abbreviations

A-D-A	Acceptor-Donor-Acceptor
AMOLED	Active Matric Organic Light Emitting Diode
BHJ	Bulk-Heterojunction
D-A	Donor-Acceptor
DSSC	Dye-Sensitised Solar Cell
DPP	Diketopyrrolopyrrole
ET	Electron Transfer
ff	Fill Factor
HOMO	Highest Occupied Molecular Orbital
IPCE	Incident Photon to Current efficiency
IR	Infra-Red
J-V	Current Density-Voltage
J_{SC}	Short Circuit Current
LED	Light Emitting Diode
LUMO	Lowest Unoccupied Molecular Orbital
NDI	Naphthalene Diimide
OFET	Organic Field Effect Transistor
OLED	Organic Light Emitting Diode
OLET	Organic Light Emitting Transistor
OPV	Organic Photovoltaic
P3HT	Poly(3-hexylthiophene-2,5-diyl)
PCBM-60	Phenyl-C61-Butyric-Acid-Methyl Ester

PCBM-70	Phenyl-C71-Butyric-Acid-Methyl Ester
PCE	Power Conversion Efficiency (η)
PEDOT	Poly(3,4-ethylenedioxythiophene)
PV	Photovoltaic
TiO_2	Titanium Dioxide
UV-Vis	Ultraviolet-Visible
V_{OC}	Open Circuit Voltage

Abstract

Solar power is fast becoming the "go-to" form of renewable energy. The most likely reason for this is the ease at which solar panels can be installed on private residences and other buildings. Government incentives and rebates in countries such as Australia have also spurred along the industry making it an affordable option for the public as well as private business. Although silicon-based panels offer moderate efficiencies and a decent return on investment newer technologies, in particular organic photovoltaics, offer an exciting alternative with the potential to give cheaper power devices with lower impact on the environment. In this body of work, the synthesis of several acceptor and donor compounds used with in the bulk-heterjunction (BHJ) architecture organic photovoltaic device, is presented.

The donor compounds, AS-1 and AS-2, were designed in order to investigate the effect that insertion of a thiophene pi-spacer would have of the properties of a triphenyl amine donor-acceptor-donor (D-A-D) compound. Results showed that the thiophene containing compound (AS-2) had far superior optical and electronic properties compaired to AS-1 as well as experiencing no ill effects on solubility or processability despite having no solubilizing alkyl chains. The thiophene insertion resulted in a lowering of the band-gap, increased light harvesting ability and superior electronic performance. In simple bulk-heterjuction cells using PCBM61 as an electron acceptor AS1 gave an open circuit voltage (V_{oc}) of 0.90 V, a current density (J_{sc}) of 3.15mA/cm^2 and a power conversion efficiency (PCE) of 1.23%. AS2 however greatly outpaced its counterpart with thanks to the thiophene spacer with a V_{oc} of 0.88 V, J_{sc} of 8.01 mA/cm^2 and a PCE of 4.01%.

The acceptor compounds consisted of two groups; class-A and class-N compounds. Both class of compounds contained diketopyrrolopyrrole (DPP) as either the central (class-A) or terminal (class-N) moiety. For the class-N compounds N6 and N7 were designed and synthesised. N6 contained a

benzothiadiazole central unit with two DPP moieties attached to create an A-D-A structure. The compound exhibited a strong absorption in the visible range and appropriate HOMO/LUMO energy levels to be paired with poly-3-hexyl thiophene (P3HT). When paired with the ever-versatile electron donor P3HT in a 1:1 blend in a bulk-heterojunction device architecture it gave a V_{oc} of 1.08 V, J_{sc} of 2.06 mA/cm^2 and a PCE of 1.08%. At the time of testing this was one of the best performing non-fullerene DPP containing small molecules.

N7 was a similar construction to N6, differing in the central moiety. N7 used an N-alkyl substituted carbazole moiety as the central unit. The compound also gave strong absorption in the visible region with appropriately placed HOMO/LUMO levels. When paired with P3HT in a 1:1.2 ratio. A V_{oc} of 1.17 V, J_{sc} of 3.16 mA/cm^2 and a PCE of 2.30% were recorded. Using N7 in these devices required no special treatment and the results obtained from them are among the highest values for a single junction bulk-heterojunction cell using a non-fullerene, small molecule acceptor.

The class-A compounds consisted of an A-A-A design, in which DPP was to be the central acceptor moiety. The other moieties were to be para-nitrophenylacetonitrile (A1), 4-(2-methoxyethoxy)-3-oxobutanenitrile (A2), 3-dibutylbarbituric acid (A3), and 2-ethyl rhodanine (A4). All compounds were synthesised simply by refluxing the bis-carbaldehyde homologue of DPP with the corresponding nucleophile. The synthesis itself appeared to be simple, the desired compound forming as the major product. There was however small amounts (typically 10 – 15%) of the mono-condensed compound. This proved troublesome and practical removal of the byproduct was only achievable for the barbituric homologue.

The inability to remove the impurity is in part due to the innate insolubility of both compounds. The optical properties of the class-A compounds however were promising, showing decent absorption in the visible region and it was for this reason A5 and A6 were subjected to photovoltaic testing, despite the poor solubility. Unfortunately they showed little to no activity, which is likely a result of poor solubility leading to inhomogeneity in the blend.

Table of Contents

Table of figures, tables and equations.

Chapter 1

Table of figures and tables Chapter 2

Table of figures and tables Chapter 3

Table of figures Chapter 4

Table of figures Chapter 5

Table of figures Chapter 6

1.0 Introduction

1.1 The Photovoltaic Effect and Early Solar Cells

In 1839 Alexandre Edmond Becquerel, a French physicist and the father of famed physicist and Nobel Laureate Antoine Henri Becquerel (who alongside Marie and Pierre Curie discovered radioactivity), conducted a simple experiment in his father's laboratory.[1] The experiment consisted of an acidic solution of silver chloride and two platinum electrodes. When the solution was illuminated Becquerel observed a small but measurable voltage across the two electrodes. At age 19 Becquerel had invented the first photovoltaic cell and at the same time discovered the photovoltaic effect, also know as the "Becquerel effect".

Becquerel's work in photovoltaics also paved the way for the work into the photoelectric effect as his experiments illustrated that a relationship did in fact exist between light and electricity. In recognition of his achievements, in 1989, the 150th anniversary of Becquerel's experiment, the European Commission founded the "Alexandre Edmond Becquerel Prize". This award is presented annually at the "European Photovoltaic Solar Energy Conference and Exhibition (EU PVSEC)" to European citizens for "outstanding merits in photovoltaics".

Although Becquerel's discovery was groundbreaking, and like most new and infant discoveries, it would take time and the work of countless others until this effect could be fully taken advantage of to make stable, functioning and usable devices. One major discovery that assisted this effort was the discovery of photoconductivity.

While working on various projects involving underwater telegraph wires an electrical engineer by the name of Willoughby Smith sought, and subsequently invented, a device that would continuously test the conductivity of these cables

as they were being laid. For this Smith needed a semiconductor material that exhibited very high resistance, and it is for this reason that selenium was chosen. Under standard laboratory conditions the system seemed to work perfectly, however when it was employed in the field the system failed to give consistent results. Smith began to troubleshoot his device and found that when exposed to intense light the resistance of the selenium rods changed dramatically. Smith had, by complete chance, discovered selenium's photoconductivity properties; this led him to publish a paper "Effect of Light on Selenium during the passage of an Electric Current" in February of 1873 in Nature.[2]

Three years later, a pair of American researchers, W.G Adams and R.E Day, built on Becquerel and Smith's work and published their research on "The Action of Light on Selenium". They discussed their research into the previously reported photoconductive properties of selenium and to determine whether or not light could induce a current in the selenium.[3] They found that, when annealed, selenium produced, under certain circumstances, an electrical current when exposed to light. Although a voltage could be measured, it was in no way usable. Nonetheless a very important property had been reported, which would allow the production, and the patent of, the first usable solar cell.

Charles Fritts patented the first "solar cell" in 1883. The design used selenium wafers coated with a thin layer of gold. This system reportedly had a power conversion efficiency (PCE) of 1%.[4] These cells, however, were extremely rudimentary and were most likely completely unusable. It wasn't until the advent of the p-n junction (Figure 1) by Russel Ohl in 1941 that real advancements could be made, not only in solar cells but also in many other avenues of electronics such as diodes and transistors, which are key to most, if not all electronic devices.[5]

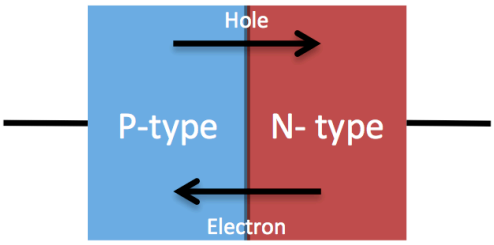

Figure 1. p-n Junction

The p-n junction is a boundary between two semiconducting materials. In the case of silicon, the crystal lattice can be doped with a material that has one extra, or one fewer, valence electron. When a material with one extra valence electron is used as the dopant, a classic example being phosphorous, the material becomes an n-type semiconductor as it has an increased concentration of electrons. The reverse is true when silicon is doped with an atom with one fewer valence electron; another classic example is the use of boron as a dopant. This creates an empty space, which an electron can occupy and is commonly referred to as a hole and the material becomes a p-type semiconductor.

When a p-type and an n-type material are joined they create an interface area where an electron from the n-type material if given some energy (say from a photon in the case of a solar cell) can migrate across the boundary and occupy a hole in the p-type material which allows current to flow. It is this system, and it's mode of operation, that has enabled most, if not all, of the advances in many electronic devices as p-n junctions are at the core of solar cells, transistors, LEDs

and many other components that have made most of modern technologies possible.[5-6]

1.2 Early Use of Solar Cells

In the mid 1950's commercial photovoltaics became a reality. Thanks to the p-n junction photovoltaic efficiencies increased to 4.5% and solar cells became a commercially viable item. This saw Hoffman Electronics, who at the time along with Bell Laboratories were a leader in solar array technology, supply the U.S Navy with six solar cell arrays for the first ever solar powered satellite, the Vanguard 1 (Figure 2).[7]

Figure 2. Vanguard 1

The success on the Vanguard mission led Les Hoffman, founder and CEO of Hoffman Electronics, to pursue the use of their solar cells in commercial devices. Although they had relatively low power output the advent of transistor technology meant it was enough to power small devices such as portable radios (Figure 3).

Figure 3. Hoffman Trans Solar Radio

This encouraged further research into these devices and it saw efficiencies increase dramatically from their humble beginnings. Solar cell technology - thanks to the efforts of researchers - has come a long way since their inception in the 1940's, and today there are classes of inorganic solar cells capable of reaching efficiencies of 44-46%[8]. Commercial cells however are typically in the 15 – 20% efficiency range.[8b, 9] This has lead to a surge in the installation of "rooftop-solar panels" on private homes. Energy independence is also becoming more and more likely thanks newer and better battery technology.[9-10]

Although traditional silicon-based solar cells have become the industry standard when choosing a renewable power source they have, like all technologies, their pros and cons. As previously mentioned their efficiencies mean that they can generate a usable amount of energy and as a result many of these devices have been installed on the roofs of homes and commercial buildings alike. Only recently came to be that traditional solar panels can produce more energy in their lifetime than it required to manufacture them in the first place. Panels are also relatively costly to produce and many of the materials used are toxic and difficult to dispose of, resulting in environmental issues when they come to the end of their usable life.[11] One way in dealing with this is to find alternate materials and methods for producing solar panels. One class of materials, known as organic semiconductors can be used to not only fabricate solar cells but many other electronic components and devices as well.[11-12] Unfortunetly in solar cells these compounds often exhibit low efficiencies, which has led to a great deal of research into finding newer and more efficient compounds as well as exploring device design. [1, 8b, 13]

1.3 Solar Cell Efficiency

As has been discussed, the quest for higher efficiencies has been the driving force behind the research into solar technology and is the most commonly used parameter used to evaluate the performance of a solar cell. The efficiency of any system is the defined as the ratio between the energy put into a system - this is light when discussing solar cells - and the energy generated, or power out of, a system (i.e electrical energy).[23, 24] For electrical systems however power is usually used, not energy.

$$\eta = \frac{P_{in}}{P_{out}}$$

Equation 1. Efficiency of a system

In electric power systems power (P) is the product of the voltage (V) and current (I) of a system.

$$P = IV$$

Equation 2. Electrical power

The power output of an electrical system can therefore be calculated through measuring voltage (V) and current (I), however with solar cells the current generated by a cell is directly proportional to the area of that cell. It is convention to therefore use current density, denoted as J, which is measured in Amps per meter squared (A/m^{-2}). This can be represented graphically as a J/V curve (Figure 1).

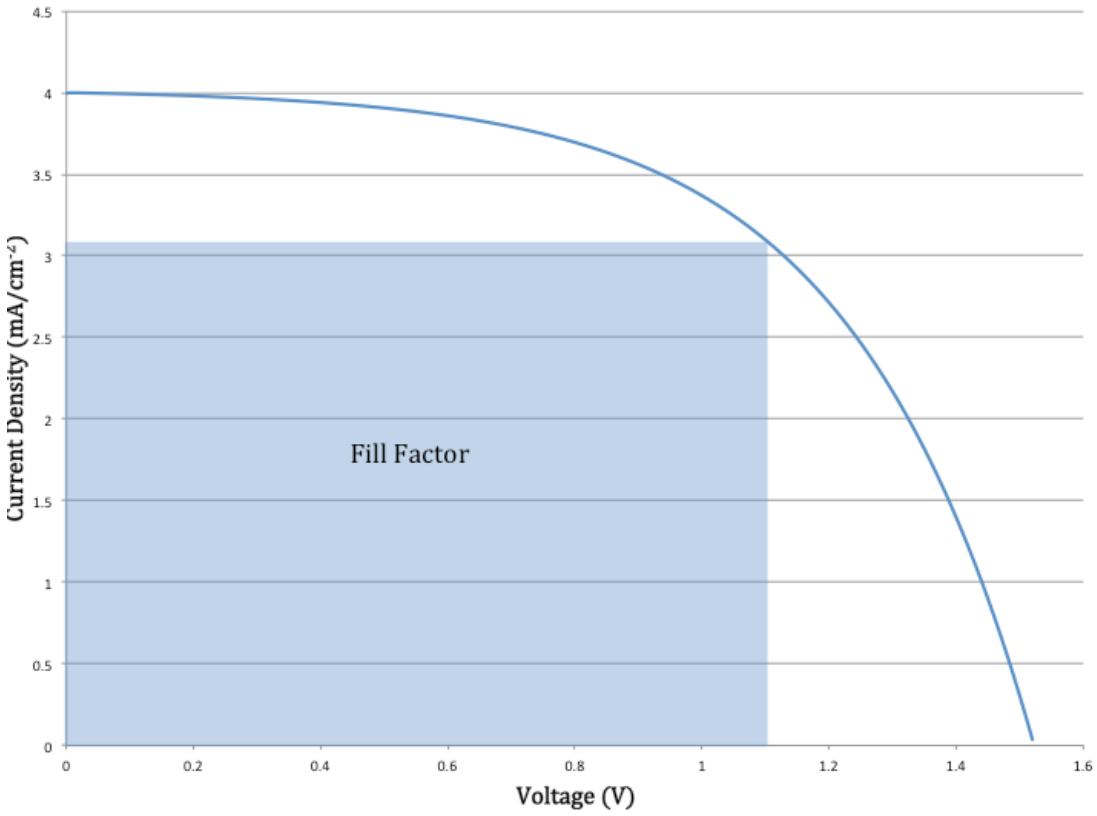

Figure 1. J/V curve with relative fill factor

When discussing solar cells, the maximum power output, P_{max}, is interchangeable with P_{out} and is defined as the product of three factors. These factors are: i) V_{oc}, which is the voltage across the cell when no current is flowing through the cell, ii) J_{sc}, which is the measured current density through the cell when the voltage across the cell is zero and iii) the fill factor (FF) which is defined as ratio between or "squareness" of the maximum power output area and the total area under the JV curve. The reason FF is included as a parameter for determining $P_{max.}$ We cannot simply multiply J_{sc} by V_{oc} as no voltage flows through the cell during short

circuit and no current flows during the open circuit, consequently no power generated at either of these points (i.e. at J_{sc}or V_{oc}). The maximum power output of a solar cell is therefore calculated using the formula below.

$$P_{max} = V_{oc} J_{sc} FF$$

Equation 3. Maximum power output of a solar cell

In the case of photovoltaic systems, P_{in} comes from a light source, which is calibrated for testing and therefore remains constant. However current is measured as a function of area, and therefore power too is represented as a function of area. It is therefore measured in either Watts per meter squared (W/m^2) or, more likely, in milliwatts per centimeter squared (mW/cm^2). Typically, procedure calls for using a 1.5 W/m^2 source, however for the purposes of the mathematics this is not strictly necessary. What is important however is proper calibration and consistency over the testing period.[25] An equation can therefore be derived as follows where η_{PVC} is the efficiency of a solar cell.

$$\eta_{PVC} = \frac{V_{oc} J_{sc} FF}{P_{in}}$$

Equation 4. Solar cell efficiency

Or put more simply:

$$\eta_{PVC} = \frac{P_{max}}{P_{in}}$$

Equation 5. Simplified solar cell efficiency

1.4 Organic Electronics

Organic electronics may hold some of the answers to the problems that are faced by traditional silicon semiconductors.[16] Rather than using silicon that has been doped with another atom, these devices use compounds that are made from predominately carbon, hence the name. In using this system, compounds with different properties can have interesting and unique conducting and semiconducting properties. These compounds are heavily conjugated and aromatic in nature resulting in low band gap and increased electron disassociation across the molecular structure, allow for facile receiving and donating of electrons. Semiconducting compounds are therefore described as either being an electron acceptor or donor. These compounds have found use in many applications such as organic light emitting diodes (OLEDs)[17], organic thin film transistors (OTFT)[13d, 18], and organic photovoltaics (OPVs)[19]. Related compounds have also seen use in chemical on/off switches and also in sensing. As these compounds are either polymers, or small molecules dispersed in a polymer semiconductor, they are inherently lightweight. They can also be fabricated into various shapes and sizes with ease. The flexible nature of many polymers can also lead to flexible and durable devices.

1.4.1 Conductive Polymers

The use and research of organic electronics has primarily seen growth in recent time due to the discovery and application of conductive polymers. These are the original organic electronic materials and without them many applications of organic semiconductors, such as flexible displays, would not be possible. These polymers are heavily conjugated and can also be heavily aromatic. Conductive polymers are not only interesting as they can conduct electricity, but they also enable other active organic materials to be incorporated into a conductive medium thus allowing the properties of other molecules to be

investigated and exploited. This has allowed for an explosion in the research and development of many types of organic electronic devices.

In 1862, Henry Letheby first prepared polyaniline (Figure 5), which is considered to be the first conductive polymer discovered, by the electrochemical oxidation of aniline. Polyaniline is both conductive and electrochromic; Letheby noted that the reduced form was colorless but became a deep blue once oxidized.

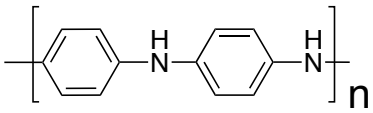

Figure 5. Structure of polyaniline

The earliest conductive polymers considered as charge transfer complexes. These compounds consist of long chains that are capped with an electron acceptor at one end and electron donor at the other. This resulted in systems that had electron density excess and one end, an electron deficiency at the other, with a long conjugated bridge through which an electron could travel upon the application of a voltage difference.

It wasn't until the work by Bolto *et al.* in 1963 that a useable conductivity in polymers was observed. They found that when iodine, in different forms, was compelexed within polypyrole, the material was conductive.[20] They hypothesised that the resistivity of the compound decreased as a result of the formation of a charge transfer complex due to the presence of the iodine, however they also expressed their belief that the data on the influence that iodine has on conductivity to be "conflicting". Furthermore, they were unable to fully estimate the degree of conjugation, as their compound was completely insoluble. Although their work was somewhat incomplete and lacking information, it laid the foundations for conductive polymer research.

In 1977, the work of Bolto *et al.* was built on in by Alan J. Heeger, Alan G. MacDiarmid and Hideki Shirakawa. They found that polyacetylene (Figure 6) became conductive when exposed to the vapors of various halogens (chlorine, bromine and iodine).[21] Their work was a much more complete and assertive attempt at understanding the relationship between the halogen content and stereochemistry of the polymer and how these factors affected its conductivity. In recognition of the impact their work has had and will continue to have Heeger, MacDiarmid and Shirakawa were awarded the Nobel Prize in Chemistry for "for the discovery and development of conductive polymers".

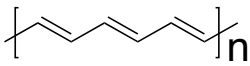

Figure 6. Structure of polyacetylene

There are now several types of conducting polymers[22] composed of a variety of monomers. However one class that not only seen extensive use but also offer versatility and simplicity are polythiophenes.[22-23] These compounds are extensively used within the construction of BHJ cells as well as thin-film field effect transistors and luminescent devices (OLEDs). This class of conductive polymers came into their own when McCullough *et al.* recognised that there was a need for consistency within structure of conducting polymers to maintain consistent electrical properties. Previous synthetic methods for these polymers lead to variances in the molecular structure, which was due to the way in which they were syntehsised, in this case asymmetric monomers with terminal coupling units, such as halogens, could often homo couple giving an inversion of the intended shape of the polymer (Figure 7).

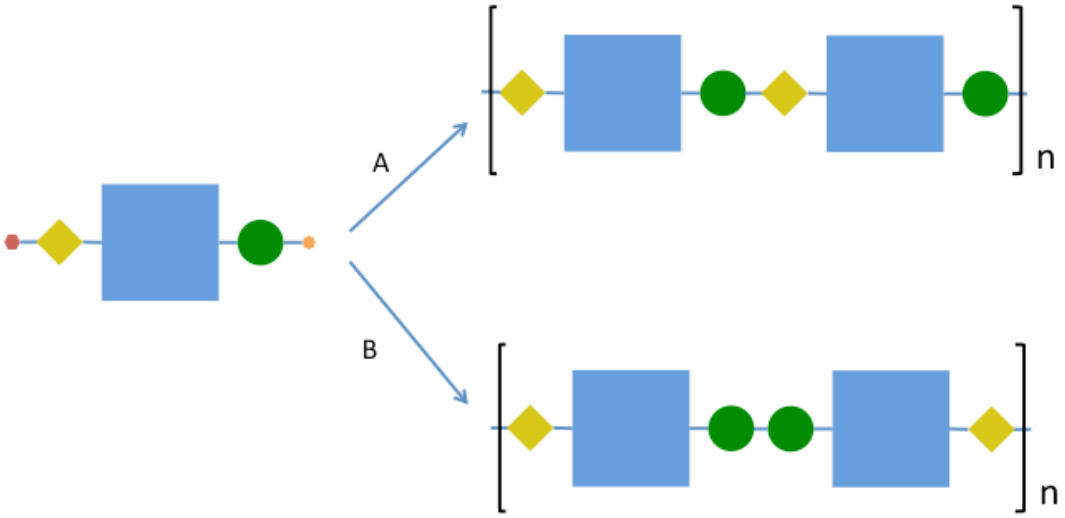

Figure 7. Representations of Polymerisation: A) desired polymerisation. B) undesired polymerization

This was relevant in McCullough's work as the solvating alkyl chain meant that the thiophene itself was asymmetric and coupling resulted in structural irregularities (Figure 8).

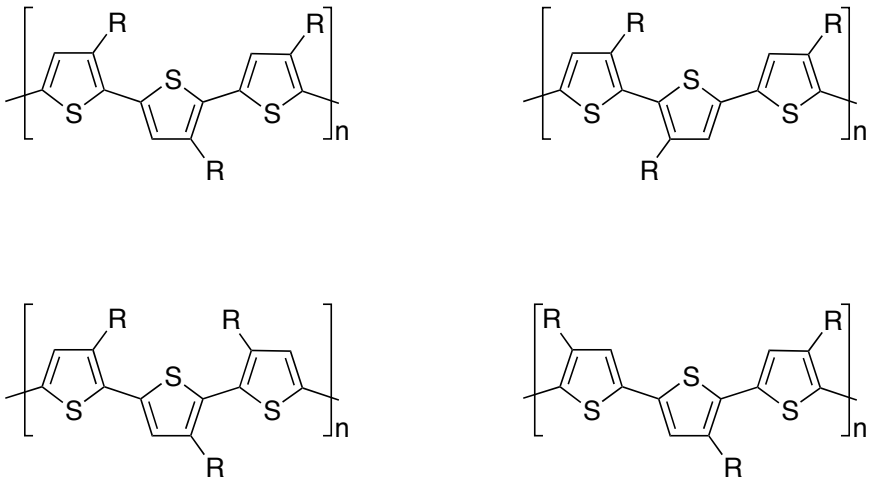

Figure 8. Polythiophenes with varying structures and inconsistencies

With structural consistency in mind, McCullough *et al.* derived a novel synthesis to produce a much higher proportion of regiosolective poly(3-alkylthiophenes). The method used α-bromo-3-alkyl substituted thiophenes as the starting material. The compounds were then converted the corresponding polymer in a multi step one-pot synthesis by generating a 2-bromo-5-magnesium bromide analogues with subsequent polymerization by using a Kumadu coupling.

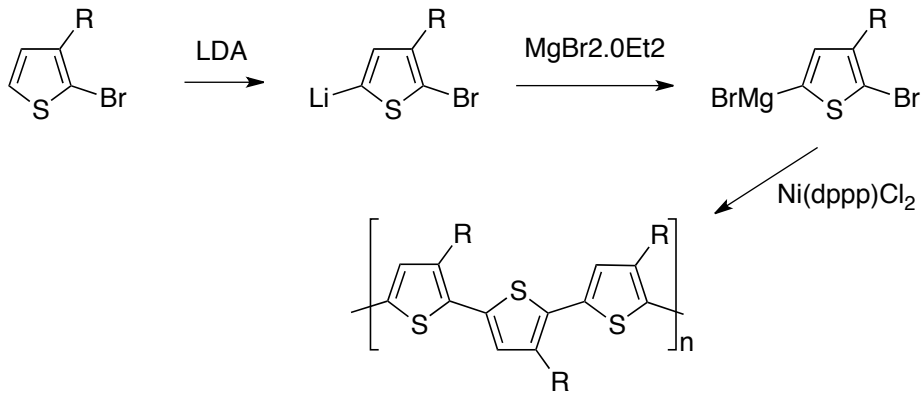

Figure 9. Synthesis of regioselective 3-alkyls substituted polythiophene

This method greatly increased the yield of a single structural unit, and as a result, the conductivity of the polymer was enhanced dramatically.

Polythiophenes are now extensively used in many areas of organic electronics this is due partly to the ease at with which they can be synthesised but also their ability to act as an electron donor material. A commonly used polythiophene derivative used is poly(3-hexylthiophene-2,5-diyl) (P3HT), This is the most commonly used medium in BHJ fabrication as it is both conductive as well as a strong electron donor.[24] It is an easily synthesised and versatile polymer that readily incorporates most dyes through both pi-pi stacking through its thiophene components and van der Waals forces through its long alkyl chains.[18b, 19b, 25]

1.4.2 Organic field effect transistors (OFETs)

Arguably the most important invention ever, the transistor, has also seen modification in composition through the use of organic semiconductors.[5, 26] Organic field effect transistors (OFETs) are simply a class of field-effect transistors that use an organic semiconductor in place of the traditional silicon and metal oxide combinations. The organic materials can either be small molecules or polymers that have semiconducting properties. Koezuka *et al.* reported the first OFET in 1987.[18c] The device was simple in construction and used polythiophene (Figure 10) as a hole transport material and showed a mobility of 2 x 10^{-5} cm^2 V^{-1} sec^{-1}. Although the hole mobility was low, the device displayed excellent stability despite having been heated to 80°C in air.

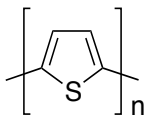

Figure 10. Structure of polythiophene

More recent devices have considerably higher mobility. Typical mobilities seen are in the range of 1 – 10 $cm^2 V^{-1} sec^{-1}$. However, rubrene-based (Figure 11) devices have mobilities as high as 40 $cm^2 V^{-1} sec^{-1}$. [27]

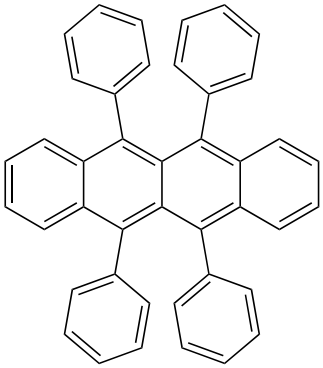

Figure 11. Structure of rubrene

OFETs have also been shown to have light emitting properties, or so-called organic light emitting transistors (OLETs). First designed in 2003 by Hepp *et al.* their device used tetracene (Figure 12) on an insulative layer of SiO_2 on top on n-doped silicon. The device had a peak emission of 540 nm and showed an average luminosity of 45 cd/m^2.[28]

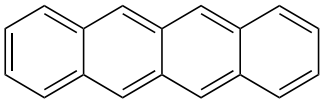

Figure 12. Structure of tetracene

OFETs have already seen use alongside OLEDs to create flexible display screens. In 2007, Sony presented a screen that was comprised of OLEDs and OFETs at the SID 2007 International Symposium. Not only was the screen durable and flexible it only weighed 1.5 g and had a maximum thickness of 0.3 mm. This was possible as the traditional glass substrates commonly used to manufacture OLEDs and OFETs in the lab can be replaced with polymers such as polyethylene terephthalate (PET).

1.4.3 Organic light emitting diodes (OLEDs)

Organic light emitting diodes (OLEDs) have already found their way into consumer products. This is in part due to their simplicity, cost and performance.[17a, 17b, 29] The compounds used in these devices are similar to OLETs however device construction is different as is the same with standard diodes and transistors. However, both are "electroluminescent" in nature, are highly efficient and can be long lasting. André Bernanose made the first report of electroluminescences in an organic material in the 1950's. He noted that when certain dyes (Gonacrine and Acridine Brilliant Orange E) were adsorbed onto a sheet of cellophane a "rather strong light emission" could be observed upon the application of an alternating current of 400–800V. He also noted that the light increased in intensity with increasing voltage, up to 2.5kV. He hypothesized that the strong electric field caused the formation of an unstable excited molecules that emit a photon upon returning to their ground state.

However it wasn't until 1987 that the first light emitting diode device was reported on by Tang *et al.* This was achieved by using a two-layer device containing a layer of tris-8-hydroxyquinolyl aluminum and a diamine in the other (Figure 13). This device reportedly needed less that 10 VDC to operate and produced more than 1000 cd/m2 and maintained an efficiency of 1.5 lm/W.[17c]

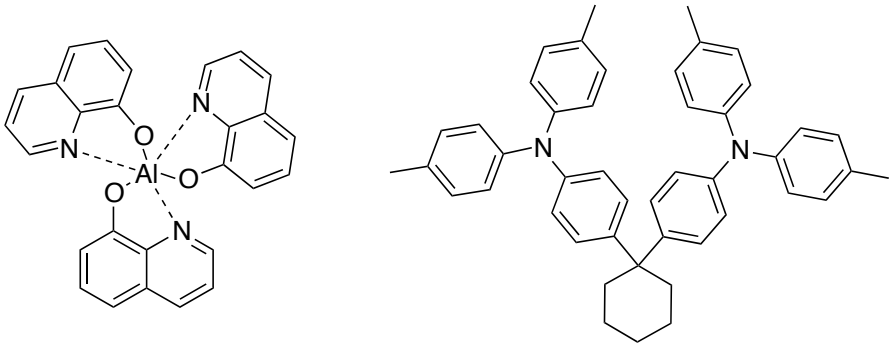

Figure 13. (left) tirs-8-hydroxyquinolyl aluminum (right) diamine used in OLED

Presently, OLEDs have been incorporated into many commercial products including battery powered lamps, but more notably in displays by combining OLEDs that emit red, green, and blue light into an active-matrix display. These devices are known as active-matrix organic light emitting diodes or AMOLEDs and have seen use in commercial applications, since 2008 most notably in smartphones of the Samsung brand (Figure 14).

Figure 14. AMOLED display in a Samsung smartphone

1.5 Organic Solar Cells

Brian O'Regan and Michael Grätzel fabricated the first usable organic solar cell in 1988 and are heralded as having invented the dye-sensitized solar cell (DSSC).[30] The cell used organic dyes, rather than the traditional doped silicone, in order to harvest light and create electron excitations needed to induce current. The device was rather simple in construction and used a glass substrate, coated in an indium tin oxide layer approximately 10 μm thick on which another layer of titanium dioxide was laid. The TiO_2 was then coated with the organo-metalic dye, a ruthenium-based complex (Figure 15). Another sheet of glass with a layer of InSnO (ITO) is placed on top of this layer and an electrolyte is injected. Upon exposure to simulated light conditions, a voltage was generated with an efficiency of 7.1 – 7.19%, with efficiencies of 12% being observed in diffused daylight. This was a major step in the development of a usable organic solar cell. There were previous reports of using organic compounds to sensitize semiconductors to light, however they were more concerned with the "switching" abilities and the devices themselves only produced a very small current. O'Regan and Gratzel's cell is even more impressive when considering that their stability and efficiency was achieved using materials that were of "low to medium purity".

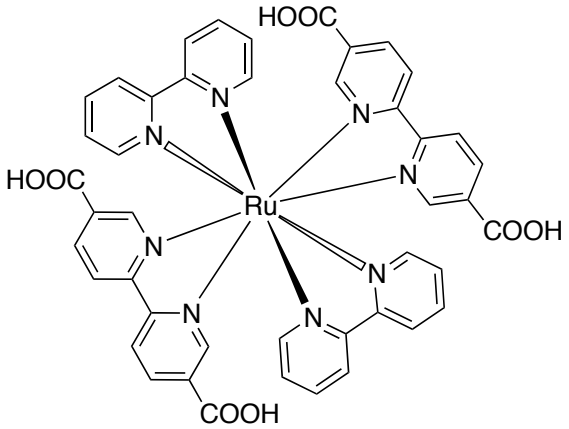

Figure 15 Ruthenium Dye

Dye-sensitized solar cells work under the principal that the dye absorbs a photon, exciting an electron which is injected into the conduction band of the semi conductor, in the case above is TiO_2. The dye itself is oxidized in this initial process and must be regenerated. This occurs at the counter electrode, normally through a redox process involving an electrolyte. It is this constant oxidation-reduction process of the dye that sees their performance dwindle overtime as the dye itself is destroyed. However, given the number of factors involved in completing one cycle, from dye oxidation to reduction, there are many areas in which improvements in the overall efficiency, stability, and simplicity of the cell can be made.

Bulk heterojunction (BHJ) devices are a way in which the organic photovoltaics (OPVs) have become much simpler. They are devices that use no electrolyte and are incredibly simple in design. They consist of an electron donor material and an electron accepting material, in essence a simple p/n junction. The materials can be either layered on top of one another or blended together and are sandwiched between two layers of a conductive material, usually a metal such as aluminium or silver (the anode), and ITO glass (cathode). This is the standard method by which laboratory cells are made but they can be made into flexible cells using sheets of thin plastics as the conductive substrates.

1.5.1 Operating Principles:

The operating principle of all photovoltaic cells is rather simple and in both organic and inorganic cells the method by which an electron migrates is very similar. In the case of organic materials it can be broken down into 3 steps, absorption/excitation, migration and transfer as illustrated in (Figure 16).[31]

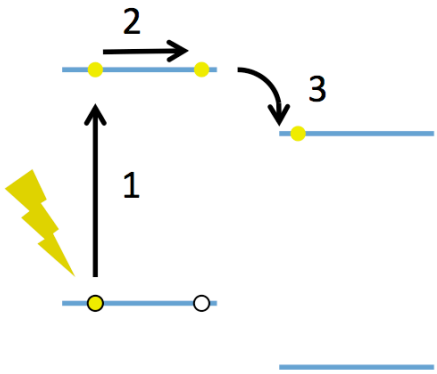

Figure 16. 1) Electron excitation 2) Electron-Hole Migration and 3) Electron transfer

Materials must be designed in order to encourage these steps to occur. In OPV materials this is achieved by having large areas of conjugated bonds, and this ensures that the electrons will interact with low energy visible light in the form of absorption and electron excitation. Consequently the further into the "red" a compound absorbs, the lower the energy requirement is and the more "active" it is.[31a, 32]

Electron migration is the process whereby the excited electron migrates towards the acceptor material; this inherently takes time and the longer the electron can remain in this excited state the longer it has to diffuse. In order to obtain this effect the hole and electron pair must not be allowed to recombine; known as electron-hole recombination or luminescence. Although there are multiple electron-hole recombination types, and in terms of organic photovoltaics it can be thought of as fluorescence.[33]

For transfer to occur, the electron accepting material used must have a LUMO lower that is of lower energy than that of the LUMO of the electron donating material. This ensures that there is an energetically favorable route for the electron to flow. In other words it must go down hill with respect to energy level.[31b, 33] The electron can then flow into the conduction band of the anode, and the hole can migrate to the cathode. This intrinsically leads to a potential difference and the electron will, if he circuit is complete, will flow through to recombine with the hole completing the cycle.[31] However when designing a cell other factors of the material need to be taken into consideration, not just its electronic properties. Although there are materials that act as excellent electron acceptors their use may be limited as a result of poor solubility in common solvents or stability, and compounds of this nature can also be hindered by cost. This must be kept in mind when designing, and synthesising compounds.[34]

Cell design can also play a significant role in the operation and efficiency of compound and subsequently the device. For optimal performance, the materials that act as an electron donors and acceptors need to be matched with one another in order to achieve electron flow. Device design and architecture is therefore an important role in the overall process of making a solar cell.

Each design has it's own pros and cons. For instance DSSCs have high efficiency and are likely to see large scale commercialization in the future. The main drawback in this design however is in the use of corrosive redox mediators in the form of liquid electrolytes. One of the major design challenges faced by manufacturers and researchers is ensuring that the electrolyte doesn't leak or dry out over time. [32a] This has spurred researchers towards finding solutions such as less volatile electrolytes as well as solid-state redox mediators.[35]

Other design types that have seen much use are the bilayer Tang *et al.* [19f] which was the first iteration of an efficient of two compounds with aligned energy levels, and the bulk hetero junction pioneered by Kraabel *et al.* (Figure 17).[36]

Again the mode of operation is similar to that which occurs in a standard silicon-based solar cell. The n-type material, the electron donor, will absorbs a photon and an electron is excited. This occurs between the highest occupied molecular orbital (HOMO) and the lowest unoccupied molecular orbital (LUMO) and it is this that gives the desired electron-hole pair. In order to induce an electrical current the electron must then enter the LUMO of the p-type, electron acceptor, material and subsequently to the anode of the device.

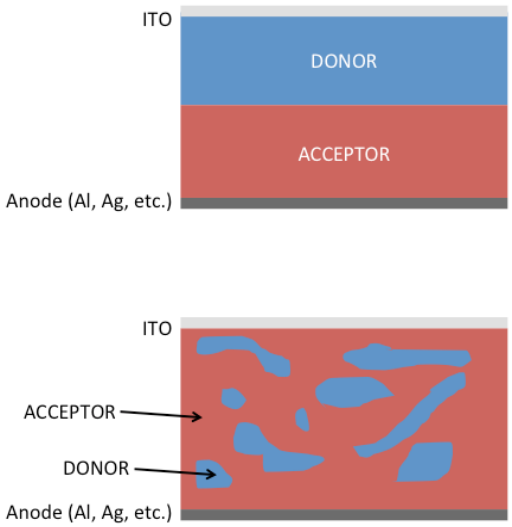

Figure 17. Bulk hetero junction cell construction, bilayer (top), dispersed (bottom)

Due to the simplicity of the design, and the ease with which devices can be made, donor and acceptor materials can be paired and tested easily which has led to a higher throughput of materials being tested. This simplistic design has also permitted variations in different aspects of their construction, such as annealing time, material thickness and solvents used. As a result, significant advances have been made in different areas pertaining to increasing the efficiencies of organic solar cells.

In very recent times, production of, a new type of semi-organic solar cell design that has seen big gains in efficiencies and an increased interest are perovskite cells. A perovskite is an inorganic material whose crystal structure is the same as $CaTiO_3$. Typically they are sensitized with an organo-metallic complex that is spin coated and annealed onto a glass substrate.

Even though they use highly crystalline material perovskites can also be fabricated using polymer substrates allowing them to be flexible, one of the main advantages that fully organic solar cells have. From their earliest reporting by Kijoma *et al.* in 2009 they have seen gains in efficiencies from 3.8% to 20%, all in six years.

1.6 Donor and Acceptor Design

The roles of an electron donor and an electron acceptor within an organic solar cell are modest ones, but they are of the utmost importance. Put simply, the cell must absorb a photon, excite an electron, and then pass the electron to the acceptor material. Although this sounds simple, it is the fundamental principle for the operation of organic solar cells. Unfortunately, in practice synthesising compounds with these properties, as well as all the other characteristics needed, such as solubility, thermal stability, appropriate molecular orbital energy levels is a challenge.[37]

Within a solar cell, the organic semiconductor can exist as either a polymer or a small molecule. Typically the compound is broken down into subunits, each with their own characteristics. The subunits are: donors (D), acceptors (D) and pi spacers (π). Acceptor subunits are typically heavily heteroatom rich and electron withdrawing, donors are usually, though not always, heteroatom poor and are electron donating. Pi-spacers are simply conjugated or aromatic units that connect the two. Compounds can be various arrangements of these units and are typically referred to using the acronyms of the subunits i.e. A-D-A or A-π-D etc.

As with all organic semiconductors, electron donor and acceptor materials consist of heavily conjugated and aromatic subunits, allowing for a delocalization of electrons and adequate HOMO/LUMO energy levels. For electron donating compounds, high energy HOMO levels and LUMO states are desirable, allowing for adequate overlap with the HOMO and LUMO energy levels of the electron acceptor, meaning an electron can migrate from the excited state in the donors LUMO the that of the acceptor.[24, 31b, 34c] The difference in energy between the HOMO/LUMO levels of a compound is referred to as the optical bandgap, this is the minimal amount of energy a photon requires in order to excite the electron from the valance band into the conduction band. Although low bandgaps are somewhat favorable there is a trade off between doing this and the V_{oc} of a cell. The V_{oc} of a cell can be roughly estimated from the molecular orbital levels of the

donor and acceptor, therefore it is benefitial to decrease badgaps by decreasing the energy level of the LUMO of a donor rather than by increasing its HOMO.[37] It is believed that the optimal bandgap for solar cells is around 1.3 eV and it is at this point that the compromise between J_{sc} and V_{oc} is optimal.[19d, 37-38]

It is therefore easy to see the importance for materials to have broad absorption profiles along with early onset of absorption in order to perform well in a bulk heterojunction device. For polymers, tuning these properties is a fairly straightforward process, as their absorption properties can be roughly estimated from the sum of the monomer units. This is, in part, why polymers reign supreme as donors within bulk-heterojunction solar cells. As photon absorption is essential for the generation of an exciton in the donor material, they must also have high absorption coefficients. Electron donor materials too must have high absorption coefficients the active layers in a cell subsequently only need to be a few tenths of a millimeter in thickness in order to absorb a sufficient amount of light in order to operate. This can be an issue when preparing the active layer of a solar cell as if there is too thick a coat then conduction is hindered as no exitons are formed, further emphasizing the importance of high absorption coefficients.[39]

There are two compounds P3HT, a donor, and PCBMPCBM-61, an acceptor, which are the industry standards when determining a compounds efficacy. These compounds will be discussed in further detail in subsequent sections. BHJ devices made from a blend of these devices typically see efficiencies in and around the 3% area but have been fabricated to achieve efficiencies in excess of 4%. However many examples of better performing devices using “paired” electron donor mixes that contain neither P3HT nor PCBMPCBM-61 do exist and illustrate the importance of harmonizing their properties.

1.6.1 Electron Donors

As electron donating material is arguably the most important part of a bulk heterojunction, cell research around them is ever increasing. Alkyl substituted polythiophenes, are some of the most widely used organic electronic materials having seen use in OLEDs, OFETs and OPVs.[40] They have strong absorption profiles, are conductive, have adequate solubility, thermally and environmentally stable and are, thanks to McCullough *et al.*,[23a] relatively easy to synthesise with a high degree of structural regularity which is important if devices are to behave consistently. One polythiophene that is extensively used is P3HT (Figure 18). This polymer consists of repeating 3-hexyl-thiophene units and has led the way as an industry standard and has become the "go-to" electron donor when testing electron acceptors within bulk heterojunction cells. Typically, when paired with a fullerene acceptor efficiencies of 3 – 4% can be achieved.[19b]

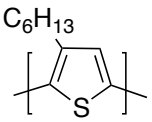

Figure 18. Structure of P3HT

As OPV devices predominantly use polymeric chromophores they are often generically labeled "plastic solar cells" and the first iteration of the cell used a polymer donor. Conjugated polymers see such use as they have all the required properties aforementioned, such as high absorption in the visible region and stability at high temperatures as well as under operating conditions. Polymers also offer ease of tunability to researchers as incorporation of a new monomer can have dramatic effects on the overall performance of a material. Within BHJ cells polymers are arguably the strongest electron donors and it is no surprise that the bulk of research into novel donor materials has revolved around their synthesis and application. This has lead to the synthesis of some very potent donors showing high performance in BHJ setups when coupled with unique donors as well as standard C_{60} derivatives and achieve efficiencies over 7%.[41]

1.6.1.1 Electron Donors (Polymers)

The first discovery of ultrafast electron transfer within a bulk heterojunction of was by Kraabel *et al.* using a blend of C_{60} and poly-3-octyl-thiophene (Figure 19). Although the study only focused on whether photoinduced electron transfer was possible no direct efficiencies were measured. However, the device architecture, and the fact that electron transfer could occur between polymers, namely poly-3-octyl-thiophene, and C_{60} paved the way for the ever-versatile and heavily used BHJ architecture.

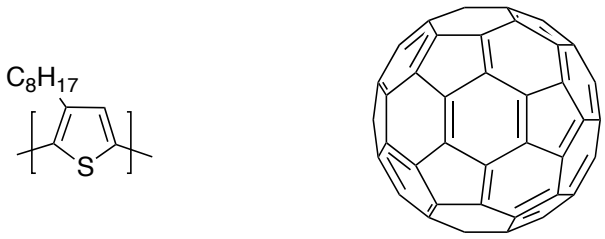

Figure 19. Structure of poly-3-octyl thiophene (left) and C_{60} (right)

In 2010 Liang *et al.* produced a polymer, PTB71, that exhibited efficiencies as high as 7.4%. The compound consisted of a benzodithiophene and bisthiophene units (Figure 20). Interestingly the compound itself showed a very high and broad internal quantum efficiency upwards of 90%.[42]

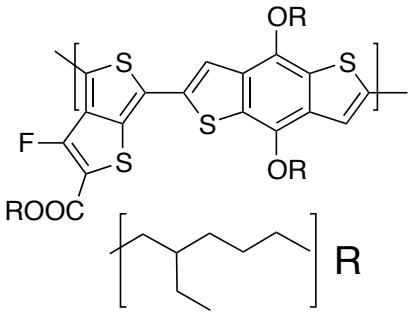

Figure 20. Structure of PTB71

Again, when paired with PCBM-71 - another benzodithiopene containing polymer, namely PBDTTPD(2EH/C7) (Figure 21), showed an impressive efficiency of 8.5% with an average of 8.3% observed over an array of devices.[43] Interestingly Cabanetos *et al.* varied alkyl chains of the ethers and imides and observed significant alteration to the overall efficiency of a compound.

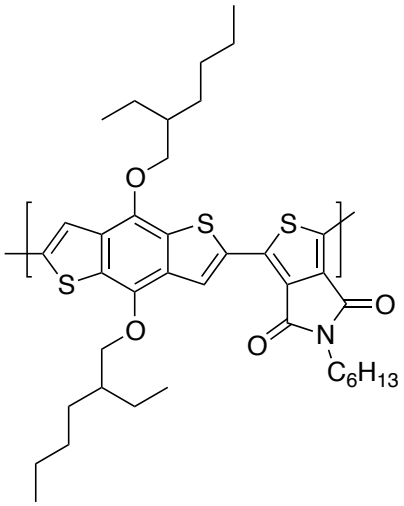

Figure 21. Structure of PBDTTPD(2E/C7)

1.6.1.2 Electron Donors (Small Molecules)

Although polymers can be potent electron donors, there has also been a steady increase in the research of small molecules as donor materials. These compounds are similar to their polymeric cousins in that they must have all the same properties and also contain moeities with electron donating and accepting properties. They are however single molecular units as opposed to repeating blocks of monomers. This means that they can be easily synthesized as well as purified and rarely suffer from problems such as region-irregularity or low solubility. They do however have their own problems, namely low power conversion efficiencies. Despite these drawbacks, small molecules have seen a great deal of success seeing efficiencies reach into the 9% range.

Some of the best performing small molecule donors come from the

Some of the best performing small molecule donors come from the benzothiadiazole family of compounds, in particular those that are paired with the silylodithiophene moiety.[44] Sun *et al.* in 2012 published on the synthesis and charecterisation of DTS(PTT2)2 (Figure 22) a novel small molecule containing a silyllobithiophene central moiety with benzyldithiazole terminal units. The compound, when paired with PCBM-71, showed an efficiency of 6.7% with a relatively high V_{oc} of 0.8 V.[45] Their discussion also emphasized the importance of fabrication procedures and the effects it has on device performance. Moreover it demonstrated that small molecules could compete with their larger polymer counterparts.

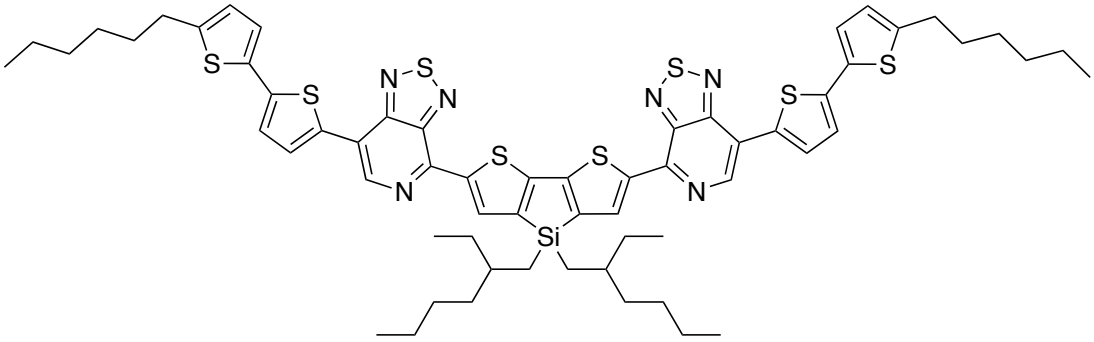

Figure 22. Structure of DTS(PTT2)2

Interestingly van der Poll *et al.* synthesised other compounds with very similar structures only varying in the dithiazole moiety and it's substitution. In 2012 they discussed p-DTS(FBTTh2)2 (Figure 23) which showed improvements over DTS(PTT2)2. Again when paired with PCBM-71 the compound showed an efficiency of 7.0% and a V_{oc} of 0.8V.[46]

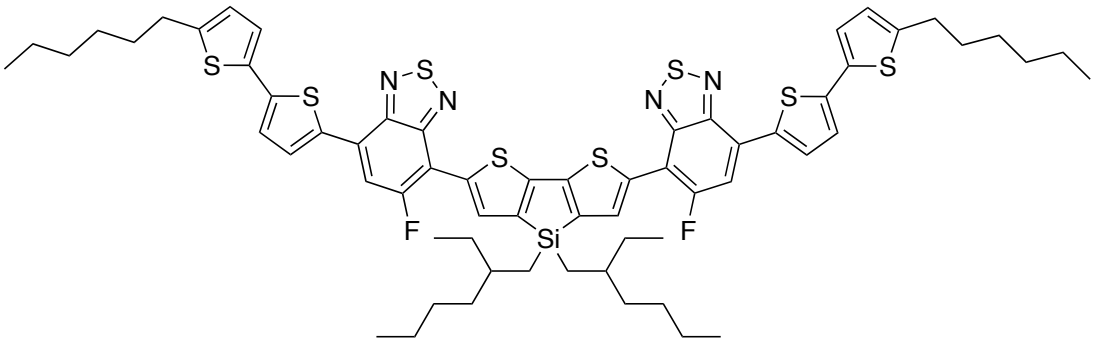

Figure 23. Structure of p-DTS(FBTTh2)2

Work by others has shown that this system, meaning those containing silylodithiophene, is particularly responsive to the subtlest of changes in heteroatom type and location.[47] Work by Takacs *et al.* varied on the work done by Sun and can be seen in Table 1.

Other compounds too have seen a great deal of success in achieving high PCE values. Among the highest, around the 9% mark and 10% in tandem cell design the compounds usually contain polythiophenes separating the donor and/or acceptor units. In particular work done by Zhang *et al.* on rhodanine-bearing polythiophene small molecules, namely DRCN7T (Figure 24).

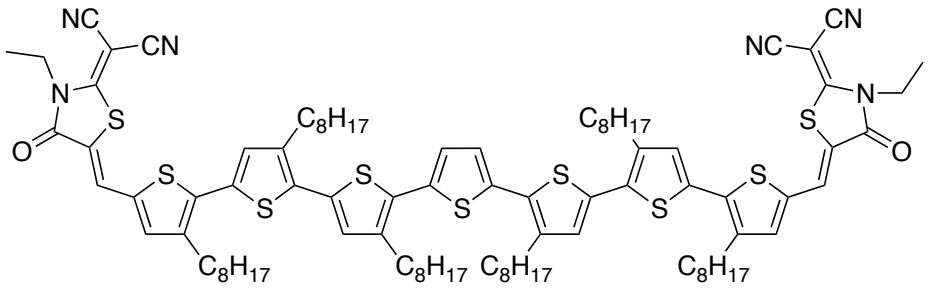

Figure 24. Structure of DRCN7T

DRCN7T is to date one of the best performing small molecule electron donors. It was synthesized by Zhang *et al., and* saw an efficiency of 9.3% with a V_{oc} of 0.91 when in a BHJ device where PCBM-71 acted as the electron acceptor. To date this is still one of the best performing small molecules and has yet to be surpassed by a small molecule in a non-tandem cell design. [48]

Table 1. High performing small molecule donor materials

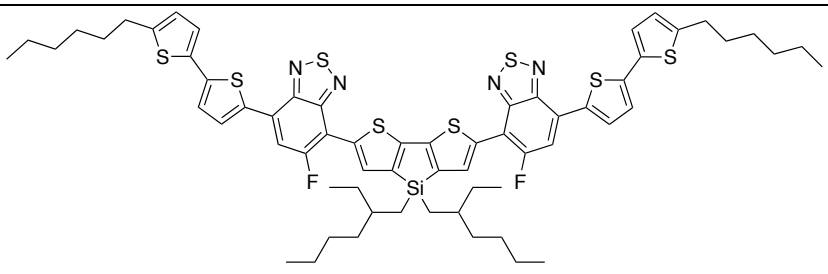	PCE: 7.1% V_{oc}: 0.81V van der Poll *et al.* [46]

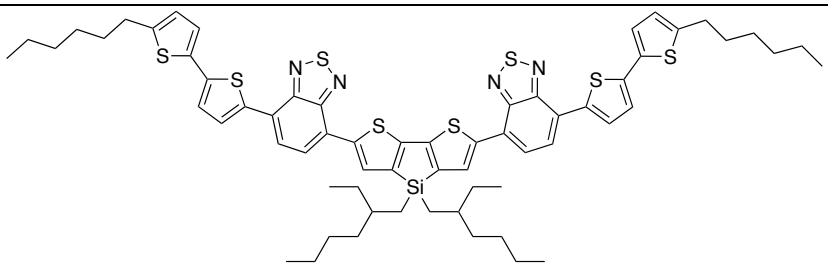	PCE: 0.19 V_{oc}: 0.83 Takacs *et al.* [47]
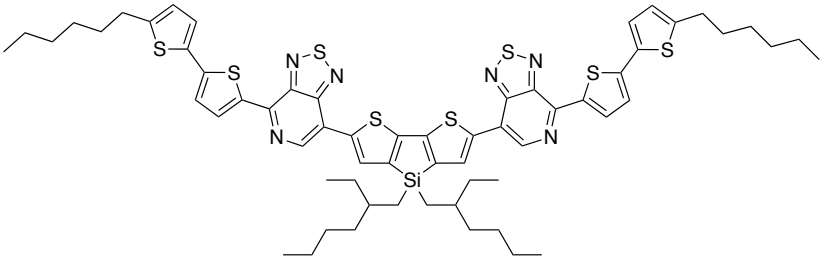	PCE: 5.6% V_{oc}: 0.73V Takacs *et al.*[47]
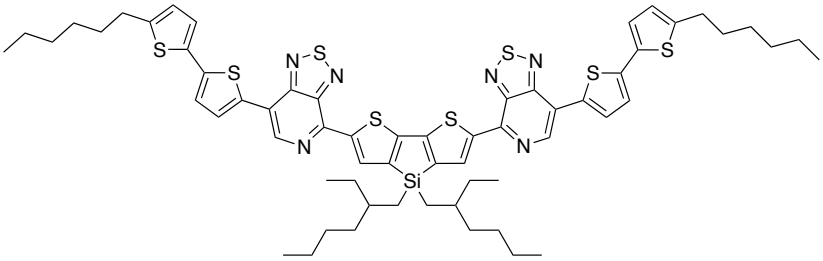	PCE: 6.7% V_{oc}: 0.78V Sun *et al.* [45]
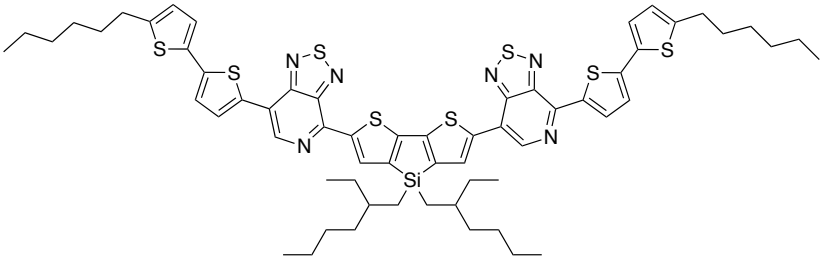	PCE: 3.16 V_{oc}: 0.72V Takacs *et al.* [47]
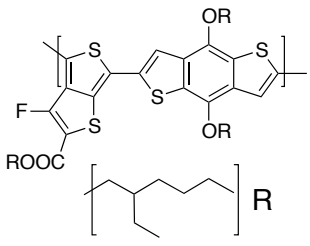	PCE: 3.16 V_{oc}: 0.75V Liang *et al.* [42]

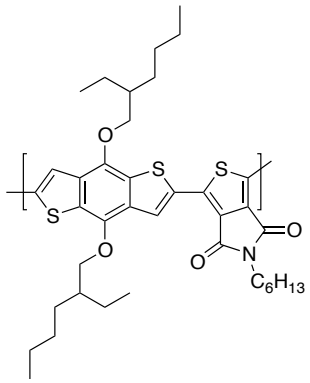	PCE: 8.5 V_{oc}: 0.97V Cabanetos *et al.* [43]
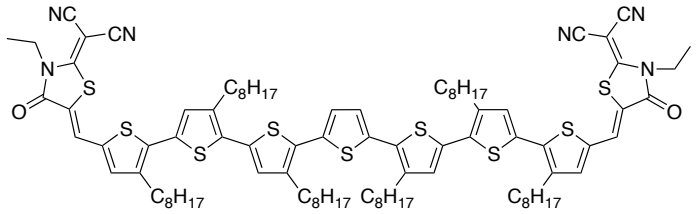	PCE: 9.3% V_{oc}: 0.91V Li *et al.*
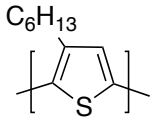	PCE: 4.4% V_{oc}: 0.61V Li *et al.* [19b]

1.6.2 Electron Acceptors

Although donor materials are arguably the most important part of a bulk heterojunction solar cell, the acceptor material is also of significant interest to researchers as increasing the potency of electron acceptors leads to better performing devices. Acceptors are typically compounds with similar characteristics to donors in terms of solubility, stability and light absorption but differ immensely in the energy of their molecular orbitals. Typically low lying HOMO and LUMO energy levels are desirable. The most potent electron acceptors are the fullerene analogues with PCBM-PCBM-61 being the industry standard for subsequent testing and evaluation of novel donor materials.

An electron acceptors role is to accept the electron that has been excited in the donor material. It must also have complementary HOMO/LUMO levels when paired with a donor. Tang pioneered the use of the donor/acceptor blend in the iteration of the first "twin-layered" solar cell. Tang used a copper porphyrin as the electron donor and a pyrelenediimide as an electron acceptor, as seen in Figure 25. Though primitive by todays standard it did result in an efficiency of approximately 0.95% and an open circuit voltage of less than 0.5 V.[19f]

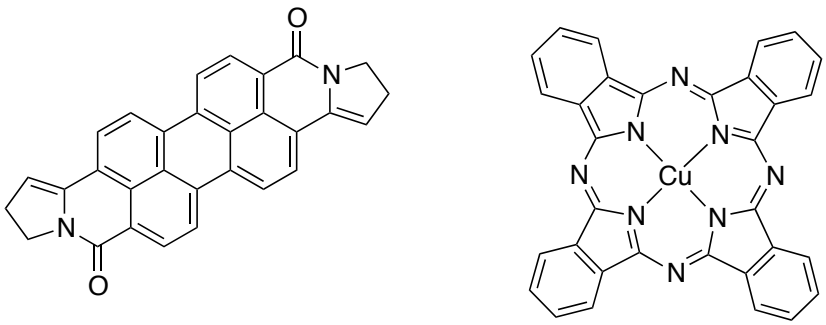

Figure 25. Analogues of perylene diimide and Cu porphyrin

Although the first acceptor within a two-compound organic solar cell was a perylene derivative, C_{60} and other fullerene derivatives have become the standard materials used in organic solar cell devices.[19f]

Harrold Kroto, James Heath, Sean O'Brein, Richard Smalley and Robert Curl first discovered buckminsterfullerene, or C_{60}, in 1985 while working at Rice University. The material was discovered when graphite was irradiated with a laser that caused the formation of C_{60}. In 1990 W. Krätschmer and D. R. Huffman developed a new synthesis in which an electrical arc was generated across two high purity electrodes, in an inert atmosphere.[49] The soot collected was then be purified by chromatography to yield pure C_{60}. This method can produce gram quantities of $C_{60,}$ however given that other fullerenes are also generated the purification step can be very costly.

Fullerenes have found extensive use in organic electronics, as their structure is inherently aromatic in nature. This leads to a large delocalisation of electrons

and as a result an electron can be easily accepted. The electron-rich environment also allows for some chemical reactions. Fullerenes can be reacted with ozone to give either epoxides or ethers depending on reaction conditions. Diels-Alder reactions can also be employed to give [2+2] cycloaddition products.[50]

However, probably the most important reaction to be employed on C_{60} that has led to its derivatives being used in organic-solar cells is the Bingel reaction. In this reaction, fullerenes can be reacted with malonates in the presence of a very strong base such sodium hydride or DBU (Figure 26).[51]

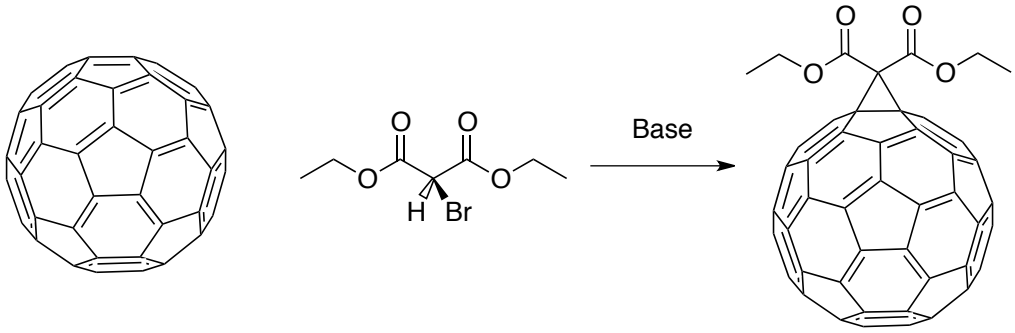

Figure 26. Synthesis of Bingel fullerene

This reaction has seen the area of fullerene research significantly expand. This also led to the synthesis of one fullerene analogue, PCBM-61 (Figure 27). This compound is the standard electron acceptor used in fullerene-based bulk heterojunction solar cells.

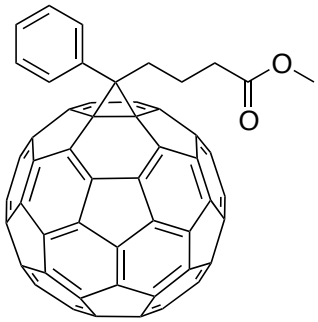

Figure 27. Structure of PCBM-61

When paired with P3HT the resulting solar cell generally gives power conversion efficiencies of 4%[52]. Fullerenes however are limited in many ways. There is a high cost involved in their synthesis, and there is also limited capacity with respect to changing their structure and properties. This has led many to seek alternative electron acceptors with varying degrees of success.

Another fullerene of note of note is PCBM-71. When used in OPV devices they see an increase in light harvesting ability in the visible region. However, it is much more expensive than its C_{60} counterpart but performs much better than PCBM-61.[53] PCBM-71 Typically sees efficiencies around 4.7%[54] when paired with P3HT; however when paired with other donors it can see efficiencies as high as 10%[55]

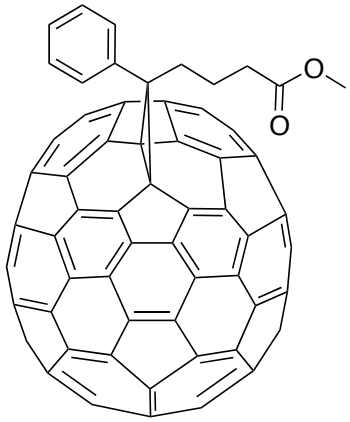

Figure 28. Structure of PCBM-71

Research into non-fullerene containing compounds for use as acceptors has also shown some promise for compounds that do not contain fullerenes. Like many compounds that are designed and used within organic electronics they can exists as either long chain polymers or as singular molecular entities. Compounds that have seen much interest are those that have areas of electron deficiency, most notably fluorenes, naphthalenediimides (NDI), diketopyrroolopyrrole (DPP) and some porphyrins. When these compounds are paired with P3HT, efficiencies below 1% are often seen, however there are compounds that have seen results that are comparable with that of PCBM-61.

One simple example of NDI as an acceptor, reported by Ahmed *et al.* is within a simple small molecule assembly with varying lengths of thiophene substitution in the 2 and 4 positions. Named NDI-nT and NDI-nTH where n is the number of thiophenes and T or TH refers to the level of alkyl substitution. When paired with P3HT the best performing acceptor, NDI-3TH (Figure 29), Ahmed *et al.* achieved an efficiency of 1.5% with a V_{oc} of 0.82 V.[56]

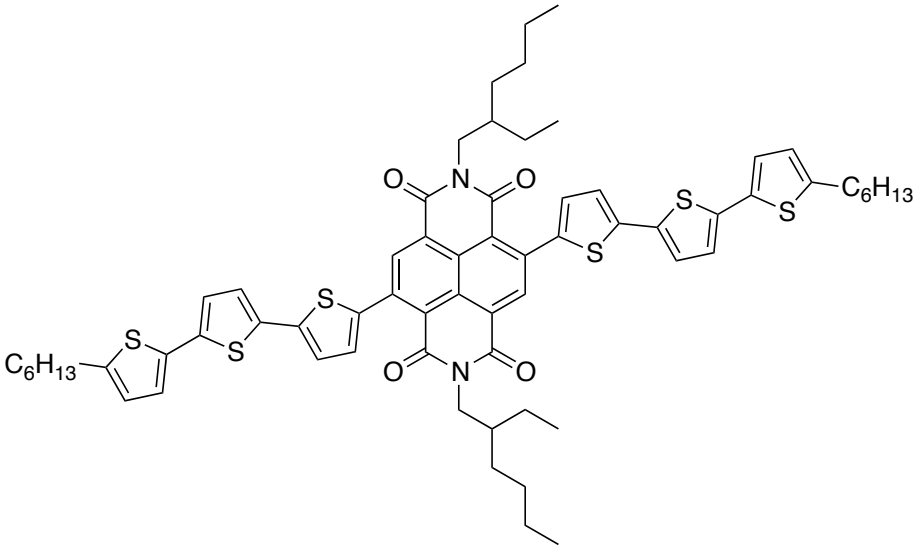

Figure 29. Structure of NDI-3TH

Other small molecules have seen success as electron acceptors. In particular the DPP class of compounds have seen not only a wide use in organic photovoltaics but also other areas of organic electronics as well as in areas such as pigments and sensors.[57]

Table 2. Acceptor performance

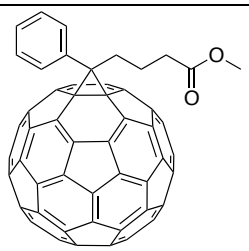	PCE: 4.4% V_{oc}: 0.61 V Li *et al.* [19b]

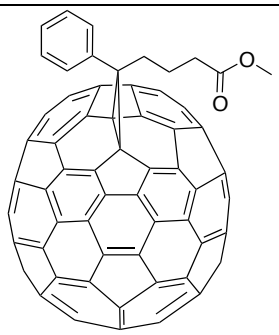	PCE: 4.7% V_{oc}: 0.66 V Shin *et al.* [54]
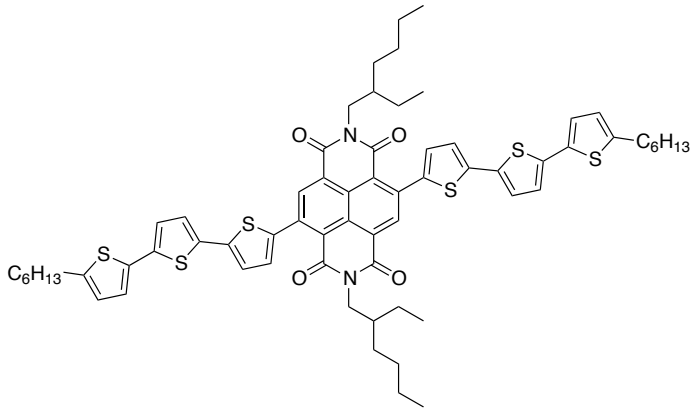	PCE: 1.5% V_{oc}: 0.82 V Ahmed *et al.* [56]

1.7 Diketopyrrolopyrrole (DPP)

Diketopyrrolopyrrole (DPP) is a widely used compound that was first discovered serendipitously in 1974 by Fumar *et al.* when they were investigating the possibility of synthesisng azetiones using similar conditions to that of the modified Reformatskii reaction that is used to derive beta-lactams and 2-azetidinones (Figure 30).[58]

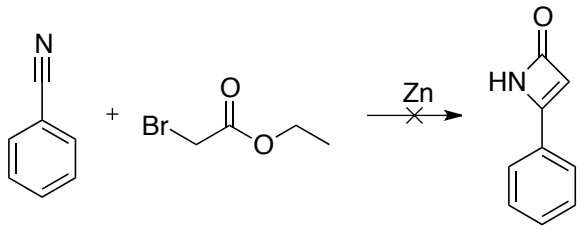

Figure 30. Attempted synthesis of azetiones

The scheme that they then designed called for refluxing ethylbromoacetate and benzylcyanide in toluene for several hours in the presence of a zinc catalyst. Fumar noted that the colour of the reaction went from "yellow, to green, to brown, to red". The reaction only gave a small yield of diphenyl-DPP (Figure 31) and no further optimization of the reaction was thoroughly conducted; in fact Fumar only published his results as he found them to be "of sufficient interest to warrant presentation".

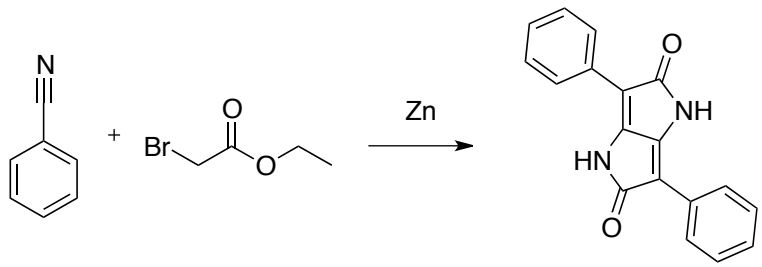

Figure 31. Synthesis of DPP

In 1983 Iqbal *et al.* filed a patent for the synthesis of DPP derivatives in high yields by condensing aryl-cyanides in the presence of alkali metals in inert organic solvents[57d]. Later, in 1997 they published their results as well as

discussing the practical aspects for DPP and its derivatives use as organic pigments. Consequently DPP's have seen extensive use in industry as pigments in plastics and paints, due to their inherent thermal and light stability. Two common pigments are Fast red 254 and Fast red 255 (Figure 32) both only vary slightly in structure.

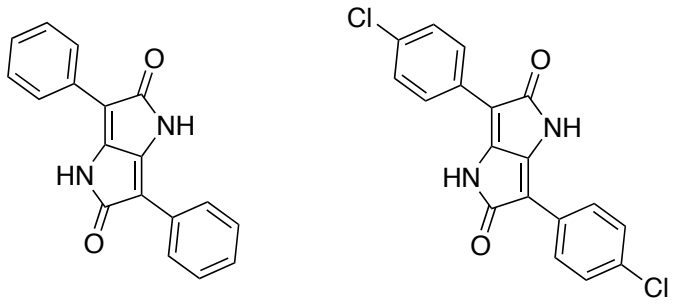

Figure 32. Fast red 254 (left) and Fast red 255 (right)

In recent times the synthesis of DPP has been explored more fully and derivatives can now be easily synthesized in good yields from arylcyanides and alkyl succinic esters in the presence of $FeCl_3$ in a caustic alcohol solution [57e]. It is this ease with which they can be made and derived that has seen them used extensively in many applications. Their vibrant colour makes them perfect for naked eye detection sensors and their broad absorption pattern also makes them perfect for use in inexpensive UV-Vis detection and sensing. There are reports in the literature that describe selective recognition for anions such as F^- and CN^- [57c, 59] and metallic cations like Hg^{2+}, Cu^{2+} and Zn^{2+}. [60]

Due to its optical properties, stability and versatility DPP has also found much use in the area of OPVs as well as other areas of organic electronics [13g, 57a, 58, 61]. In 1993 Chan *et al.* first described the photo-reactivity and photo-conductivity of a DPP-based polymer (Figure 33) and found that a small current was observed when the polymer was irradiated by a laser.[62] The UV-Vis spectra of the polymer showed the presence of monomer bands, however they were red shifted which is indicative of lowering the band-gap between HOMO and LUMO energy levels. This broad absorption profile and their high charge mobility makes them excellent candidates for use in OPV studies.[57b, 57e, 63]

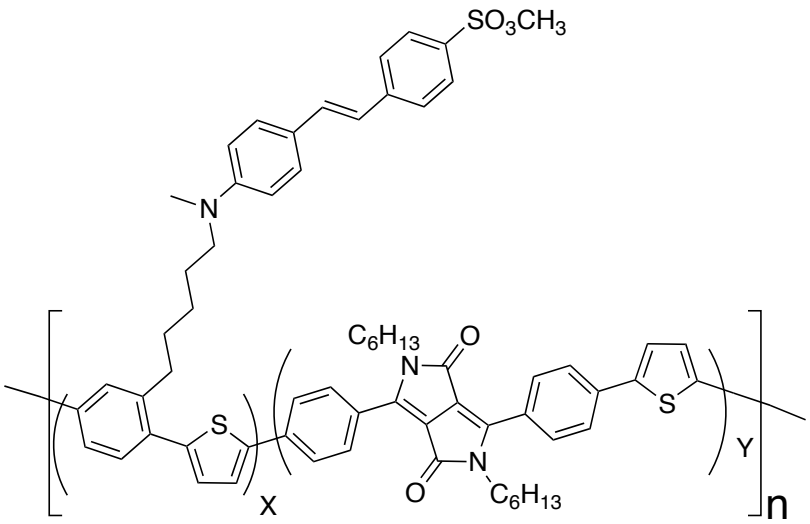

Figure 33. First DPP polymer synthesised for organoelectronic studies

Most commonly used as a monomer unit in long chain polymers DPP devices have seen power conversion efficiencies as high as 8% when the material is used as an electron donor.[64] These compounds are usually synthesised by a coupling reaction (Suzuki, Stille, Negishi etc.) in which the DPP will be di-functionalised to have two terminal coupling sites such as tri-butyl tin, boronic acids or halide. These compounds can then be polymerized with a corresponding compound that has a matching terminal coupling site.

One such compound, PDPPTPT (Figure 34) has seen use in this manner and has also been coupled with various pi spacers. Derivatives show very good solubility which is a key requirement for optimal device performance[13f] As well they have a

respectable PCE of 4.5% when PCBM-61 was used as an acceptor and 5.5% when coupled with PCBM-70 as the acceptor. This illustrates not only the importance of compound design but also the importance in the design of the device and the acceptor used.[65]

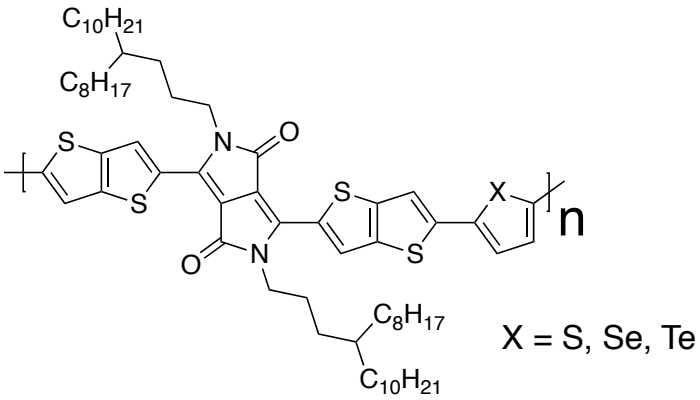

Figure 34. Structure of PDPPTPT

Although many improvements in the area of DPP polymers and their applications in OPV have been made, as well as other areas of organic electronics, there has also been work into its use as a component in small molecules either as a central or terminal acceptor moiety.[13g, 61c, 66] The advantage of using such compounds is the ease with which they can be synthesized as well as purified, which avoids many of the hurdles and inconsistencies that can arise from using polymeric compounds.[13e] When using DPP as an electron donor (p-type) component within small molecules for use in solution processable BHJ devices PCEs in excess of 5% are often observed and in some cases PCEs as high as 15% are observed. [13g, 61c, 66].

Table 3. High performing DPP electron donor polymers

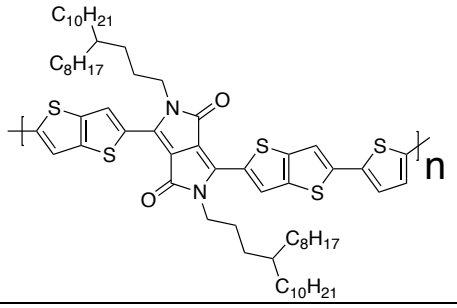	PCBM-61 PCE: 6.5% V_{oc}: 0.61 V PCBM-71 PCE: 8.5% V_{oc}: 0.59 V Ashraf *et al.* [65]
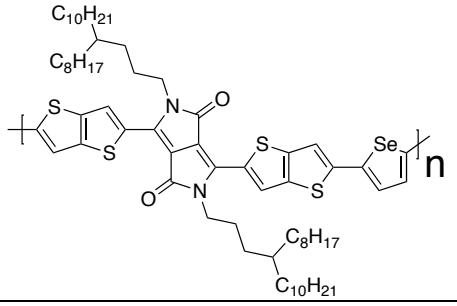	PCBM-61 PCE: 5.8% V_{oc}: 0.57 V PCBM-71 PCE: 7.0% V_{oc}: 0.61 V Ashraf *et al.* [65]
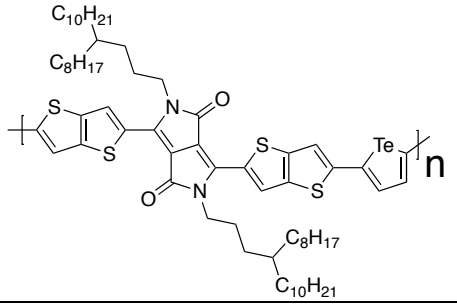	PCBM-61 PCE: 4.6% V_{oc}: 0.57V PCBM-71 PCE: 7.1% V_{oc}: 0.52 V Ashraf *et al.* [65]
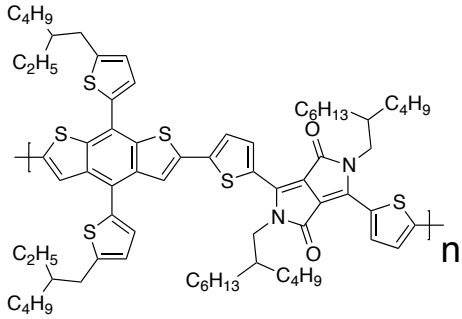	PCBM-61 PCE: 6.5% V_{oc}: 0.73 V Dou *et al.* [64]
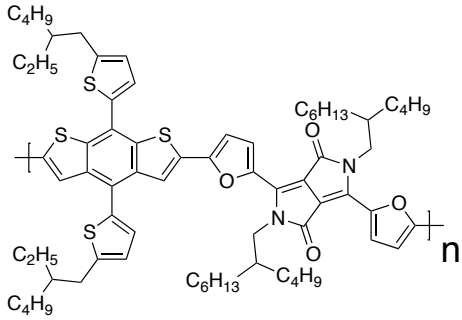	PCBM-61 PCE; 5.5% V_{oc}; 0.77 V Dou *et al.* [64]

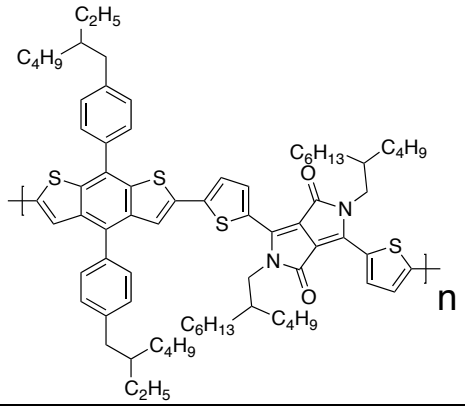	PCBM-61 PCE: 6.0% V_{oc}: 0.76 V Dou *et al.* [64]
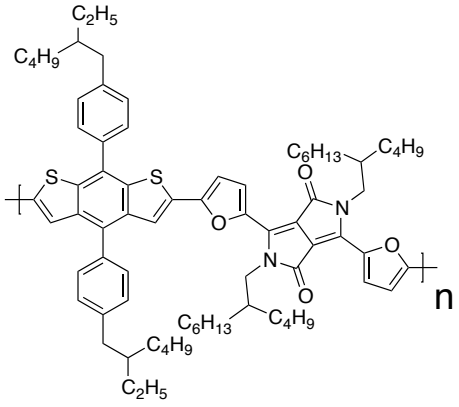	PCBM-61 PCE: 3.0% V_{oc}: 0.77 V Dou *et al.* [64]

1.8 DPP Containing Small Molecule Electron Acceptors

The versatility of DPPs have also led to its use within small molecules used as electron acceptors. Dubbed "non-fullerene" acceptors, these compounds traditionally have lower PCE and V_{oc} when paired with P3HT. However they do offer an cheaper and more chemically diverse alternative to fullerene containing electron acceptors. Recent work has seen a steady increase in V_{oc} to a comparable, and in some instances higher, level to P3HT:PBM61. Work on increasing efficiency has also seen a steady increase from levels below 1% to levels above 2% in only a few years.

A simple use of DPP within small molecules was explored by Karsten *et al.*. They investigated two simple DPP analogues as potential electron acceptors. Their use in a system based on a thenaldehyde derivative bearing either one (DPP-T1) or two (DPP-T2) thiophene moieties (Figure 35).[57a]

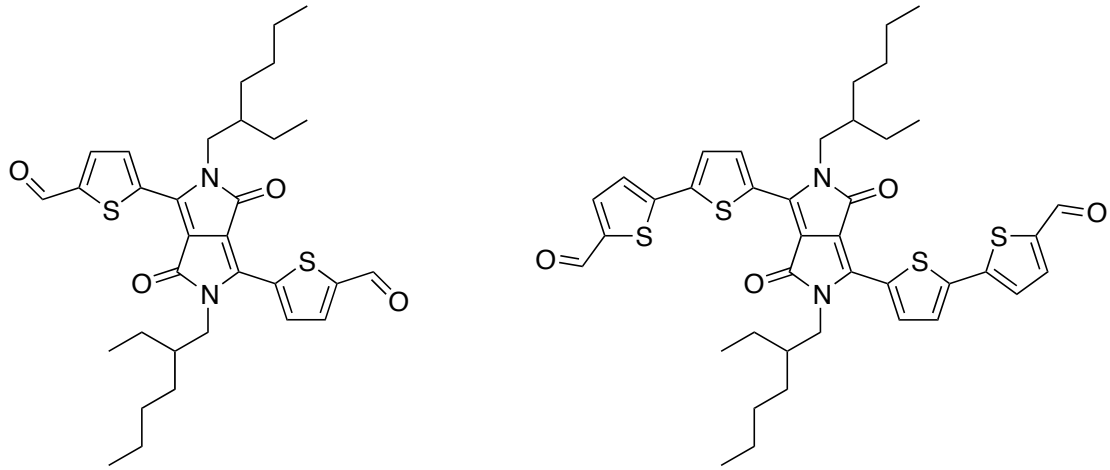

Figure 35. Structures of DPP-T1 (left) and DPP-T2 (right)

Both compounds showed the desired optical properties and also had sufficiently placed HOMO/LUMO orbitals to be used in conjunction with P3HT. The devices fabricated from these compounds showed that DPP-TA1 had a maximum efficiency of 0.31% and a V_{oc} of 0.52V and DPP-T2 showed a PCE of 0.24% and a V_{oc} of 0.85V. These results clearly illustrate the potential use of DPP within a BHJ

as a non-fullerene acceptor. As well, these DPP aldehyde compounds are also interesting starting materials for use in other DPP chemistry.

Work from Sonar *et al.*. has also seen DPP used within a BHJ device as a non-fullerene electron acceptor. Using DPP as a central moiety end capped with poly fluorinated aromatics has given comparable V_{oc} to that of a P3HT:PCBM-61 cell with an efficiency of 1%, namely TFPDPP (Figure 36).[67]

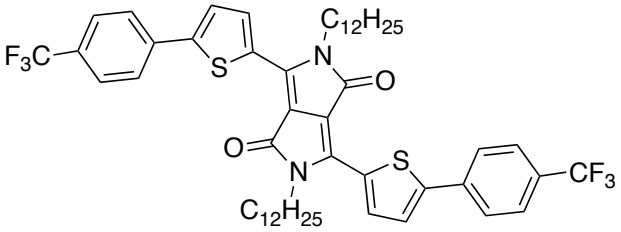

Figure 36. Structure of TFPDPP

Other compounds synthesised in their study also showed some level of conversion, typically in the 0.5% mark with moderate V_{oc} values around the 0.25 – 0.6 V range.

DPP has also seen use as a terminal moiety - so called bis-DPP compounds. Typically they show high V_{oc} and moderate PCE values. They also show suitable optical and electronic properties with suitably positioned HOMO/LUMO orbitals. Work by Patil *et al.* on such compounds yielded a simple bis-DPP (DPP-1) molecule (Figure 37) with a high V_{oc} of 1.1 V and moderate PCE of 1.2%.[68] The amount of solubilizing alkyl chains allowed for simple and efficient solution processing and interestingly the processing methods also showed to have an affect on the performance of the device.

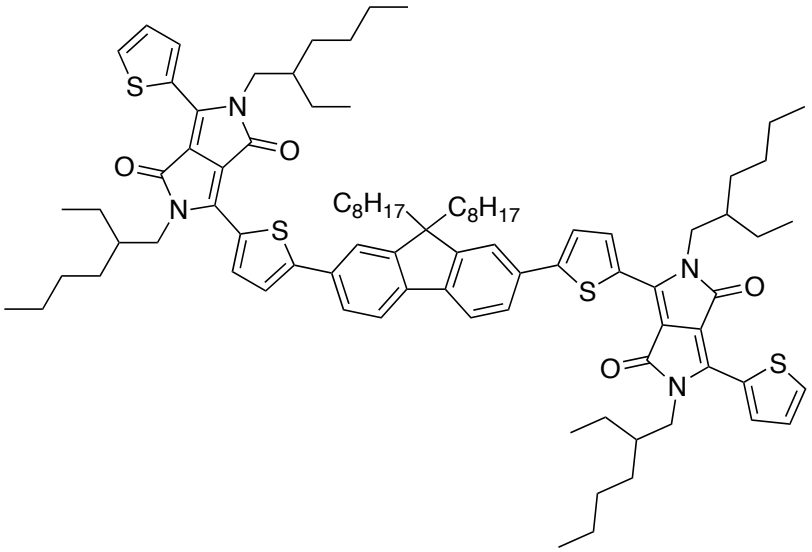

Figure 37. Structure of DPP-1

More recently, Lin *et al.* developed a bis-DPP compound with a dibenzosilole central moiety (DBS-2DPP) (Figure 38), a similar molecule to that of Patil *et al..* [68] As with other bis-DPP molecules both the optical and electronic properties of the compound were suitable for use with P3HT. The compound also showed excellent physical and processing properties, mainly in part to the large number of alkyl-solubilising groups. DBS-2DPP showed an impressive PCE of 2%, almost on par with that of PCBMPCBM-61, and a decent V_{oc} of 0.97 V.

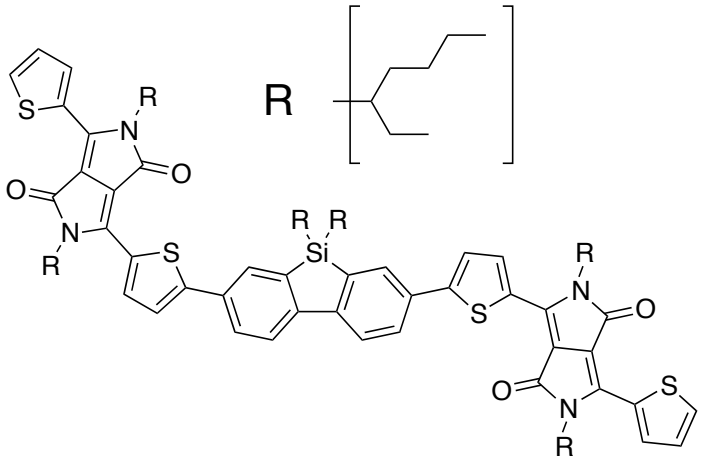

Figure 38. Structure of DBS-2DPP

One DPP compound in particular is of interest given its structure. It is in part similar to the bis-DPP molecules but uses a triphenyl amine (TPA) as its central core and has three terminal DPP units, namely S(TPA-DPP). Synthesised and evaluated as a non fullerene acceptor by Lin *et al.* the compound showed decent PCE of 1.2%, but had a very impressive V_{oc} of almost 1.2V.[69]

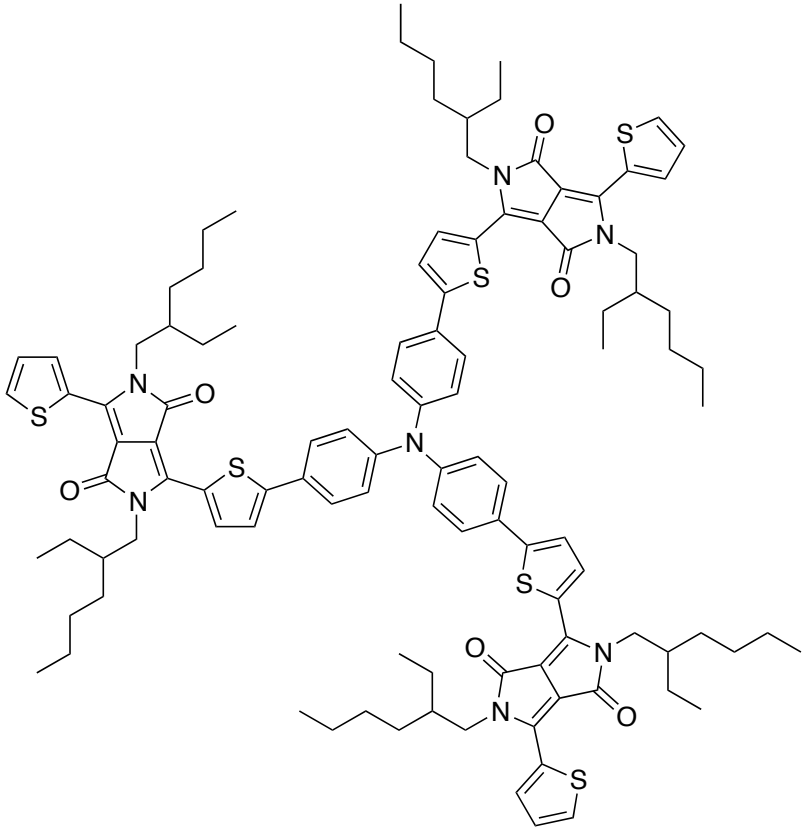

Figure 39. Structure of S(TPA-DPP)

Table 4. High performing small molecule DPP compounds

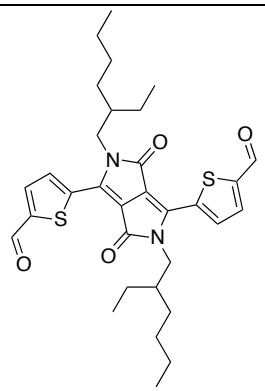	PCE: 0.31% V_{oc}: 0.52 V Karsten *et al.* [57a]

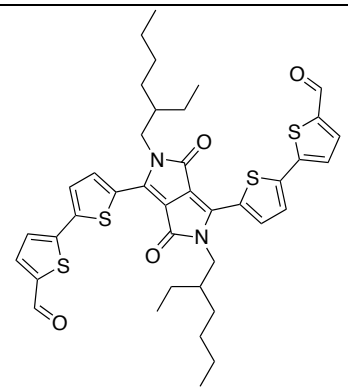	PCE: 0.24% V_{oc}: 0.85 V Karsten *et al.* [57a]
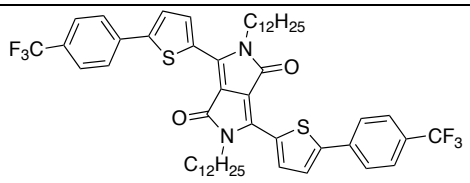	PCE: 1% V_{oc}: 0.25 – 0.6 V Sonar *et al.* [67]
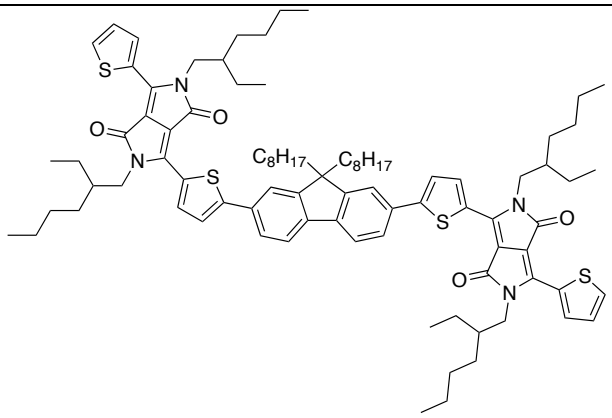	PCE: 1.2% V_{oc}: 1.1 V Patil *et al.* [61a]
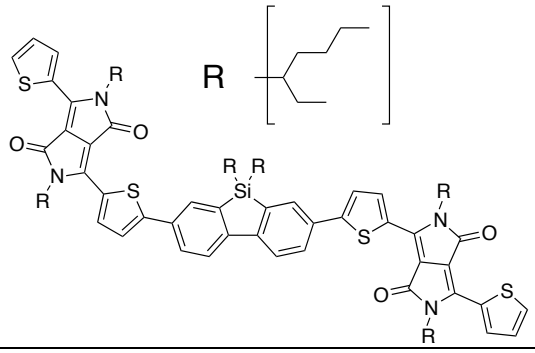	PCE: 2.0% V_{oc}: 0.97 V Lin *et al.* [68]

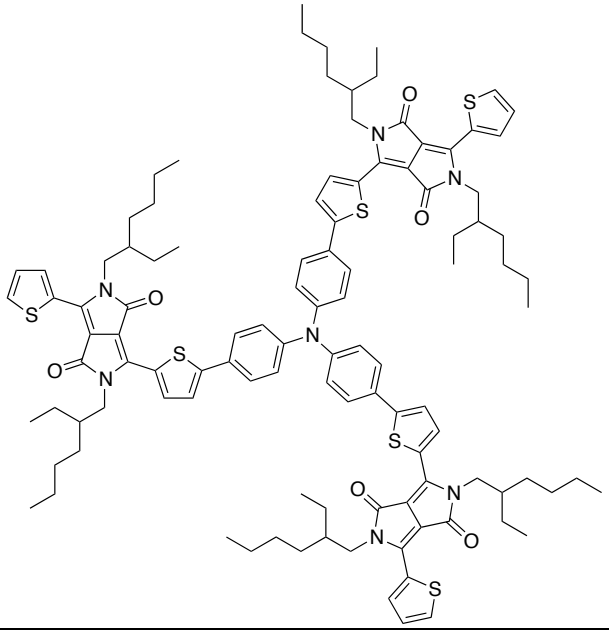	PCE: 1.2% V_{oc}: 1.2 V Lin *et al.* [69]

1.9 Literature limitations and Project Aims.

Small molecules are only now starting to push the boundaries to where they can see actual use in real world applications.[19d, 70] In general, heavily aromatized and conjugated small molecules suffer from poor solubility leading to either poor formation of heterogeneous mixtures as well as the formation of aggregates.[25a, 71] They may also have poor absorption profiles, especially in the visible region, which inevitably leads to poor device performance.[39b, 72] Multistep synthesis and isolation of products can also be an issue, particularly when synthesizing compounds with poor solubility. The purification and isolation of compounds commonly used such as fullerene derivatives and heavily regio-regular polymers are also big factors in contributing to the high cost. This cost can have implications on the viability and usability of newer technology stemming from organic electronics.[12, 16c]

The overall aims of the project were to synthesise compounds, both acceptors and donors, with high efficiencies and high V_{oc}. The compounds themselves must also be soluble in common laboratory solvents (i.e. chloroform, toluene, dichloromethane etc.) if they are to be easily purified and processed. It is also the aim of this project to determine the effects of different separator units and pi spacers have on a compounds performance within a bulk heterojunction cell. It would also be desirable for the compounds to be simple in construction relying on simple well-understood reactions as well as using relatively cheap starting materials.

1.9.1 Overcoming the Issues Described in the Literature

In order to overcome the issues proposed in the literature simple molecules must be synthesised that have strong absorption profiles in the visible and near-IR regions, have good solubility and possess appropriate HOMO/LUMO levels. The project's aim was to address these points by the synthesis of novel mono-

and bis-DPP homologues through simple means such as Knovelnagel and Suzuki couplings. Novel TPA homologues, will also be prepared, for use as electron donors within the small molecules.

Both DPP and TPA have shown use, even together, within organic photovoltaics. The aim here was to use the already well-known properties of these small molecules to produce simple compounds with novel structures and their application in solution processable bulk hetero junction cells. An overview of which is outlined for each homologue below

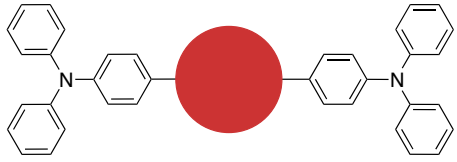 DONOR ACCEPTOR DONOR	AS1 and AS2, TPA D-A-D Small molecule electron donor
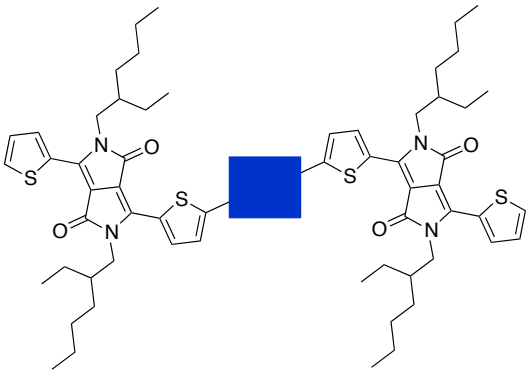 ACCEPTOR DONOR ACCEPTOR	N7 and N8, bis-DPP small molecule A-D-A electron acceptors.
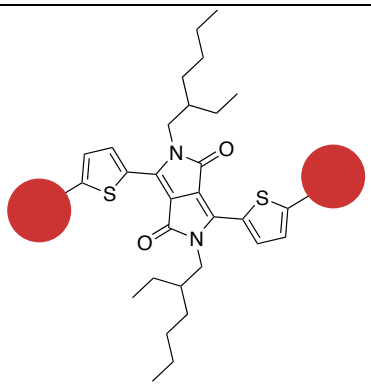 ACEEPTOR ACCEPTOR ACCEPTOR	A1 – A4, mono-DPP A-A-A small molecules electron acceptors.

Table 5. Generic structures of compounds synthesised in this project

1.10 Outline of Chapters 2 – 5

1.10.1 Outline of "Significant Improvement of Optoelectronic and Photovoltaic Properties by Incorporating Thiophene in a Solution-Processable D–A–D Modular Chromophore"

The compounds AS1 ((2*Z*,2'*Z*)-2,2'-(1,4-phenylene)bis(3-(4-(diphenyl-amino)phenyl)acrylonitrile) and AS2 ((2*Z*,2'*Z*)-2,2'-(1,4-phenylene)bis(3-(5-(4-(diphenylamino)phenyl)thiophen-2-yl)acrylonitrile) (Figure 40), were synthesised using condensation reactions between 1,4-phenylacetonitrile and the appropriate aldehyde. The compounds differ only in the added thiophene π-spacer that exists in AS2. They were obtained in moderate yields and the purification of AS2 can be achieved by simple recrystallisation. AS1 was isolated as an off-white amorphous powder whereas AS2 was isolated as brick red needle-like crystals. The optical properties AS2 shows a far superior light harvesting ability than AS1 in both the film and solution form. AS2 also showed a decrease in bandgap with a corresponding red shift of the UV-Vis spectrum. When paired with PCBM-61 AS1 gave a PCE of 1.23% whereas AS2 saw a greater than three times increase of PCE to 4.1%, greater than that of a similar device from P3HT fabricated in similar fashion.

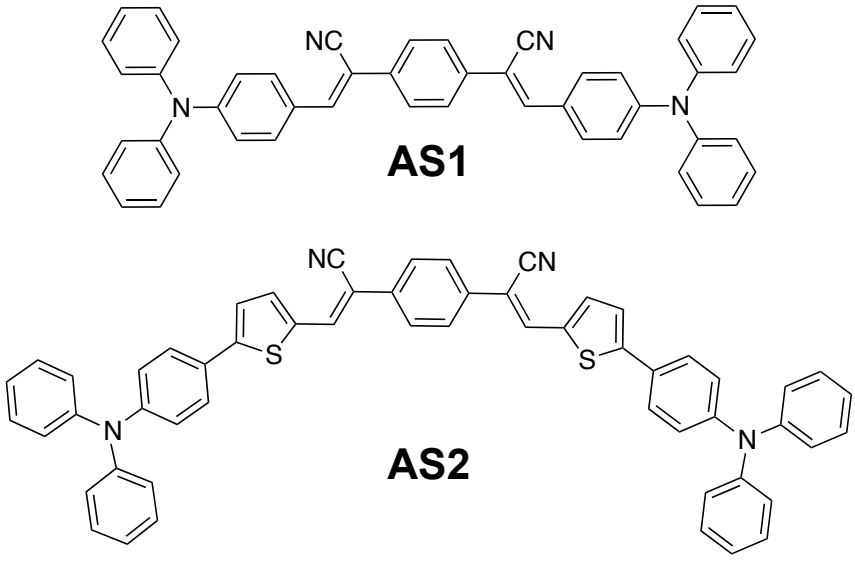

Figure 40. Structures of AS1 (top) and AS2 (bottom)

1.10.2 Outline of "A diketopyrrolopyrrole and benzothiadiazole based small molecule electron acceptor: design, synthesis, characterization and photovoltaic properties"

Compound N6 (6,6'-(5,5'-(benzo[*c*][1,2,5]thiadiazole-4,7-diyl)bis(thiophene-5,2-diyl))bis(2,5-bis(2-ethylhexyl)-3-(thiophen-2-yl)pyrrolo[3,4-*c*]pyrrole-1,4(2*H*,5*H*)-dione) (Figure 41), a simple solution-processable small molecule electron acceptor was designed and synthesized. Based on the bis-DPP model using benzothiadiazole as a central moiety, the compound displayed excellent solubility and strong absorption in the visible range in both solution and film form. When paired with P3HT as a donor in a BHJ device, a PCE of 1.16% with an impressively high V_{oc} of 1.1 V, amongst the best performing DPP non-fullerene electron acceptors at the time of publication.

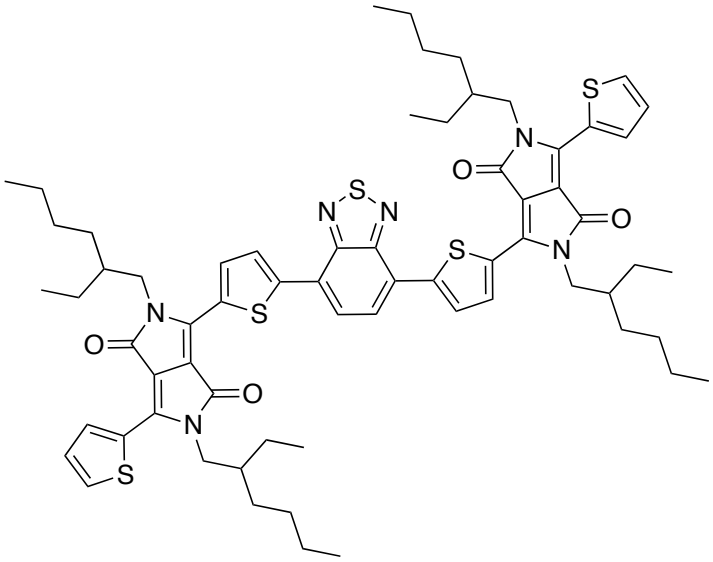

Figure 41. Structure of N6

1.10.3. Outline of "A non-fullerene electron acceptor based on central carbazole and terminal diketopyrrolopyrrole functionalities for efficient, reproducible and solution-processable bulk-heterojunction devices"

Another bis-DPP molecule, N7 (6,6'-(5,5'-(9-(heptadecan-9-yl)-9*H*-carbazole-2,7-diyl)bis(thiophene-5,2-diyl))bis(2,5-bis(2-ethylhexyl)-3-(thiophen-2-yl)pyrrolo[3,4-*c*]pyrrole-1,4(2*H*,5*H*)-dione) (Figure 42), is a non-fullerene acceptor composed of a central carbazole moiety with terminal DPP units. The compound shows excellent solubility and was purified simply by preparative thin layer chromatography. The compound showed strong absorption in the visible range and excellent solubility in common organic solvents due to the alkylation of the carbazole unit. When paired with P3HT the compound showed high efficiency giving a PCE of 2.3% with an V_{oc} of ~1.2 V, among the highest for the simple device architecture.

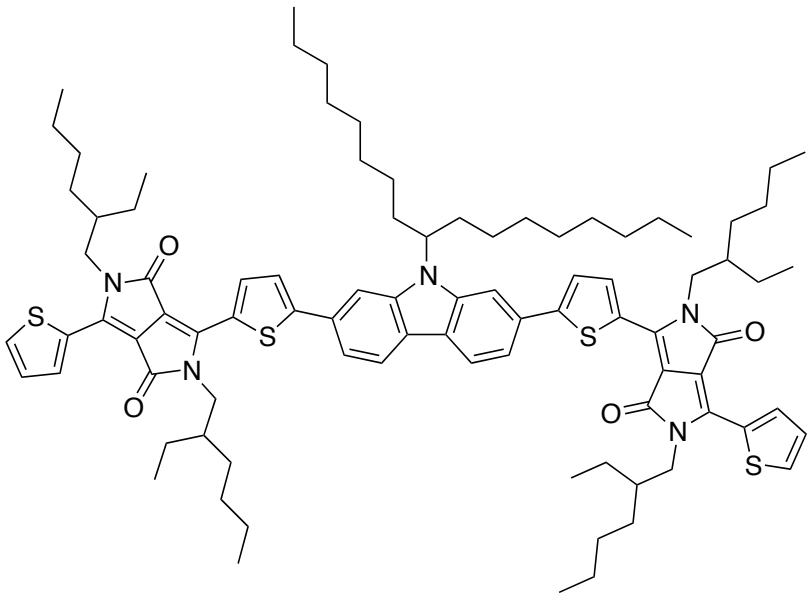

Figure 42. Structure of N7

1.10.4 Outline of A-class compounds

The A-class compounds (Figure 43) were designed with simplicity in mind. For this DPP was chosen as a central moiety to which a number of known electron acceptor units were bound *via* condensation reaction from the corresponding DPP bis-aldehyde. The compounds showed good absorption in the UV region and, given the compounds structure and previous success from other groups with mono DPP analogues,[67] had potential for use as electron acceptors in a BHJ device. Unfortunately their inherent insolubility in common, and even exotic, solvents meant that purification was difficult, leading to a mixture of the mono- and di-condensed compounds that were nearly impossible to separate. Consequently poor OPV performances in a BHJ were observed for two of the compounds (A3 and A4) and the later two were retired as a result of this outcome.

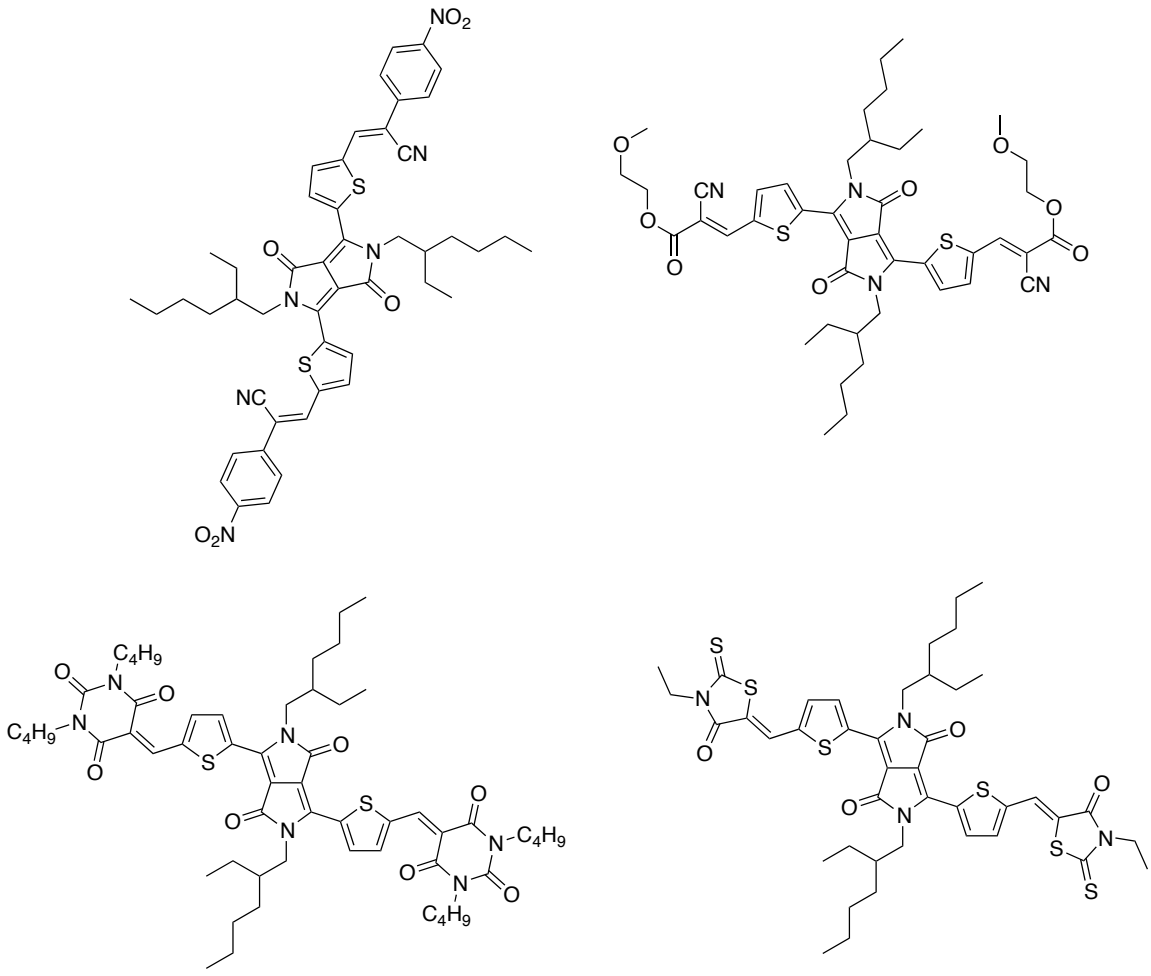

Figure 43. Strucutres of A1 (top-left), A2 (top right), A3 (bottom left) and A4 (bottom right)

References

1. Fraas, L. M.; Partain, L. D., Solar Cells and Their Applications. 2 ed.; Wiley: Hoboken, 2010.
2. Smith, W., Effect of Light on Selenium During the Passage of An Electric Current*. *Nature* **1873,** *7* (173), 303-303.
3. Adams, W. G.; Day, R. E., The Action of Light on Selenium. *Philosophical Transactions of the Royal Society of London* **1877,** *167* (0), 313-349.
4. Fritts, C. E., On a new form of selenium cell, and some electrical discoveries made by its use. *American Journal of Science* **1883,** *s3-26* (156), 465-472.
5. Shockley, W., The Theory ofp-nJunctions in Semiconductors andp-nJunction Transistors. *Bell System Technical Journal* **1949,** *28* (3), 435-489.
6. Kitai, A., Principles of Solar Cells, LEDs and Diodes The role of the PN junction Introduction. *Principles of Solar Cells, Leds and Diodes: The Role of the Pn Junction* **2011**, Xi-Xiii.
7. Rauschenbach, H. S., **1980**.
8. (a) Dimroth, F.; Grave, M.; Beutel, P.; Fiedeler, U.; Karcher, C.; Tibbits, T. N. D.; Oliva, E.; Siefer, G.; Schachtner, M.; Wekkeli, A.; Bett, A. W.; Krause, R.; Piccin, M.; Blanc, N.; Drazek, C.; Guiot, E.; Ghyselen, B.; Salvetat, T.; Tauzin, A.; Signamarcheix, T.; Dobrich, A.; Hannappel, T.; Schwarzburg, K., Wafer bonded four-junction GaInP/GaAs//GaInAsP/GaInAs concentrator solar cells with 44.7% efficiency. *Progress in Photovoltaics: Research and Applications* **2014,** *22* (3), 277-282; (b) Green, M. A.; Emery, K.; Hishikawa, Y.; Warta, W.; Dunlop, E. D., Solar cell efficiency tables (Version 45). *Progress in Photovoltaics: Research and Applications* **2015,** *23* (1), 1-9.
9. (a) Elliman, R.; Gould, C.; Al-Tai, M., Review of current and future electrical energy storage devices. In *Power Engineering Conference (UPEC)*, IEEE: 2015; pp 1-5; (b) Ismail, A. M.; Ramirez-Iniguez, R.; Asif, M.; Munir, A. B.; Muhammad-Sukki, F., Progress of solar photovoltaic in ASEAN countries: A review. *Renewable and Sustainable Energy Reviews* **2015,** *48*, 399-412.
10. Hosenuzzaman, M.; Rahim, N. A.; Selvaraj, J.; Hasanuzzaman, M.; Malek, A. B. M. A.; Nahar, A., Global prospects, progress, policies, and environmental impact of solar photovoltaic power generation. *Renewable and Sustainable Energy Reviews* **2015,** *41*, 284-297.
11. (a) Louwen, A.; van Sark, W.; Schropp, R.; Faaij, A., A cost roadmap for silicon heterojunction solar cells. *Sol. Energy Mater. Sol. Cells* **2016,** *147*, 295-314; (b) Chen, W.; Hong, J.; Yuan, X.; Liu, J., Environmental impact assessment of monocrystalline silicon solar photovoltaic cell production: a case study in China. *Journal of Cleaner Production* **2016,** *112*, 1025-1032.
12. Ito, M.; Lespinats, S.; Merten, J.; Malbranche, P.; Kurokawa, K., Life cycle assessment and cost analysis of very large-scale PV systems and suitable locations in the world. *Progress in Photovoltaics: Research and Applications* **2016,** *24* (2), 159-174.
13. (a) Abrusci, A.; Stranks, S. D.; Docampo, P.; Yip, H.-L.; Jen, A. K. Y.; Snaith, H. J., High-Performance Perovskite-Polymer Hybrid Solar Cells via Electronic

Coupling with Fullerene Monolayers. *Nano Lett.* **2013,** *13* (7), 3124-3128; (b) Chen, C.-C.; Bae, S.-H.; Chang, W.-H.; Hong, Z.; Li, G.; Chen, Q.; Zhou, H.; Yang, Y., Perovskite/polymer monolithic hybrid tandem solar cells utilizing a low-temperature, full solution process. *Mater. Horiz.* **2015,** *2* (2), 203-211; (c) Kojima, A.; Teshima, K.; Shirai, Y.; Miyasaka, T., Organometal Halide Perovskites as Visible-Light Sensitizers for Photovoltaic Cells. *J. Am. Chem. Soc.* **2009,** *131* (17), 6050-6051; (d) Jung, B. J.; Sun, J.; Lee, T.; Sarjeant, A.; Katz, H. E., Low-Temperature-Processible, Transparent, and Air-Operable n-Channel Fluorinated Phenylethylated Naphthalenetetracarboxylic Diimide Semiconductors Applied to Flexible Transistors. *Chem. Mater.* **2009,** *21* (1), 94-101; (e) Bobe, S. R.; Gupta, A.; Rananaware, A.; Bilic, A.; Bhosale, S. V.; Bhosale, S. V., Improvement of optoelectronic and photovoltaic properties through the insertion of a naphthalenediimide unit in donor–acceptor oligothiophenes. *RSC Adv.* **2015,** *5* (6), 4411-4415; (f) Lee, J. S.; Son, S. K.; Song, S.; Kim, H.; Lee, D. R.; Kim, K.; Ko, M. J.; Choi, D. H.; Kim, B.; Cho, J. H., Importance of Solubilizing Group and Backbone Planarity in Low Band Gap Polymers for High Performance Ambipolar field-effect Transistors. *Chem. Mater.* **2012,** *24* (7), 1316-1323; (g) Huang, J.; Jia, H.; Li, L.; Lu, Z.; Zhang, W.; He, W.; Jiang, B.; Tang, A.; Tan, Z. a.; Zhan, C.; Li, Y.; Yao, J., Fine-tuning device performances of small molecule solar cells via the more polarized DPP-attached donor units. *PCCP* **2012,** *14* (41), 14238.

14. (a) Espinosa, N.; García-Valverde, R.; Urbina, A.; Krebs, F. C., A life cycle analysis of polymer solar cell modules prepared using roll-to-roll methods under ambient conditions. *Sol. Energy Mater. Sol. Cells* **2011,** *95* (5), 1293-1302; (b) Espinosa, N.; Hösel, M.; Angmo, D.; Krebs, F. C., Solar cells with one-day energy payback for the factories of the future. *Energy Environ. Sci.* **2012,** *5* (1), 5117-5132.

15. Shrotriya, V.; Li, G.; Yao, Y.; Moriarty, T.; Emery, K.; Yang, Y., Accurate Measurement and Characterization of Organic Solar Cells. *Adv. Funct. Mater.* **2006,** *16* (15), 2016-2023.

16. (a) McCulloch, I., Organic Electronics. *Adv. Mater.* **2013,** *25* (13), 1811-1812; (b) Kelley, T. W.; Baude, P. F.; Gerlach, C.; Ender, D. E.; Muyres, D.; Haase, M. A.; Vogel, D. E.; Theiss, S. D., Recent Progress in Organic Electronics: Materials, Devices, and Processes. *Chem. Mater.* **2004,** *16* (23), 4413-4422; (c) Forrest, S. R., The path to ubiquitous and low-cost organic electronic appliances on plastic. *Nature* **2004,** *428* (6986), 911-918.

17. (a) Sekitani, T.; Nakajima, H.; Maeda, H.; Fukushima, T.; Aida, T.; Hata, K.; Someya, T., Stretchable active-matrix organic light-emitting diode display using printable elastic conductors. *Nature Materials* **2009,** *8* (6), 494-499; (b) Liao, L. S.; Slusarek, W. K.; Hatwar, T. K.; Ricks, M. L.; Comfort, D. L., Tandem Organic Light-Emitting Diode using Hexaazatriphenylene Hexacarbonitrile in the Intermediate Connector. *Adv. Mater.* **2008,** *20* (2), 324-329; (c) Tang, C. W.; VanSlyke, S. A., Organic electroluminescent diodes. *Appl. Phys. Lett.* **1987,** *51* (12), 913.

18. (a) Zhou, W.; Wen, Y.; Ma, L.; Liu, Y.; Zhan, X., Conjugated Polymers of Rylene Diimide and Phenothiazine for n-Channel Organic Field-Effect Transistors. *Macromolecules* **2012,** *45* (10), 4115-4121; (b) Ortiz, R. o. P.; Herrera, H.; Blanco, R. l.; Huang, H.; Facchetti, A.; Marks, T. J.; Zheng, Y.; Segura, J. L., Organic n-Channel Field-Effect Transistors Based on Arylenediimide-Thiophene Derivatives. *J. Am. Chem. Soc.* **2010,** *132* (24), 8440-8452; (c)

Koezuka, H.; Tsumura, A.; Ando, T., Field-effect transistor with polythiophene thin film. *Synth. Met.* **1987,** *18* (1-3), 699-704.
19. (a) Yu, G.; Gao, J.; Hummelen, J. C.; Wudl, F.; Heeger, A. J., Polymer Photovoltaic Cells: Enhanced Efficiencies via a Network of Internal Donor-Acceptor Heterojunctions. *Science* **1995,** *270* (5243), 1789-1791; (b) Li, G.; Zhu, R.; Yang, Y., Polymer solar cells. *Nature Photonics* **2012,** *6* (3), 153-161; (c) Li, Z.; Dong, Q.; Li, Y.; Xu, B.; Deng, M.; Pei, J.; Zhang, J.; Chen, F.; Wen, S.; Gao, Y.; Tian, W., Design and synthesis of solution processable small molecules towards high photovoltaic performance. *J. Mater. Chem.* **2011,** *21* (7), 2159-2168; (d) Lin, Y.; Li, Y.; Zhan, X., Small molecule semiconductors for high-efficiency organic photovoltaics. *Chem. Soc. Rev.* **2012,** *41* (11), 4245; (e) Kearns, D.; Calvin, M., Photovoltaic Effect and Photoconductivity in Laminated Organic Systems. *The Journal of Chemical Physics* **1958,** *29* (4), 950; (f) Tang, C. W., Two-layer organic photovoltaic cell. *Appl. Phys. Lett.* **1986,** *48* (2), 183.
20. Bolto, B. A.; McNeill, R.; Weiss, D. E., Electronic Conduction in Polymers. III. Electronic Properties of Polypyrrole. *Aust. J. Chem.* **1963,** *16* (6), 1090.
21. Shirakawa, H.; Louis, E. J.; MacDiarmid, A. G.; Chiang, C. K.; Heeger, A. J., Synthesis of electrically conducting organic polymers: halogen derivatives of polyacetylene, (CH) x. *J. Chem. Soc., Chem. Commun.* **1977,** (16), 578.
22. Inzelt, G., *Conducting polymers: a new era in electrochemistry*. Springer Science & Business Media: 2012.
23. (a) McCullough, R. D., The Chemistry of Conducting Polythiophenes. *Adv. Mater.* **1998,** *10* (2), 93-116; (b) Sato, M.-a.; Tanaka, S.; Kaeriyama, K., Soluble conducting polythiophenes. *J. Chem. Soc., Chem. Commun.* **1986,** (11), 873.
24. Chen, Q.; Mao, L.; Li, Y.; Kong, T.; Wu, N.; Ma, C.; Bai, S.; Jin, Y.; Wu, D.; Lu, W.; Wang, B.; Chen, L., Quantitative operando visualization of the energy band depth profile in solar cells. *Nature Communications* **2015,** *6*, 7745.
25. (a) Roncali, J., Molecular Bulk Heterojunctions: An Emerging Approach to Organic Solar Cells. *Acc. Chem. Res.* **2009,** *42* (11), 1719-1730; (b) Facchetti, A., π-Conjugated Polymers for Organic Electronics and Photovoltaic Cell Applications†. *Chem. Mater.* **2011,** *23* (3), 733-758.
26. (a) Riordan, M.; Hoddeson, L.; Herring, C., The invention of the transistor. *Reviews of Modern Physics* **1999,** *71* (2), S336; (b) Shukla, D.; Nelson, S. F.; Freeman, D. C.; Rajeswaran, M.; Ahearn, W. G.; Meyer, D. M.; Carey, J. T., Thin-Film Morphology Control in Naphthalene-Diimide-Based Semiconductors: High Mobility n-Type Semiconductor for Organic Thin-Film Transistors. *Chem. Mater.* **2008,** *20* (24), 7486-7491; (c) Hwang, D. K.; Dasari, R. R.; Fenoll, M.; Alain-Rizzo, V.; Dindar, A.; Shim, J. W.; Deb, N.; Fuentes-Hernandez, C.; Barlow, S.; Bucknall, D. G.; Audebert, P.; Marder, S. R.; Kippelen, B., Stable Solution-Processed Molecularn-Channel Organic Field-Effect Transistors. *Adv. Mater.* **2012,** *24* (32), 4445-4450.
27. Klauk, H., Organic thin-film transistors. *Chem. Soc. Rev.* **2010,** *39* (7), 2643.
28. Hepp, A.; Heil, H.; Weise, W.; Ahles, M.; Schmechel, R.; von Seggern, H., Light-Emitting Field-Effect Transistor Based on a Tetracene Thin Film. *Phys. Rev. Lett.* **2003,** *91* (15).
29. Park, Y.-S.; Kang, J.-W.; Kang, D. M.; Park, J.-W.; Kim, Y.-H.; Kwon, S.-K.; Kim, J.-J., Efficient, Color Stable White Organic Light-Emitting Diode Based on High Energy Level Yellowish-Green Dopants. *Adv. Mater.* **2008,** *20* (10), 1957-1961.

30. O'Regan, B.; Grätzel, M., A low-cost, high-efficiency solar cell based on dye-sensitized colloidal TiO2 films. *Nature* **1991,** *353* (6346), 737-740.
31. (a) Choy, W. C. H., *Organic Solar Cells Materials And Device Physics*. Springer: 2013; (b) Hoppe, H.; Sariciftci, N. S., Organic solar cells: An overview. *J. Mater. Res.* **2011,** *19* (07), 1924-1945.
32. (a) Robertson, N., Optimizing Dyes for Dye-Sensitized Solar Cells. *Angew. Chem. Int. Ed.* **2006,** *45* (15), 2338-2345; (b) Tamayo, A. B.; Dang, X.-D.; Walker, B.; Seo, J.; Kent, T.; Nguyen, T.-Q., A low band gap, solution processable oligothiophene with a dialkylated diketopyrrolopyrrole chromophore for use in bulk heterojunction solar cells. *Appl. Phys. Lett.* **2009,** *94* (10), 103301.
33. Brabec, C. J.; Zerza, G.; Cerullo, G.; De Silvestri, S.; Luzzati, S.; Hummelen, J. C.; Sariciftci, S., Tracing photoinduced electron transfer process in conjugated polymer/fullerene bulk heterojunctions in real time. *Chem. Phys. Lett.* **2001,** *340* (3-4), 232-236.
34. (a) Hou, J.; Guo, X., Active Layer Materials for Organic Solar Cells. **2013**, 17-42; (b) Gupta, A.; Ali, A.; Gao, M.; Singh, T. B.; Bilic, A.; Watkins, S. E.; Bach, U.; Evans, R. A., Small molecules containing rigidified thiophenes and a cyanopyridone acceptor unit for solution-processable bulk-heterojunction solar cells. *Dyes and Pigments* **2015,** *119*, 122-132; (c) Li, Y.; Guo, Q.; Li, Z.; Pei, J.; Tian, W., Solution processable D–A small molecules for bulk-heterojunction solar cells. *Energy & Environmental Science* **2010,** *3* (10), 1427.
35. (a) O'Regan, B.; Lenzmann, F.; Muis, R.; Wienke, J., A Solid-State Dye-Sensitized Solar Cell Fabricated with Pressure-Treated P25−TiO2and CuSCN: Analysis of Pore Filling and IV Characteristics. *Chem. Mater.* **2002,** *14* (12), 5023-5029; (b) Murakoshi, K.; Kogure, R.; Wada, Y.; Yanagida, S., Fabrication of solid-state dye-sensitized TiO2 solar cells combined with polypyrrole. *Sol. Energy Mater. Sol. Cells* **1998,** *55* (1-2), 113-125.
36. Kraabel, B.; Lee, C. H.; McBranch, D.; Moses, D.; Sariciftci, N. S.; Heeger, A. J., Ultrafast photoinduced electron transfer in conducting polymer—buckminsterfullerene composites. *Chem. Phys. Lett.* **1993,** *213* (3-4), 389-394.
37. Scharber, M. C.; Mühlbacher, D.; Koppe, M.; Denk, P.; Waldauf, C.; Heeger, A. J.; Brabec, C. J., Design Rules for Donors in Bulk-Heterojunction Solar Cells—Towards 10 % Energy-Conversion Efficiency. *Adv. Mater.* **2006,** *18* (6), 789-794.
38. Shockley, W.; Queisser, H. J., Detailed Balance Limit of Efficiency of p-n Junction Solar Cells. *J. Appl. Phys.* **1961,** *32* (3), 510.
39. (a) Liu, C.; Wang, K.; Gong, X.; Heeger, A. J., Low bandgap semiconducting polymers for polymeric photovoltaics. *Chem. Soc. Rev.* **2016**; (b) Li, Y., Molecular Design of Photovoltaic Materials for Polymer Solar Cells: Toward Suitable Electronic Energy Levels and Broad Absorption. *Acc. Chem. Res.* **2012,** *45* (5), 723-733.
40. Yamamoto, T., Molecular assembly and properties of polythiophenes. *NPG Asia Materials* **2010,** *2* (2), 54-60.
41. Benten, H.; Mori, D.; Ohkita, H.; Ito, S., Recent research progress of polymer donor/polymer acceptor blend solar cells. *J. Mater. Chem. A* **2016**.
42. Liang, Y.; Xu, Z.; Xia, J.; Tsai, S.-T.; Wu, Y.; Li, G.; Ray, C.; Yu, L., For the Bright Future-Bulk Heterojunction Polymer Solar Cells with Power Conversion Efficiency of 7.4%. *Adv. Mater.* **2010,** *22* (20), E135-E138.
43. Cabanetos, C.; El Labban, A.; Bartelt, J. A.; Douglas, J. D.; Mateker, W. R.; Fréchet, J. M. J.; McGehee, M. D.; Beaujuge, P. M., Linear Side Chains in Benzo[1,2-

b:4,5-b′]dithiophene–Thieno[3,4-c]pyrrole-4,6-dione Polymers Direct Self-Assembly and Solar Cell Performance. *J. Am. Chem. Soc.* **2013,** *135* (12), 4656-4659.
44. (a) Zhang, L.; Pu, M.; Zhou, W.; Hu, X.; Zhang, Y.; Xie, Y.; Liu, B.; Chen, Y., Poly(3-butylthiophene) Inducing Crystallization of Small Molecule Donor for Enhanced Photovoltaic Performance. *The Journal of Physical Chemistry C* **2015,** *119* (41), 23310-23318; (b) Liu, X.; Sun, Y.; Perez, L. A.; Wen, W.; Toney, M. F.; Heeger, A. J.; Bazan, G. C., Narrow-Band-Gap Conjugated Chromophores with Extended Molecular Lengths. *J. Am. Chem. Soc.* **2012,** *134* (51), 20609-20612; (c) Coughlin, J. E.; Henson, Z. B.; Welch, G. C.; Bazan, G. C., Design and Synthesis of Molecular Donors for Solution-Processed High-Efficiency Organic Solar Cells. *Acc. Chem. Res.* **2014,** *47* (1), 257-270.
45. Sun, Y.; Welch, G. C.; Leong, W. L.; Takacs, C. J.; Bazan, G. C.; Heeger, A. J., Solution-processed small-molecule solar cells with 6.7% efficiency. *Nature Materials* **2011,** *11* (1), 44-48.
46. van der Poll, T. S.; Love, J. A.; Nguyen, T.-Q.; Bazan, G. C., Non-Basic High-Performance Molecules for Solution-Processed Organic Solar Cells. *Adv. Mater.* **2012,** *24* (27), 3646-3649.
47. Takacs, C. J.; Sun, Y.; Welch, G. C.; Perez, L. A.; Liu, X.; Wen, W.; Bazan, G. C.; Heeger, A. J., Solar Cell Efficiency, Self-Assembly, and Dipole–Dipole Interactions of Isomorphic Narrow-Band-Gap Molecules. *J. Am. Chem. Soc.* **2012,** *134* (40), 16597-16606.
48. Zhang, Q.; Kan, B.; Liu, F.; Long, G.; Wan, X.; Chen, X.; Zuo, Y.; Ni, W.; Zhang, H.; Li, M.; Hu, Z.; Huang, F.; Cao, Y.; Liang, Z.; Zhang, M.; Russell, T. P.; Chen, Y., Small-molecule solar cells with efficiency over 9%. *Nature Photonics* **2014,** *9* (1), 35-41.
49. Krätschmer, W.; Lamb, L. D.; Fostiropoulos, K.; Huffman, D. R., Solid C60: a new form of carbon. *Nature* **1990,** *347* (6291), 354-358.
50. (a) Langa De La Puente, F.; Nierengarten, J.-F., **2011**; (b) Akasaka, T.; Ando, W.; Kobayashi, K.; Nagase, S., Organic chemical derivatization of fullerenes. 2. Photochemical [2 + 3] cycloaddition of C60 with disiliranes. *J. Am. Chem. Soc.* **1993,** *115* (22), 10366-10367.
51. Nakamura, Y.; Suzuki, M.; Imai, Y.; Nishimura, J., Synthesis of [60]Fullerene Adducts Bearing Carbazole Moieties by Bingel Reaction and Their Properties. *Org. Lett.* **2004,** *6* (16), 2797-2799.
52. Schilinsky, P.; Waldauf, C.; Brabec, C. J., Recombination and loss analysis in polythiophene based bulk heterojunction photodetectors. *Appl. Phys. Lett.* **2002,** *81* (20), 3885.
53. Wienk, M. M.; Kroon, J. M.; Verhees, W. J. H.; Knol, J.; Hummelen, J. C.; van Hal, P. A.; Janssen, R. A. J., Efficient Methano[70]fullerene/MDMO-PPV Bulk Heterojunction Photovoltaic Cells. *Angew. Chem. Int. Ed.* **2003,** *42* (29), 3371-3375.
54. Shin, W. S.; Hwang, Y. M.; So, W.-W.; Yoon, S. C.; Lee, C. J.; Moon, S.-J., Performance of P3HT/C70-PCBM Polymer Photovoltaic Devices According to Manufacturing Conditions. *Molecular Crystals and Liquid Crystals* **2008,** *491* (1), 331-338.
55. Yao, H.; Zhao, W.; Zheng, Z.; Cui, Y.; Zhang, J.; Wei, Z.; Hou, J., PBDT-TSR: a highly efficient conjugated polymer for polymer solar cells with a regioregular structure. *J. Mater. Chem. A* **2016,** *4* (5), 1708-1713.

56. Ahmed, E.; Ren, G.; Kim, F. S.; Hollenbeck, E. C.; Jenekhe, S. A., Design of New Electron Acceptor Materials for Organic Photovoltaics: Synthesis, Electron Transport, Photophysics, and Photovoltaic Properties of Oligothiophene-Functionalized Naphthalene Diimides. *Chem. Mater.* **2011,** *23* (20), 4563-4577.
57. (a) Karsten, B. P.; Bijleveld, J. C.; Janssen, R. A. J., Diketopyrrolopyrroles as Acceptor Materials in Organic Photovoltaics. *Macromol. Rapid Commun.* **2010,** *31* (17), 1554-1559; (b) Li, Y.; Sonar, P.; Singh, S. P.; Soh, M. S.; van Meurs, M.; Tan, J., Annealing-Free High-Mobility Diketopyrrolopyrrole–Quaterthiophene Copolymer for Solution-Processed Organic Thin Film Transistors. *J. Am. Chem. Soc.* **2011,** *133* (7), 2198-2204; (c) Kaur, M.; Cho, M. J.; Choi, D. H., Chemodosimeter approach: Selective detection of fluoride ion using a diketopyrrolopyrrole derivative. *Dyes and Pigments* **2014,** *103*, 154-160; (d) Hao, Z.; Iqbal, A., Some aspects of organic pigments. *Chem. Soc. Rev.* **1997,** *26* (3), 203; (e) Kaur, M.; Choi, D. H., Diketopyrrolopyrrole: brilliant red pigment dye-based fluorescent probes and their applications. *Chem. Soc. Rev.* **2015,** *44* (1), 58-77.
58. Farnum, D. G.; Mehta, G.; Moore, G. G. I.; Siegal, F. P., Attempted Reformatskii Reaction of Benzonitrile, 1,4-Diketo-3,6-Diphenylpyrrolo[3,4-C]Pyrrole - Lactam Analog of Pentalene. *Tetrahedron Lett.* **1974,** (29), 2549-2552.
59. Jeong, Y.-H.; Lee, C.-H.; Jang, W.-D., A Diketopyrrolopyrrole-Based Colorimetric and Fluorescent Probe for Cyanide Detection. *Chemistry - An Asian Journal* **2012,** *7* (7), 1562-1566.
60. (a) Zhang, G.; Li, H.; Bi, S.; Song, L.; Lu, Y.; Zhang, L.; Yu, J.; Wang, L., A new turn-on fluorescent chemosensor based on diketopyrrolopyrrole (DPP) for imaging Zn2+ in living cells. *The Analyst* **2013,** *138* (20), 6163; (b) Kaur, M.; Choi, D. H., Dual channel receptor based on diketopyrrolopyrrole alkyne conjugate for detection of Hg2+/Cu2+ by "naked eye" and fluorescence. *Sensors and Actuators B: Chemical* **2014,** *190*, 542-548.
61. (a) Patil, H.; Zu, W. X.; Gupta, A.; Chellappan, V.; Bilic, A.; Sonar, P.; Rananaware, A.; Bhosale, S. V.; Bhosale, S. V., A non-fullerene electron acceptor based on fluorene and diketopyrrolopyrrole building blocks for solution-processable organic solar cells with an impressive open-circuit voltage. *Phys. Chem. Chem. Phys.* **2014,** *16* (43), 23837-23842; (b) Raynor, A. M.; Gupta, A.; Patil, H.; Bilic, A.; Bhosale, S. V., A diketopyrrolopyrrole and benzothiadiazole based small molecule electron acceptor: design, synthesis, characterization and photovoltaic properties. *RSC Adv.* **2014,** *4* (101), 57635-57638; (c) Ryan, J. W.; Matsuo, Y., Increased Efficiency in Small Molecule Organic Solar Cells Through the Use of a 56-π Electron Acceptor – Methano Indene Fullerene. *Scientific Reports* **2015,** *5*, 8319.
62. Chan, W. K.; Chen, Y.; Peng, Z.; Yu, L., Rational designs of multifunctional polymers. *J. Am. Chem. Soc.* **1993,** *115* (25), 11735-11743.
63. Zhang, X.; Richter, L. J.; DeLongchamp, D. M.; Kline, R. J.; Hammond, M. R.; McCulloch, I.; Heeney, M.; Ashraf, R. S.; Smith, J. N.; Anthopoulos, T. D.; Schroeder, B.; Geerts, Y. H.; Fischer, D. A.; Toney, M. F., Molecular Packing of High-Mobility Diketo Pyrrolo-Pyrrole Polymer Semiconductors with Branched Alkyl Side Chains. *J. Am. Chem. Soc.* **2011,** *133* (38), 15073-15084.
64. Dou, L.; Gao, J.; Richard, E.; You, J.; Chen, C.-C.; Cha, K. C.; He, Y.; Li, G.; Yang, Y., Systematic Investigation of Benzodithiophene- and Diketopyrrolopyrrole-

Based Low-Bandgap Polymers Designed for Single Junction and Tandem Polymer Solar Cells. *J. Am. Chem. Soc.* **2012,** *134* (24), 10071-10079.
65. Ashraf, R. S.; Meager, I.; Nikolka, M.; Kirkus, M.; Planells, M.; Schroeder, B. C.; Holliday, S.; Hurhangee, M.; Nielsen, C. B.; Sirringhaus, H.; McCulloch, I., Chalcogenophene Comonomer Comparison in Small Band Gap Diketopyrrolopyrrole-Based Conjugated Polymers for High-Performing Field-Effect Transistors and Organic Solar Cells. *J. Am. Chem. Soc.* **2015,** *137* (3), 1314-1321.
66. (a) Lee, O. P.; Yiu, A. T.; Beaujuge, P. M.; Woo, C. H.; Holcombe, T. W.; Millstone, J. E.; Douglas, J. D.; Chen, M. S.; Fréchet, J. M. J., Efficient Small Molecule Bulk Heterojunction Solar Cells with High Fill Factors via Pyrene-Directed Molecular Self-Assembly. *Adv. Mater.* **2011,** *23* (45), 5359-5363; (b) Huang, J.; Zhan, C.; Zhang, X.; Zhao, Y.; Lu, Z.; Jia, H.; Jiang, B.; Ye, J.; Zhang, S.; Tang, A.; Liu, Y.; Pei, Q.; Yao, J., Solution-Processed DPP-Based Small Molecule that Gives High Photovoltaic Efficiency with Judicious Device Optimization. *ACS Applied Materials & Interfaces* **2013,** *5* (6), 2033-2039.
67. Sonar, P.; Ng, G.-M.; Lin, T. T.; Dodabalapur, A.; Chen, Z.-K., Solution processable low bandgap diketopyrrolopyrrole (DPP) based derivatives: novel acceptors for organic solar cells. *J. Mater. Chem.* **2010,** *20* (18), 3626.
68. Lin, Y.; Li, Y.; Zhan, X., A Solution-Processable Electron Acceptor Based on Dibenzosilole and Diketopyrrolopyrrole for Organic Solar Cells. *Advanced Energy Materials* **2013,** *3* (6), 724-728.
69. Lin, Y.; Cheng, P.; Li, Y.; Zhan, X., A 3D star-shaped non-fullerene acceptor for solution-processed organic solar cells with a high open-circuit voltage of 1.18 V. *Chem. Commun.* **2012,** *48* (39), 4773.
70. (a) Günes, S.; Neugebauer, H.; Sariciftci, N. S., Conjugated Polymer-Based Organic Solar Cells. *Chem. Rev.* **2007,** *107* (4), 1324-1338; (b) Huang, Q.; Li, H., Recent progress of bulk heterojunction solar cells based on small-molecular donors. *Chin. Sci. Bull.* **2013,** *58* (22), 2677-2685.
71. (a) Kanimozhi, C.; Yaacobi-Gross, N.; Burnett, E. K.; Briseno, A. L.; Anthopoulos, T. D.; Salzner, U.; Patil, S., Use of side-chain for rational design of n-type diketopyrrolopyrrole-based conjugated polymers: what did we find out? *PCCP* **2014,** *16* (32), 17253; (b) Lloyd, M. T.; Anthony, J. E.; Malliaras, G. G., Photovoltaics from soluble small molecules. *Mater. Today* **2007,** *10* (11), 34-41.
72. Gupta, A.; Ali, A.; Bilic, A.; Gao, M.; Hegedus, K.; Singh, B.; Watkins, S. E.; Wilson, G. J.; Bach, U.; Evans, R. A., Absorption enhancement of oligothiophene dyes through the use of a cyanopyridone acceptor group in solution-processed organic solar cells. *Chem. Commun.* **2012,** *48* (13), 1889.

2.0 Significant Improvement of Optoelectronic and Photovoltaic Properties by Incorporating Thiophene in a Solution-Processable D–A–D Modular Chromophore

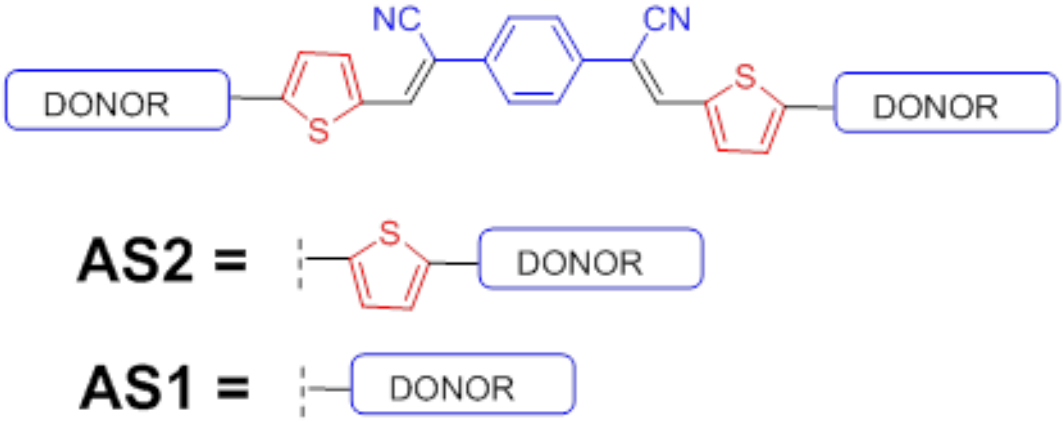

Journal article published in *Molecules* **2015**, *20,* 21787–21801 presented as **Chapter 2**.

molecules

MDPI

Article

Significant Improvement of Optoelectronic and Photovoltaic Properties by Incorporating Thiophene in a Solution-Processable D–A–D Modular Chromophore

Aaron M. Raynor [1], Akhil Gupta [1,2,*], Christopher M. Plummer [1], Sam L. Jackson [1], Ante Bilic [3], Hemlata Patil [1], Prashant Sonar [4,*] and Sheshanath V. Bhosale [1,*]

Received: 6 October 2015 ; Accepted: 25 November 201 5; Published: 4 December 2015
Academic Editor: Sergei Manzhos

1 School of Applied Sciences, The Royal Melbourne Institute of Technology (RMIT) University, GPO Box 2476, Melbourne Victoria 3001, Australia; aaron.raynor@rmit.edu.au (A.M.R.); chris.plummer@rmit.edu.au (C.M.P.); sam.jackson@rmit.edu.au (S.L.J.); hemlatap2@gmail.com (H.P.)
2 Medicinal Chemistry, Monash Institute of Pharmaceutical Sciences, Monash University, Parkville Victoria 3052, Australia
3 Virtual Nanoscience Lab, Commonwealth Scientific and Industrial Research Organization (CSIRO) Manufacturing, Parkville Victoria 3052, Australia; ante.bilic@csiro.au
4 School of Chemistry, Physics and Mechanical Engineering, Queensland University of Technology (QUT), GPO Box 2434, Brisbane QLD 4001, Australia
* Correspondence: akhil.gupta@monash.edu (A.G.); sonar.prashant@qut.edu.au (P.S.); sheshanath.bhosale@rmit.edu.au (S.V.B.); Tel./Fax: +61-3-9925-2680 (S.V.B.)

Abstract: Through the incorporation of a thiophene functionality, a novel solution-processable small organic chromophore was designed, synthesized and characterized for application in bulk-heterojunction solar cells. The new chromophore, (2*Z*,2′*Z*)-2,2′-(1,4-phenylene)bis(3-(5-(4-(diphenylamino)phenyl)thiophen-2-yl)acrylonitrile) (coded as **AS2**), was based on a donor–acceptor–donor (D–A–D) module where a simple triphenylamine unit served as an electron donor, 1,4-phenylenediacetonitrile as an electron acceptor, and a thiophene ring as the π-bridge embedded between the donor and acceptor functionalities. **AS2** was isolated as brick-red, needle-shaped crystals, and was fully characterized by ^{1}H- and ^{13}C-NMR, IR, mass spectrometry and single crystal X-ray diffraction. The optoelectronic and photovoltaic properties of **AS2** were compared with those of a structural analogue, (2*Z*,2′*Z*)-2,2′-(1,4-phenylene)bis(3-(4-(diphenylamino)phenyl)-acrylonitrile) (**AS1**). Benefiting from the covalent thiophene bridges, compared to **AS1** thin solid film, the **AS2** film showed: (1) an enhancement of light-harvesting ability by 20%; (2) an increase in wavelength of the longest wavelength absorption maximum (497 nm *vs.* 470 nm) and (3) a narrower optical band-gap (1.93 eV *vs.* 2.17 eV). Studies on the photovoltaic properties revealed that the best **AS2**-[6,6]-phenyl-C_{61}-butyric acid methyl ester ($PC_{61}BM$)-based device showed an impressive enhanced power conversion efficiency of 4.10%, an approx. 3-fold increase with respect to the efficiency of the best **AS1**-based device (1.23%). These results clearly indicated that embodiment of thiophene functionality extended the molecular conjugation, thus enhancing the light-harvesting ability and short-circuit current density, while further improving the bulk-heterojunction device performance. To our knowledge, **AS2** is the first example in the literature where a thiophene unit has been used in conjunction with a 1,4-phenylenediacetonitrile accepting functionality to extend the π-conjugation in a given D–A–D motif for bulk-heterojunction solar cell applications.

Keywords: solution-processable; bulk-heterojunction devices; donor–acceptor–donor; triphenylamine; thiophene; 1,4-phenylenediacetonitrile

1. Introduction

The development of renewable energy technologies is pivotal for accommodating the ever increasing energy demands of the modern society. Such technologies are also important for lowering environmental pollution and greenhouse gas emissions. Towards this objective, many approaches to harvest solar energy have been investigated. The fabrication of bulk-heterojunction (BHJ) devices is one such promising strategy that has attracted considerable attention over the past two decades due to their advantages of being lightweight, low cost and their flexibility in large-area applications [1–7]. Such devices are comprised of an interpenetrating network of organic donor and acceptor domains that is formed during their fabrication via solution processing. Conventionally, semiconducting donor polymers such as poly(3-hexylthiophene) (P3HT) and acceptors such as soluble fullerene derivatives, $PC_{61}BM$ and its C_{71} analogue ($PC_{71}BM$), have been used to obtain a deeper understanding of device design and morphology [8–13]. Apart from archetypal P3HT, conjugated polymers have also been developed and significant progress has been attained with promising BHJ architecture. Power conversion efficiency (PCE) values above 10% has been reported with such polymeric donors [14–17]. In the interim, solution-processed small molecular donor-based BHJ devices have also aroused interest, mainly due to their advantages of well-defined chemical structure, convenient purification methods, such as simple column chromatography, and monodisperse molecular weight [18–23]. These advantages allow and encourage researchers to exert efforts for the design and development of small molecular donors. Recently, immense efforts have been dedicated to developing small molecular-based solution-processable organic solar cells [1,21] and so far, the highest PCE of 9.95% was achieved by Kan *et al.* [24] which is analogous to those of the polymer-based solution-processable devices. Thus, in view of such reports and the fact that BHJ devices incorporating small molecular donors can compete with polymer-based devices, there is an overwhelming interest in developing small molecular donors.

Recent years have seen a dramatic surge not only in terms of device efficiency using small molecular donors but also in their design and efficient synthetic development. A variety of small molecule donor materials based on donor–acceptor (D–A) combinations such as D–A–D [25–27], A–D–A [28,29], D–π–A [18,19,30] and star-shaped architectures [31] have been reported. The D–A–D design in particular is one of the most promising and successful modules based on which various donor and acceptor units have been explored for high-performance solution-processable photovoltaic devices. A finite number of central accepting units, such as naphthalene diimide [25], diketopyrrolopyrrole [27], 2-pyran-4-ylidenemalononitrile [32] and thiazolothiazole [33] have been reported to suit the D–A–D module. Not only that the availability and selection of such accepting blocks is limited, it is furthermore imperative that the target chromophore must possess a low optical band gap, broad absorption profile, high mobility and appropriately tuned highest occupied molecular orbital (HOMO) and lowest unoccupied molecular orbital (LUMO) energy levels using such blocks. Such requirements do possess a challenge for an organic chemist who must consider such factors while designing a new chromophore based on the D–A–D module. Therefore, it is not surprising that there exists an enormous scope for the design and development of new light-harvesting materials based on the challenging D–A–D module and is an aspiration for most of the researchers.

In our own studies of small molecule chromophores and charge transport materials based on a variety of D–A combinations, we have reported examples of successful solution-processable BHJ photovoltaic devices [18,19,25,34–37]. Furthermore, we are highly interested to extend our efforts on the design and development of new chromophores that are inspired by the D–A–D module. In this study, we report the design, facile synthesis and characterization of the optoelectronic and photovoltaic properties of two small organic chromophores, **AS2** and **AS1**, (shown in Figure 1), and their direct comparison. Both materials are based on a D–A–D structural motif where a triphenyl-amine functionality has been chosen as a common donor at both ends of the central acceptor unit, 1,4-phenylenediacetonitrile (PDA), so as to get symmetrical **AS2** and **AS1**. **AS2** is a structural analogue of **AS1** where a thiophene ring has been introduced between the donor and acceptor functionalities in order to vary the optoelectronic and photovoltaic properties (Figure 1).

When compared with the commonly used accepting groups, such as dicyanovinylidene, aromatizable cyanopyridone, indenedione or oxoindenemalononitrile [38,39], PDA can be an acceptor of choice for extended π-conjugation over the whole molecular backbone, mainly due to its bidentate nature. It is notable to mention that the use of the PDA unit for electroluminescent conjugated polymers has been reported in the literature [40,41] as well as one- and two-photon spectroscopy studies [42–46]. However, its suitability as an acceptor in small molecular chromophores, particularly D–A–D modular, for BHJ applications is still unknown [4,21]. This provides an encouragement and some strong incentive for its investigation. Owing to the exploration of PDA acceptor unit in the D–A–D module, this study continues our search for the generation of new organic chromophores for BHJ applications.

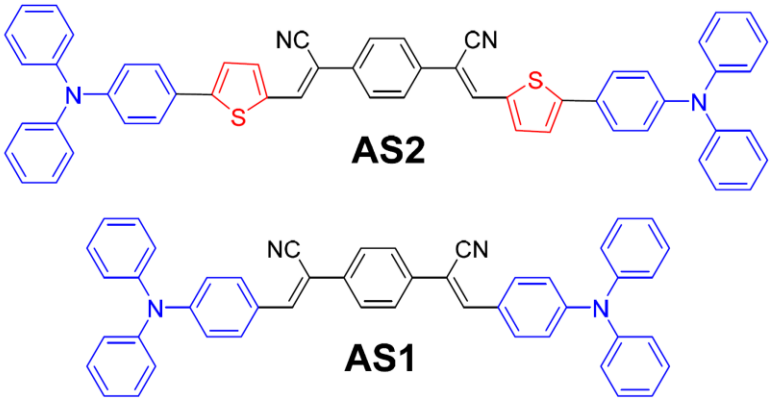

Figure 1. Molecular structures of the newly designed **AS2** and reference **AS1** materials investigated in this study.

2. Results and Discussion

2.1. Design Strategy, Synthesis

The materials **AS2** and **AS1** were synthesized via the Knoevenagel condensation of appropriate aldehydes with active methylene groups of the PDA acceptor unit and their chemical structures were confirmed by ^{1}H- and ^{13}C-NMR, mass spectrometry, and, where possible (**AS2** only), by single crystal X-ray diffraction (XRD). The synthetic methodology for synthesizing **AS1** was similar to an old literature report [42], albeit dissimilar base and solvent were used to deal with a homogeneous reaction solution. Knoevenagel condensation reaction of an aldehyde with active methylene group is an efficient way of generating a double bond between a π-bridge and acceptor functionality. The use of such chemistry is a common strategy to generate organic sensitizers for dye-sensitized solar cells [47]. However, the use of same strategy to develop small molecular chromophores for BHJ applications is still limited [4,21]. Herein, not only we are demonstrating the Knoevenagel condensation reaction of PDA acceptor unit but also the fabrication of solution-processable BHJ devices incorporating a fullerene acceptor ($PC_{61}BM$) and either **AS2** or **AS1** as a donor component (Figure 1). To the best of our knowledge, this is the first time PDA has been used to generate D–A–D modular small molecular chromophores for BHJ applications. Initial screening of the BHJ devices revealed that greater PCE was achieved for **AS2** (4.10% for **AS2** compared with 1.23% for **AS1**), as confirmed by the increased short-circuit current density (8.01 mA$\cdot$cm^{-2} for **AS2** and 3.15 mA$\cdot$cm^{-2} for **AS1**), under simulated AM 1.5 illumination (100 mW$\cdot$cm^{-2}).

Both materials were based on the D–A–D module and the central acceptor moiety was directly linked to the terminal donor functionalities in order to create a conjugated structure. The development of these target materials incorporates the use of two identical donor units (triphenylamine) on each side of the central core, resulting in symmetrical chromophores. Insertion of a planar, conjugated functionality, such as thiophene in **AS2**, between the donor and acceptor components of a target

material can provide greater absorption over visible light spectrum when compared with otherwise structurally similar compounds [38,48]. Moreover, the selection of thiophene over highly aromatic, conjugating functionalities, such as phenyl, was based on the earlier work reported by Würthner *et al.* [49] and Gupta *et al.* [50] where it has been demonstrated that replacement of a phenyl group with thiophene can provide significant spectral red-shifts and is advantageous for superior charge delocalization. As a result, **AS2** is deemed to exhibit a large red shift of lambda maximum when compared with the reference compound **AS1**. Both of the materials were synthesized per the reaction shown in Scheme 1 and were purified by simple column chromatography. Brick-red, needle-shaped crystals, suitable for single crystal XRD, were prepared by diffusing methanol into a dichloromethane solution of **AS2**, over approximately three days. However, no crystal growth was observed for **AS1**. Both materials were synthesized in moderate to high yields (**AS2** = 63% and **AS1** = 86%) and were highly soluble in a variety of common organic solvents, for example chlorobenzene, chloroform, and toluene. The solubility of organic p-type materials is paramount for fabricating solution-processable BHJ devices and both the materials fulfill this criterion. In fact, the solubility of **AS2** was found to be higher by 50% w/v when compared with **AS1**.

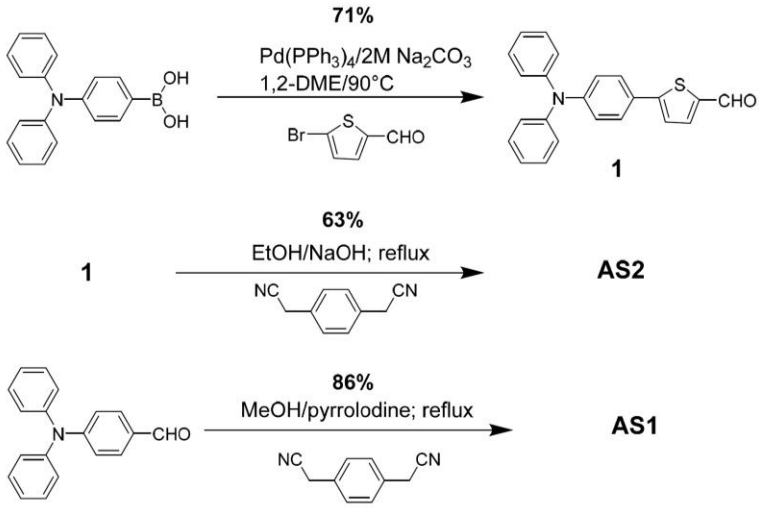

Scheme 1. Reaction scheme for the synthesis of **AS2** and **AS1**.

The precursor aldehyde **1** of **AS2** was also crystallized by diffusion of methanol into chloroform to obtain yellow, needle-shaped crystals. Diffraction measurements were performed at 200 K on a Bruker Apex II CCD diffractometer using Mo Kα radiation(λ = 0.71073 Å) The structure were solved using dual space methods using the program SHELX-2014/7 [51] using the Olex2 1.2 GUI [52], with anisotropic thermal parameters for all non-hydrogen atoms. All non-hydrogen atoms were refined anisotropically by full-matric least-squares methods SHELX-2014/7. Molecular drawings were obtained using Mercury [53]. The utility of **1** for dye-sensitized solar cells has been reported [54], however, its use to generate small molecular chromophores for BHJ applications is seldom reported [4,21]. This state of affairs encourages us and provides a strong incentive to report its synthesis and crystal growth strategy.

The compound **1** was crystallized in the monoclinic space group (P $2_1/c$) with four asymmetric units in one cell. The thiophene group and the adjacent phenyl groups are planar with pendant phenyl groups displaced around nitrogen. The packing consist of a two-fold screw axis with centers of inversion between sulfur molecules as well as a glide plane perpendicular to the thiophene plane. The packing is dominated by π-π face-to-face stacking between the thiophene and phenyl groups. The pendant phenyl groups are stabilized by π-π edge-to-face stacking with distances in the range 2.771–3.283 Å as shown in Figure 2.

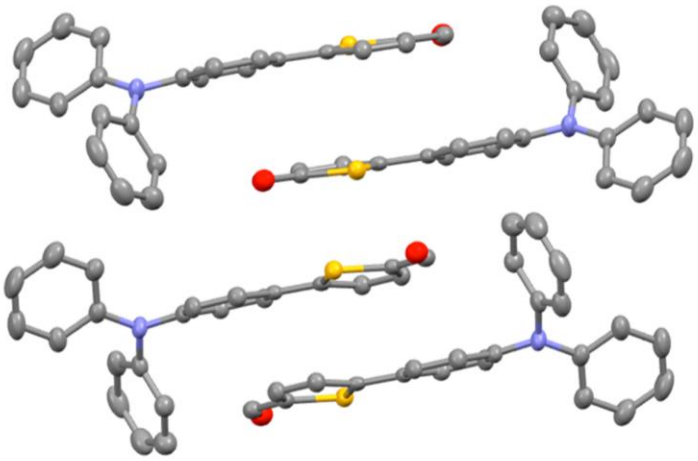

Figure 2. Packing of **1** along the *b* axis.

AS2 co-crystallizes with chloroform in the triclinic space group (P-1) with a center of symmetry around the central phenyl group. The packing is dominated by face-to-face π-π stacking between central phenyls and thiophenes, and by edge-to-face π-π-stacking between pendant phenyl groups with the distance 2.772 Å as shown in Figure 3. The details of packing structure, formula, crystal size of **1** and **AS2** are described in Table 1.

Table 1. Details of crystal data and structure refinement parameters of **1** and **AS2**.

Identification Code	CCDC: 1420377 (1)	CCDC: 1420378 (AS2)
Empirical formula	$C_{23}H_{17}NOS$	$C_{31}H_{22}OS$
Formula weight	355.43	442.55
Temperature/K	200(2)	200(2)
Crystal system	monoclinic	monoclinic
Space group	$P2_1/c$	$P2_1$
a/Å	19.916(3)	5.5812(7)
b/Å	6.6680(9)	47.120(6)
c/Å	13.4336(16)	9.2435(11)
α/°	90	90
β/°	96.613(3)	103.343(3)
γ/°	90	90
Volume/Å^3	1772.1(4)	2365.3(5)
Z	4	4
ρ_{calc}g/cm^3	1.332	1.243
μ/mm^{-1}	0.194	0.158
F(000)	744.0	928.0
Crystal size/mm^3	0.292 × 0.076 × 0.063	0.667 × 0.137 × 0.087
Radiation	MoKα (λ = 0.71073)	MoKα (λ = 0.71073)
2Θ range for data collection/	4.118 to 48.588	3.458 to 67.842
Index ranges	$-22 \leqslant h \leqslant 23, -7 \leqslant k \leqslant 7, -15 \leqslant l \leqslant 15$	$-8 \leqslant h \leqslant 8, -73 \leqslant k \leqslant 73, -14 \leqslant l \leqslant 12$
Reflections collected	15255	83,300
Independent reflections	2883 [R_{int} = 0.0707, R_{sigma} = 0.0447]	19,180 [R_{int} = 0.0616, R_{sigma} = 0.0596]
Data/restraints/parameters	2883/0/235	19180/1/595
Goodness-of-fit on F^2	0.949	1.028
Final R indexes [I ⩾ 2σ (I)]	R_1 = 0.0412, wR_2 = 0.1095	R_1 = 0.0659, wR_2 = 0.1531
Final R indexes [all data]	R_1 = 0.0720, wR_2 = 0.1274	R_1 = 0.0972, wR_2 = 0.1684
Largest diff. peak/hole/e Å^{-3}	0.17/−0.26	0.29/−0.39

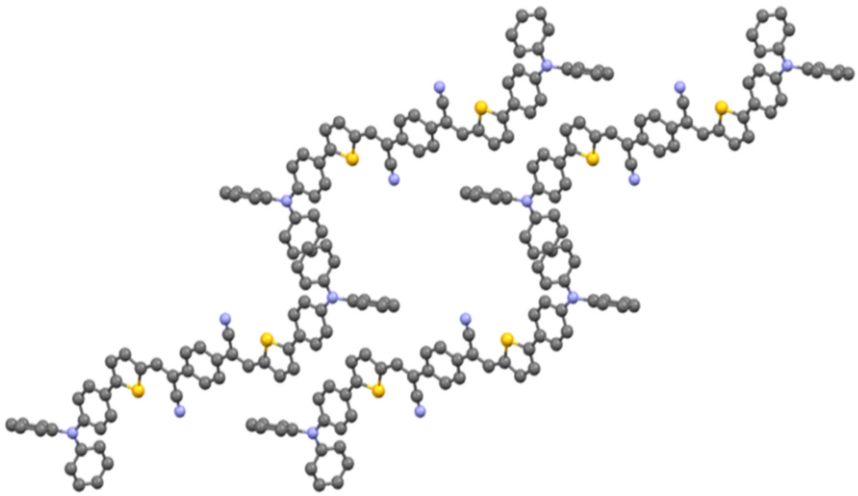

Figure 3. Packing of **AS2** along the *c* axis.

2.2. Optoelectronic Properties

The optical properties of **AS2** and **AS1** were investigated by measuring their ultraviolet–visible (UV–Vis) absorption spectra in chloroform solution and in pristine spin-cast films (Figure 4). The longest wavelength absorption maximum (λ_{max}) exhibited by **AS2** in solution form was at 459 nm which was red-shifted by 23 nm when compared with the solution λ_{max} of **AS1**. Both the absorption maximum and extinction coefficient (**AS2** = 59,000 $M^{-1} \cdot cm^{-1}$; **AS1** = 49,000 $M^{-1} \cdot cm^{-1}$) increased with the insertion of thiophene functionality. With the insertion of thiophene ring we found enhancement to the peak molar absorptivity of >20% of **AS2** compared with **AS1**. This enhanced profile allows a larger amount of the solar spectrum to be absorbed, thus exhibiting greater intramolecular charge transfer (ICT) transition. We observed a similar bathochromic absorption shift in the thin film spectrum of **AS2** compared with that of **AS1** (Figure 4). The strong red-shift is attributed to the extended π-conjugation within the molecular backbone of **AS2** that became possible with the insertion of thiophene functionality. This type of control over the absorption profile through the insertion of a strongly conjugated unit can help to fine tune optical energy levels, to enhance light harvesting and BHJ device performance.

Density functional theory (DFT) calculations using the Gaussian 09 suite of programs [55] and the B3LYP/6-311 + G(d,p)//B3LYP/6-31G(d) level of theory indicated that the HOMO orbital densities of both **AS2** and **AS1** have a major distribution over the whole molecular backbone and the LUMO densities were delocalized through the central acceptor functionality and adjacent rings (Figure 5). Inserted thiophene rings in case of **AS2** can accommodate LUMO density with almost equal contribution as the central PDA, thus sparing the adjoining phenyl rings of the donor triphenylamine for an efficient segregation of HOMO and LUMO densities. Such separation is ideal for the ICT transition and is attributed to the presence of a strong conjugated unit, of which thiophene is an example, in the given D–A–D system. Experimental estimation of the HOMO energies was carried out using photo electron spectroscopy in air (PESA) and the LUMO energies were calculated by adding the optical band gap (film spectra) to the HOMO values (see Figure 6 for energy level diagram and Figure S1 [see Supplementary Material] for the PESA curve). Film spectra indicated that insertion of thiophene reduces the band gap of **AS2** by 0.24 eV when compared with **AS1**. Furthermore, the estimation of HOMO using PESA revealed that the HOMO energy level of **AS2** was raised by 0.18 eV when compared with the HOMO level of **AS1**. This is in agreement with the DFT calculations that the presence of thiophene indeed plays a crucial role for: (1) density segregation; (2) tuning the optical energy levels; and (3) theoretical and experimental band gap reduction. These measurements

and calculations provide a strong rational for our design strategy that the induction of a conjugated functionality can indeed improve the optoelectronic properties of a given chromophore. The energy level diagram advised that the band gaps of these materials are all in the range required of donor materials for BHJ devices. **AS2** optical band gap is somewhat narrower in magnitude than 2.0 eV measured for the conventional P3HT. The optical and electrochemical properties of both the materials in solution and film form are summarized in Supplementary Material Table S1.

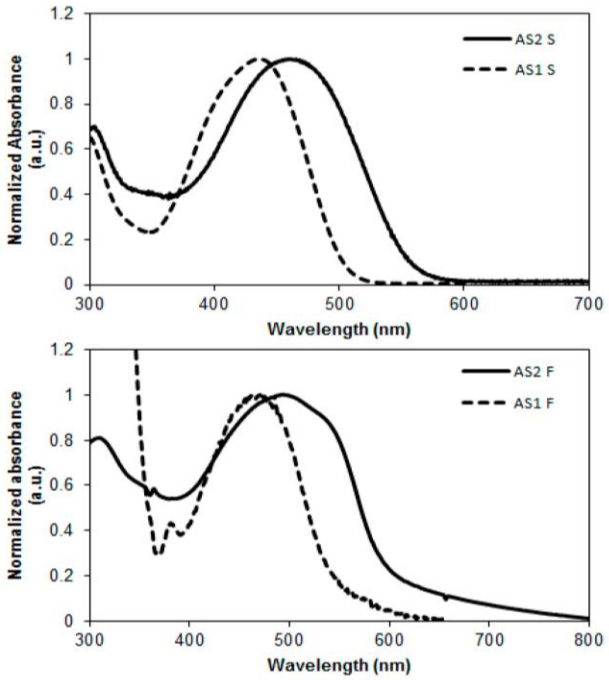

Figure 4. Normalized absorption spectra of compounds **AS2** and **AS1** in $CHCl_3$ solutions (**upper**) and for pristine as-casted films (**lower**); (films of **AS2** and **AS1** were spin-coated at 2000 rpm for 1 min to give a film thickness of ~70 nm).

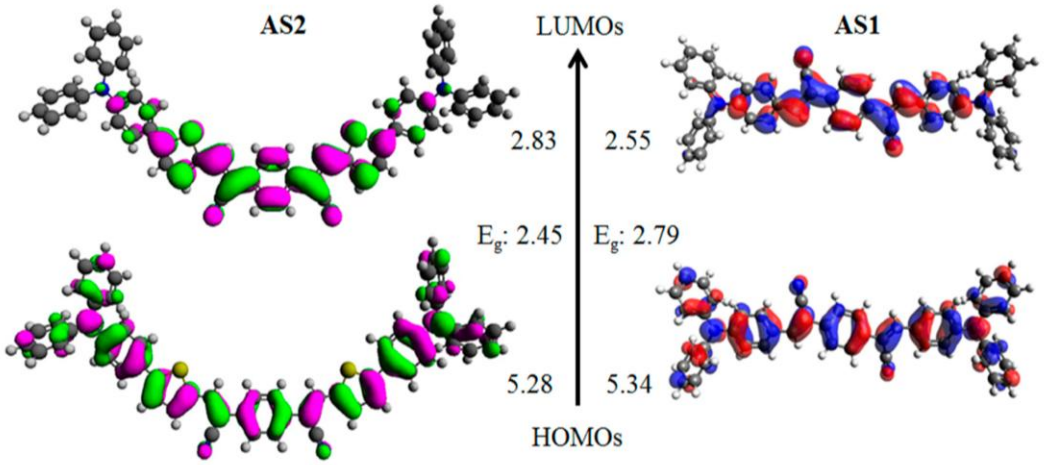

Figure 5. Orbital density distribution for the frontier molecular orbitals of **AS2** and **AS1**. DFT calculations were performed using the Gaussian 09 suite of programs and the B3LYP/6-311 + G(d,p)//B3LYP/6-31G(d) level of theory. Theoretical HOMO/LUMO energy levels and band-gaps (*vs.* Vac scale) are also shown.

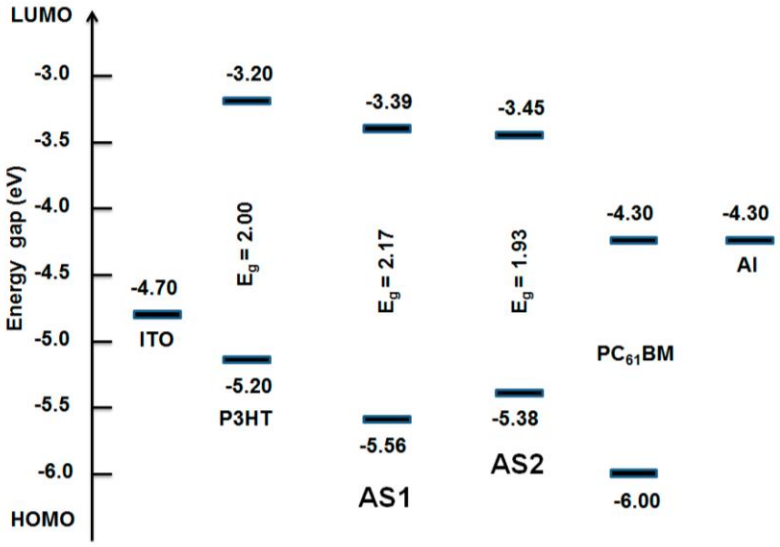

Figure 6. Energy level diagram depicting the band gaps of AS2 and AS1 in comparison with P3HT and $PC_{61}BM$. Experimental estimation of the HOMO energies was carried out using PESA and the LUMO energies were calculated by adding the optical band gap (film spectra) to the HOMO values.

Encouraging though the optoelectronic properties are, the compounds must display thermal stability given the rigorous conditions used in device fabrication such as annealing at temperature in the excess of 100 °C. In line with this requirement and to determine the thermal stability of **AS2** and **AS1**, thermogravimetric analysis (TGA) was conducted. TGA (Supplementary Material Figure S2) indicated that both **AS2** and **AS1** are thermally stable and will not degrade during the annealing of BHJ devices.

After correlating the optoelectronic properties of **AS2** and **AS1** with those of the conventional $PC_{61}BM$ acceptor (see Figure 6), we screened their potency as donor materials (p-type) in solution-processable BHJ devices under simulated sunlight and monochromatic light illumination. The blend solutions of both the materials and $PC_{61}BM$ were used to cast an active layer on top of the PEDOT:PSS surface. The BHJ device architecture used was ITO/PEDOT:PSS (38 nm)/active layer/Ca (20 nm)/Al (100 nm) where the active layer was a solution processed blend of either **AS2** or **AS1** and $PC_{61}BM$. For **AS2**, a promising PCE of 4.10% was achieved when the film was spin-coated from a chlorobenzene solution as a 1:1 blend with $PC_{61}BM$. By contrast, the maximum PCE obtained for a device based on **AS1** was 1.23%, when fabricated under similar conditions. The comparative current–voltage curves for the optimized blends of **AS2** and **AS1** with $PC_{61}BM$ are shown in Figure 7. High boiling solvents such as chlorobenzene are better not only from processing point of view but also for achieving smoother films without crystallization occurring on the active surfaces. Latter was particularly true as our efforts to construct BHJ devices using a low-boiling solvent, such as chloroform, afforded either uneven surfaces or minor cracks on the active surfaces.

The optimized devices based on **AS2** exhibited a decreased open circuit voltage (V_{oc}) than the devices based on **AS1**. This in fact is consistent with the measured HOMO values where a higher HOMO for **AS2** would predict a lower V_{oc}. On the other hand, the short circuit current density (J_{sc}) for the devices fabricated using **AS2** was higher than the J_{sc} extracted from the devices based on **AS1**. This was in agreement with the observed bathochromic shift in the absorption spectrum of **AS2** compared with **AS1**. The photovoltaic cell parameters for **AS2**-based devices were 0.88 V [open circuit voltage, V_{oc}], 8.01 mA$\cdot$cm^{-2} [current density, (J_{sc})], 0.58 [fill factor, (FF)] and 4.10% [power conversion efficiency, (PCE)]. Initial screening of the BHJ devices based on **AS1**:$PC_{61}BM$ showed moderate device performance with a high V_{oc} of 0.90 V, FF of 43% J_{sc} of 3.15 mA/cm^2 and an overall PCE of 1.23%. Taken as a whole, the insertion of thiophene functionality into the studied D–A–D

structural motif incorporating PDA acceptor functionality resulted in significant enhancement of J_{sc} and PCE values by factors >2 and >3, respectively, thus promoting the use of a smaller conjugated functionality, such as thiophene, as an interesting structural concept for the design and development of highly efficient BHJ materials. Furthermore, it is notable to mention that **AS2** showed optimal performance with inexpensive $PC_{61}BM$ and simple device architecture, thus providing some strong incentive to apply the design concept reported in this work to the new generations of BHJ materials.

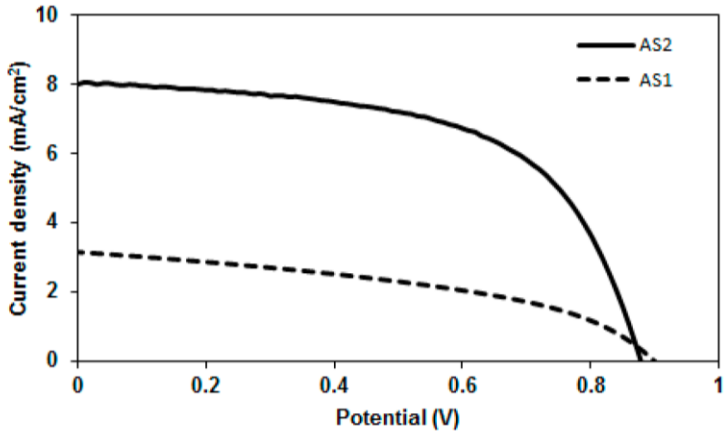

Figure 7. Current–voltage curves for the optimized devices based on AS2 and AS1 in blends with $PC_{61}BM$ (1:1 w/w) under simulated sunlight (AM 1.5, 1000 $W \cdot m^{-2}$). Device structure was: ITO/PEDOT-PSS (38 nm)/active layer/Ca (20 nm)/Al (100 nm) where the active layers were the blends of either **AS2** or **AS1** and $PC_{61}BM$ spun on top of the films of PEDOT:PSS using chlorobenzene solvent.

The incident photon-to-current-conversion efficiency (IPCE) spectra of these BHJ devices are shown in Figure 8. The IPCE measurement of these BHJ devices was broad spectrum, typically covering most of the visible range, from 350 to 750 nm. **AS2** and **AS1** exhibited high plateaus at ~40% and ~27% for the best BHJ devices respectively. The IPCE spectrum of **AS2**, which carried a thiophene functionality, was red-shifted when compared with **AS1**, a finding that is consistent with the result of thin film absorption spectrum. The significantly higher peak IPCE of **AS2** compared to **AS1** indicated that the superior performance of **AS2** can be rationalized in terms of enhanced light-harvesting and appropriately tuned optical energy levels, thereby corroborating the design principle.

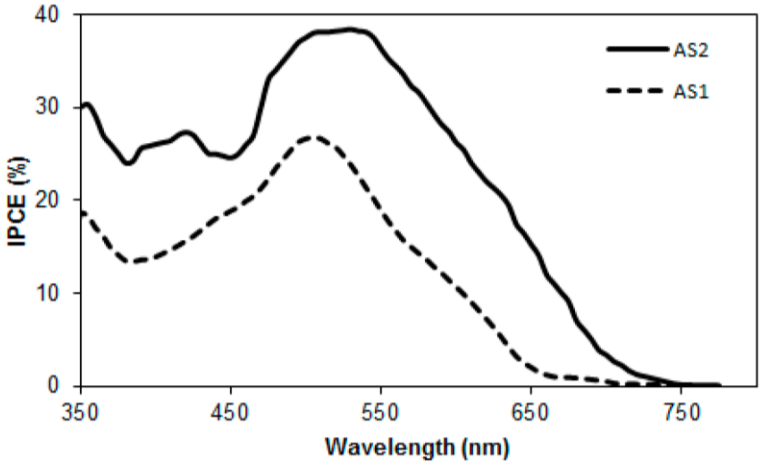

Figure 8. IPCE spectra of **AS2** and **AS1** with $PC_{61}BM$blends.

To examine the physical microstructure of the blend surface, we used atomic force microscopy (AFM) in tapping mode. The actual surface morphology of the blend films of **AS2**/**AS1**:$PC_{61}BM$ (1:1 w/w) is shown in Figure 9. Physically, both the blends were found to be smooth and the root mean square roughness of 0.41 nm and 0.35 nm was observed for **AS2** and **AS1** respectively. No cracks were observed on the film surfaces when the films were spin-casted using chlorobenzene (3000 rpm). The processing of active films of BHJ devices using a high boiling solvent such as chlorobenzene is advantageous over low boiling solvent such as chloroform and is in agreement with the AFM morphology. Our attempts to fabricate BHJ devices using chloroform resulted in very poor photovoltaic performance. This was mainly due to inferior film quality. Though **AS2** exerted promising PCE in this preliminary work, ample scope still exists to explore device strategies to enhance PCE. The performance might be improved by (1) using $PC_{71}BM$ or (2) effective interlayer, such as metal oxide interlayer, which can facilitate the efficient charge extraction, and (3) devising processing methods, such as use of additives. Work towards some of such strategies is the subject of on-going work in our laboratories. The discovery of potential materials, such as **AS2**, exhibiting promising optoelectronic and photovoltaic properties opens up the way to develop D–A–D modular small organic chromophores, with the use of PDA acceptor in particular, and paves the way for such materials to be used for other organic electronic applications.

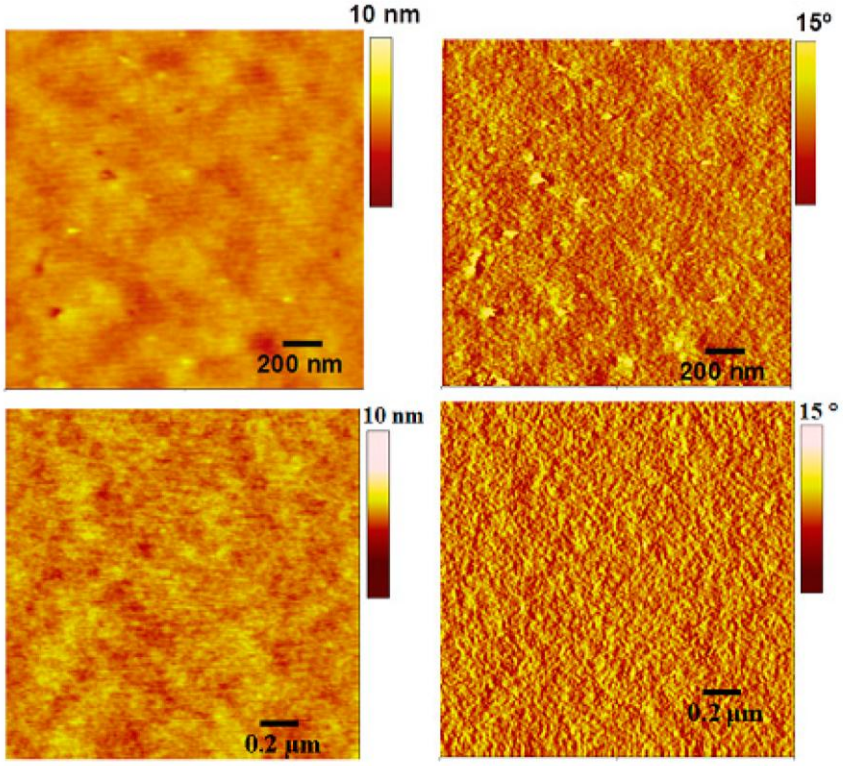

Figure 9. AFM images of 1:1 blends of **AS2** (**top**) and **AS1** (**bottom**) with $PC_{61}BM$ as-casted from chlorobenzene solution. Topographic (**left**) and phase images (**right**) are shown.

3. Experimental Section

3.1. Materials and Instruments

All reagents and chemicals used, unless otherwise specified, were purchased from Sigma-Aldrich (Sydney, Australia). The solvents used for reactions were obtained from Merck Speciality Chemicals (Sydney, Australia) and were used as received. Unless otherwise specified, all ^{1}H- and ^{13}C-NMR spectra

washed with cold EtOH (50.0 mL) followed by cold hexane (50.0 mL), and dried under high vacuum at 40 °C. The solid was crystallized using $CHCl_3$/hexane to afford 574 mg of **AS2** (63%) as a brick-red solid. m. p. >240 °C (decomposed at 240 °C); IR (solid film, cm^{-1}) 3674, 2988, 2208 (-CN str), 1578, 1486, 1440, 1421, 1324, 1271, 1238, 1179, 1064, 922, 829. ^{1}H-NMR (300 MHz, CD_2Cl_2): δ = 7.77–7.76 (m, 3H), 7.65–7.63 (m, 1H), 7.60–7.59 (m, 2H), 7.36–7.31 (m, 5H) 7.18–7.15 (m, 5H), 7.12–7.08 (m, 3H); ^{13}C-NMR (300 MHz, $CDCl_3$) δ = 149.9, 148.6, 147.1, 136.1, 134.8, 134.7, 134.4, 129.4, 127.0, 126.7, 126.0, 124.9, 123.6, 122.8, 122.7, 118.1, 105.7; LRMS (MALDI-TOF): m/z = 830.229; HRMS (APCI): calculated for $C_{56}H_{39}N_4S_2$ $[M + H]^+$ 831.2611; found 831.2602.

3.2.4. X-ray Crystallography

CCDC's **1420377** for **1** and **1420378** for **AS2** contain the supplementary crystallographic data for this paper. These data can be obtained free of charge via http://www.ccdc.cam.ac.uk/conts/retrieving.html (or from the CCDC, 12 Union Road, Cambridge CB2 1EZ, UK; Fax: +44 1223 336033; E-mail: deposit@ccdc.cam.ac.uk).

4. Conclusions

In conclusion, we have demonstrated the first use of the PDA acceptor functionality in conjunction with a thiophene unit for the design and development of a BHJ chromophore, **AS2**, where PDA was used in the D–A–D modular arrangement. The incorporation of this strong conjugating thiophene unit helped to improve light-harvesting, photocurrent density and PCE of **AS2** when compared with an analogue, **AS1**. The incorporation of the thiophene functionality was of clear benefit in improving the BHJ performance and indicates a potential to be broadly applicable in the design and development of future high performance BHJ chromophores.

Supplementary Materials: Supplementary materials can be accessed at: http://www.mdpi.com/1420-3049/20/12/19798/s1.

Acknowledgments: S.V.B. (RMIT) acknowledges financial support from the Australian Research Council (ARC), Australia, under a Future Fellowship Scheme (FT110100152). The CSIRO Division of Materials Science and Engineering, Clayton, Victoria is acknowledged for providing support through a visiting fellow position (A.G.). P.S. is thankful to the ARC Future Fellowship Scheme (FT130101337) at Queensland University of Technology, Brisbane, Queensland.

Author Contributions: A.M.R. synthesis, characterization, properties of materials and fabrication of devices; S.L.J and C.M.P.: single crystal structure determinations; A.G. and H.P. device fabrication and characterization; A.B.: performance of DFT calculation; P.S: results and discussion part, and S.V.B.: design, supervision and analysis of data. All the authors contributed for the manuscript preparation.

Conflicts of Interest: The authors declare no conflict of interests.

References

1. Chen, Y.; Wan, X.; Long, G. High performance photovoltaic applications using solution-processed small molecules. *Acc. Chem. Res.* **2013**, *46*, 2645–2655. [CrossRef] [PubMed]
2. Duan, C.; Huang, F.; Cao, Y. Recent development of push–pull conjugated polymers for bulk-heterojunction photovoltaics: Rational design and fine tailoring of molecular structures. *J. Mater. Chem.* **2012**, *22*, 10416–10434. [CrossRef]
3. Günes, S.; Neugebauer, H.; Sariciftci, N.S. Conjugated polymer-based organic solar cells. *Chem. Rev.* **2007**, *107*, 1324–1338. [CrossRef] [PubMed]
4. Lin, Y.; Li, Y.; Zhan, X. Small molecule semiconductors for high-efficiency organic photovoltaics. *Chem. Soc. Rev.* **2012**, *41*, 4245–4272. [CrossRef] [PubMed]
5. Huang, Y.; Kramer, E.J.; Heeger, A.J.; Bazan, G.C. Bulk heterojunction solar cells: Morphology and performance relationships. *Chem. Rev.* **2014**, *114*, 7006–7043. [CrossRef] [PubMed]
6. Heegar, A.J. 25th Anniversary article: Bulk heterojunction solar cells: Understanding the mechanism of operation. *Adv. Mater.* **2014**, *26*, 10–28. [CrossRef] [PubMed]

7. Scharber, M.C.; Sariciftci, N.S. Efficiency of bulk-heterojunction organic solar cells. *Prog. Polym. Sci.* **2013**, *38*, 1929–1940. [CrossRef] [PubMed]
8. Boudreault, P.-L.T.; Najari, A.; Leclerc, M. Processable Low-Bandgap Polymers for Photovoltaic Applications. *Chem. Mater.* **2011**, *23*, 456–469. [CrossRef]
9. Facchetti, A. π-Conjugated polymers for organic electronics and photovoltaic cell applications. *Chem. Mater.* **2011**, *23*, 733–758. [CrossRef]
10. Gupta, A.; Watkins, S.E.; Scully, A.D.; Singh, T.B.; Wilson, G.J.; Rozanski, L.J.; Evans, R.A. Band-gap tuning of pendant polymers for organic light-emitting devices and photovoltaic applications. *Synth. Met.* **2011**, *161*, 856–863. [CrossRef]
11. He, Y.; Li, Y. Fullerene derivative acceptors for high performance polymer solar cells. *Phys. Chem. Chem. Phys.* **2011**, *13*, 1970–1983. [CrossRef] [PubMed]
12. Laquai, F.; Andrienko, D.; Mauer, R.; Blom, P.W.M. Charge carrier transport and photogeneration in P3HT:PCBM photovoltaic blends. *Macromol. Rapid Commun.* **2015**, *36*, 1001–1025. [CrossRef] [PubMed]
13. Dang, M.T.; Hirsch, L.; Wantz, G.; Wuest, J.D. Controlling the morphology and performance of bulk heterojunctions in solar cells. Lessons learned from the benchmark poly(3-hexylthiophene): [6,6]-phenyl-C61-butyric acid methyl ester system. *Chem. Rev.* **2013**, *113*, 3734–3765. [CrossRef] [PubMed]
14. You, J.; Chen, C.-C.; Hong, Z.; Yoshimura, K.; Ohya, K.; Xu, R.; Ye, S.; Gao, J.; Li, G.; Yang, Y. 10.2% Power conversion efficiency polymer tandem solar cells consisting of two identical sub-cells. *Adv. Mater.* **2013**, *25*, 3973–3978. [CrossRef] [PubMed]
15. You, J.; Dou, L.; Yoshimura, K.; Kato, T.; Ohya, K.; Moriarty, T.; Emery, K.; Chen, C.-C.; Gao, J.; Li, G.; *et al.* A polymer tandem solar cell with 10.6% power conversion efficiency. *Nat. Commun.* **2013**, *4*. [CrossRef] [PubMed]
16. Lu, L.; Zheng, T.; Wu, Q.; Schneider, A.M.; Zhao, D.; Yu, L. Recent advances in bulk heterojunction polymer solar cells. *Chem. Rev.* **2015**. [CrossRef] [PubMed]
17. Guo, X.; Baumgarten, M.; Muellen, K. Designing π-conjugated polymers for organic electronics. *Prog. Polym. Sci.* **2013**, *38*, 1832–1908. [CrossRef]
18. Gupta, A.; Ali, A.; Bilic, A.; Gao, M.; Hegedus, K.; Singh, B.; Watkins, S.E.; Wilson, G.J.; Bach, U.; Evans, R.A. Absorption enhancement of oligothiophene dyes through the use of a cyanopyridone acceptor group in solution-processed organic solar cells. *Chem. Commun.* **2012**, *48*, 1889–1891. [CrossRef] [PubMed]
19. Kumar, R.J.; Churches, Q.I.; Subbiah, J.; Gupta, A.; Ali, A.; Evans, R.A.; Holmes, A.B. Enhanced photovoltaic efficiency via light-triggered self-assembly. *Chem. Commun.* **2013**, *49*, 6552–6554. [CrossRef] [PubMed]
20. Li, Y.; Guo, Q.; Li, Z.; Pei, J.; Tian, W. Solution processable D-A small molecules for bulk-heterojunction solar cells. *Energy Environ. Sci.* **2010**, *3*, 1427–1436. [CrossRef]
21. Mishra, A.; Bäuerle, P. Small molecule organic semiconductors on the move: Promises for future solar energy technology. *Angew. Chem. Int. Ed.* **2012**, *51*, 2020–2067. [CrossRef] [PubMed]
22. Liu, J.; Walker, B.; Nguyen, T.-Q. Solution-processed molecular bulk heterojunction solar cells. In *Organic Photovoltaics*, 2nd ed.; Brabec, C.J., Scherf, U., Dyakonov, V., Eds.; Wiley-VCH Verlag GmbH & Co. KGaA: Weinheim, Germany, 2014; pp. 95–137.
23. Roncali, J.; Leriche, P.; Blanchard, P. Molecular materials for organic photovoltaics: Small is beautiful. *Adv. Mater.* **2014**, *26*, 3821–3838. [CrossRef] [PubMed]
24. Kan, B.; Zhang, Q.; Li, M.; Wan, X.; Ni, W.; Long, G.; Wang, Y.; Yang, X.; Feng, H.; Chen, Y. Solution-processed organic solar cells based on dialkylthiol-substituted benzodithiophene unit with efficiency near 10%. *J. Am. Chem. Soc.* **2014**, *136*, 15529–15532. [CrossRef] [PubMed]
25. Patil, H.; Gupta, A.; Bilic, A.; Jackson, S.L.; Latham, K.; Bhosale, S.V. Donor-acceptor-donor modular small organic molecules based on the naphthalene diimide acceptor unit for solution-processable photovoltaic devices. *J. Electron. Mater.* **2014**, *43*, 3243–3254. [CrossRef]
26. Sonar, P.; Williams, E.T.; Singh, S.P.; Manzhos, S.; Dodabalapur, A. A benzothiadiazole end capped donor-acceptor based small molecule for organic electronics. *Phys. Chem. Chem. Phys.* **2013**, *15*, 17064–17069. [CrossRef] [PubMed]
27. Walker, B.; Tamayo, A.B.; Dang, X.-D.; Zalar, P.; Seo, J.H.; Garcia, A.; Tantiwiwat, M.; Nguyen, T.-Q. Nanoscale phase separation and high photovoltaic efficiency in solution-processed, small-molecule bulk heterojunction solar cells. *Adv. Funct. Mater.* **2009**, *19*, 3063–3069. [CrossRef]

28. Loser, S.; Bruns, C.J.; Miyauchi, H.; Ortiz, R.O.P.; Facchetti, A.; Stupp, S.I.; Marks, T.J. A naphthodithiophene-diketopyrrolopyrrole donor molecule for efficient solution-processed solar cells. *J. Am. Chem. Soc.* **2011**, *133*, 8142–8145. [CrossRef] [PubMed]
29. Yong, W.; Zhang, M.; Xin, X.; Li, Z.; Wu, Y.; Guo, X.; Yang, Z.; Hou, J. Solution-processed indacenodithiophene-based small molecule for bulk heterojunction solar cells. *J. Mater. Chem. A* **2013**, *1*, 14214–14220. [CrossRef]
30. Gupta, A.; Ali, A.; Gao, M.; Singh, T.B.; Bilic, A.; Watkins, S.E.; Bach, U.; Evans, R.A. Small molecules containing rigidified thiophenes and a cyanopyridone acceptor unit for solution-processable bulk-heterojunction solar cells. *Dyes Pigm.* **2015**, *119*, 122–132. [CrossRef]
31. Yuan, M.-S.; Wang, Q.; Wang, W.-J.; Li, T.-B.; Wang, L.; Deng, W.; Du, Z.-T.; Wang, J.-R. Symmetrical and asymmetrical (multi)branched truxene compounds: Structure and photophysical properties. *Dyes Pigm.* **2012**, *95*, 236–243. [CrossRef]
32. Li, Z.; Dong, Q.; Li, Y.; Xu, B.; Deng, M.; Pei, J.; Zhang, J.; Chen, F.; Wen, S.; Gao, Y.; *et al.* Design and synthesis of solution processable small molecules towards high photovoltaic performance. *J. Mater. Chem.* **2011**, *21*, 2159–2168. [CrossRef]
33. Shi, Q.; Cheng, P.; Li, Y.; Zhan, X. A solution processable D-A-D molecule based on thiazolothiazole for high performance organic solar cells. *Adv. Energy Mater.* **2012**, *2*, 63–67. [CrossRef]
34. Gupta, A.; Hangarge, R.V.; Wang, X.; Alford, B.; Chellapan, V.; Jones, L.A.; Rananaware, A.; Bilic, A.; Sonar, P.; Bhosale, S.V. Crowning of dibenzosilole with a naphthalenediimide functional group to prepare an electron acceptor for organic solar cells. *Dyes Pigm.* **2015**, *120*, 314–321. [CrossRef]
35. Patil, H.; Gupta, A.; Alford, B.; Ma, D.; Privér, S.H.; Bilic, A.; Sonar, P.; Bhosale, S.V. Conjoint use of dibenzosilole and indan-1,3-dione functionalities to prepare an efficient non-fullerene acceptor for solution-processable bulk-heterojunction solar cells. *Asian J. Org. Chem.* **2015**. [CrossRef]
36. Patil, H.; Zu, W.X.; Gupta, A.; Chellappan, V.; Bilic, A.; Sonar, P.; Rananaware, A.; Bhosale, S.V.; Bhosale, S.V. A non-fullerene electron acceptor based on fluorene and diketopyrrolopyrrole building blocks for solution-processable organic solar cells with an impressive open-circuit voltage. *Phys. Chem. Chem. Phys.* **2014**, *16*, 23837–23842. [CrossRef] [PubMed]
37. Raynor, A.M.; Gupta, A.; Patil, H.; Bilic, A.; Bhosale, S.V. A diketopyrrolopyrrole and benzothiadiazole based small molecule electron acceptor: Design, synthesis, characterization and photovoltaic properties. *RSC Adv.* **2014**, *4*, 57635–57638. [CrossRef]
38. Gupta, A.; Ali, A.; Singh, T.B.; Bilic, A.; Bach, U.; Evans, R.A. Molecular engineering for panchromatic absorbing oligothiophene donor-π-acceptor organic semiconductors. *Tetrahedron* **2012**, *68*, 9440–9447. [CrossRef]
39. Kronenberg, N.M.; Deppisch, M.; Würthner, F.; Lademann, H.W.A.; Deing, K.; Meerholz, K. Bulk heterojunction organic solar cells based on merocyanine colorants. *Chem. Commun.* **2008**, *48*, 6489–6491. [CrossRef] [PubMed]
40. Grimsdale, A.C.; Chan, K.L.; Martin, R.E.; Jokisz, P.G.; Holmes, A.B. Synthesis of light-emitting conjugated polymers for applications in electroluminescent devices. *Chem. Rev.* **2009**, *109*, 897–1091. [CrossRef] [PubMed]
41. Halliday, D.A.; Burn, P.L.; Friend, R.H.; Bradley, D.D.C.; Holmes, A.B. Determination of the average molecular weigth of poly(p-phenylenevinylene). *Synth. Met.* **1993**, *55*, 902–907. [CrossRef]
42. Pond, S.J.K.; Rumi, M.; Levin, M.D.; Parker, T.C.; Beljonne, D.; Day, M.W.; Brédas, J.-L.; Marder, S.R.; Perry, J.W. One- and two-photon spectroscopy of donor−acceptor−donor distyrylbenzene derivatives: Effect of cyano substitution and distortion from planarity. *J. Phys. Chem. A* **2002**, *106*, 11470–11480. [CrossRef]
43. Maurin, M.; Vurth, L.; Vial, J.-C.; Baldeck, P.; Marder, S.R.; van der Sanden, B.; Stephan, O. Pluronic organic fluorescent probes for two-photon vascularisation imaging. *Nonlinear Opt. Quantum Opt.* **2010**, *40*, 175–181.
44. Fang, H.-H.; Chen, Q.-D.; Yang, J.; Xia, H.; Gao, B.-R.; Feng, J.; Ma, Y.-G.; Sun, H.-B. Two-photon pumped amplified spontaneous emission from cyano-substituted oligo(p-phenylenevinylene) crystals with aggregation-induced emission enhancement. *J. Phys. Chem. C* **2010**, *114*, 11958–11961. [CrossRef]
45. Yan, Z.-Q.; Yang, Z.-Y.; Wang, H.; Li, A.-W.; Wang, L.-P.; Yang, H.; Gao, B.-R. Study of aggregation induced emission of cyano-substituted oligo(p-phenylenevinylene) by femtosecond time resolved fluorescence. *Spectrochim Acta A Mol Biomol Spectrosc.* **2011**, *78*, 1640–1645. [CrossRef] [PubMed]

46. Maurin, M.; Stephan, O.; Vial, J.-C.A.; Marder, S.R.; van der Sanden, B.P.J. Deep *in vivo* two-photon imaging of blood vessels with a new dye encapsulated in pluronic nanomicelles. *J. Biomed. Opt.* **2011**, *16*, 1–6. [CrossRef] [PubMed]
47. Xiang, W.; Gupta, A.; Kashif, M.K.; Duffy, N.; Bilic, A.; Evans, R.A.; Spiccia, L.; Bach, U. Cyanomethylbenzoic acid: An acceptor for donor–π–acceptor chromophores used in dye-sensitized solar cells. *ChemSusChem* **2013**, *6*, 256–260. [CrossRef] [PubMed]
48. Bobe, S.R.; Gupta, A.; Rananaware, A.; Bilic, A.; Bhosale, S.V.; Bhosale, S.V. Improvement of optoelectronic and photovoltaic properties through the insertion of a naphthalenediimide unit in donor–acceptor oligothiophenes. *RSC Adv.* **2015**, *5*, 4411–4415. [CrossRef]
49. Würthner, F.; Wortmann, R.; Matschiner, R.; Lukaszuk, K.; Meerholz, K.; DeNardin, Y.; Bittner, R.; Brauchle, C.; Sens, R. Merocyanine dyes in the cyanine limit: A new class of chromophores for photorefractive materials. *Angew. Chem. Int. Ed.* **1997**, *36*, 2765–2768. [CrossRef]
50. Gupta, A.; Armel, V.; Xiang, W.; Fanchini, G.; Watkins, S.E.; MacFarlane, D.R.; Bach, U.; Evans, R.A. The effect of direct amine substituted push-pull oligothiophene chromophores on dye-sensitized and bulk heterojunction solar cells performance. *Tetrahedron* **2013**, *69*, 3584–3592. [CrossRef]
51. Sheldrick, G.M. A short history of SHELX. *Acta. Cryst.* **2008**, *64*, 112–122. [CrossRef] [PubMed]
52. Dolomanov, O.V.; Bourhis, L.J.; Gildea, R.J.; Howard, J.A.K.; Puschmann, H. OLEX2: A complete structure solution, refinement and analysis program. *J. Appl. Cryst.* **2009**, *42*, 339–341. [CrossRef]
53. Sheldrick, G.M. Crystal structure refinement with SHELXL. *Struct. Chem.* **2014**, *71*, 3–8.
54. Hagberg, D.P.; Marinado, T.; Karlsson, K.M.; Nonomura, K.; Qin, P.; Boschloo, G.; Brinck, T.; Hagfeldt, A.; Sun, L. Tuning the HOMO and LUMO energy levels of organic chromophores for dye sensitized solar cells. *J. Org. Chem.* **2007**, *72*, 9550–9556. [CrossRef] [PubMed]
55. Frisch, M.J.; Trucks, G.W.; Schlegel, H.B.; Scuseria, G.E.; Robb, M.A.; Cheeseman, J.R.; Scalmani, G.; Barone, V.; Mennucci, B.; Petersson, G.A.; *et al. Gaussian 09, revision D.01*; Gaussian Incorporation: Wallingford, CT, USA, 2013.

Sample Availability: Samples of the compounds **S10** and **S11** are available from the authors.

Experimental Part

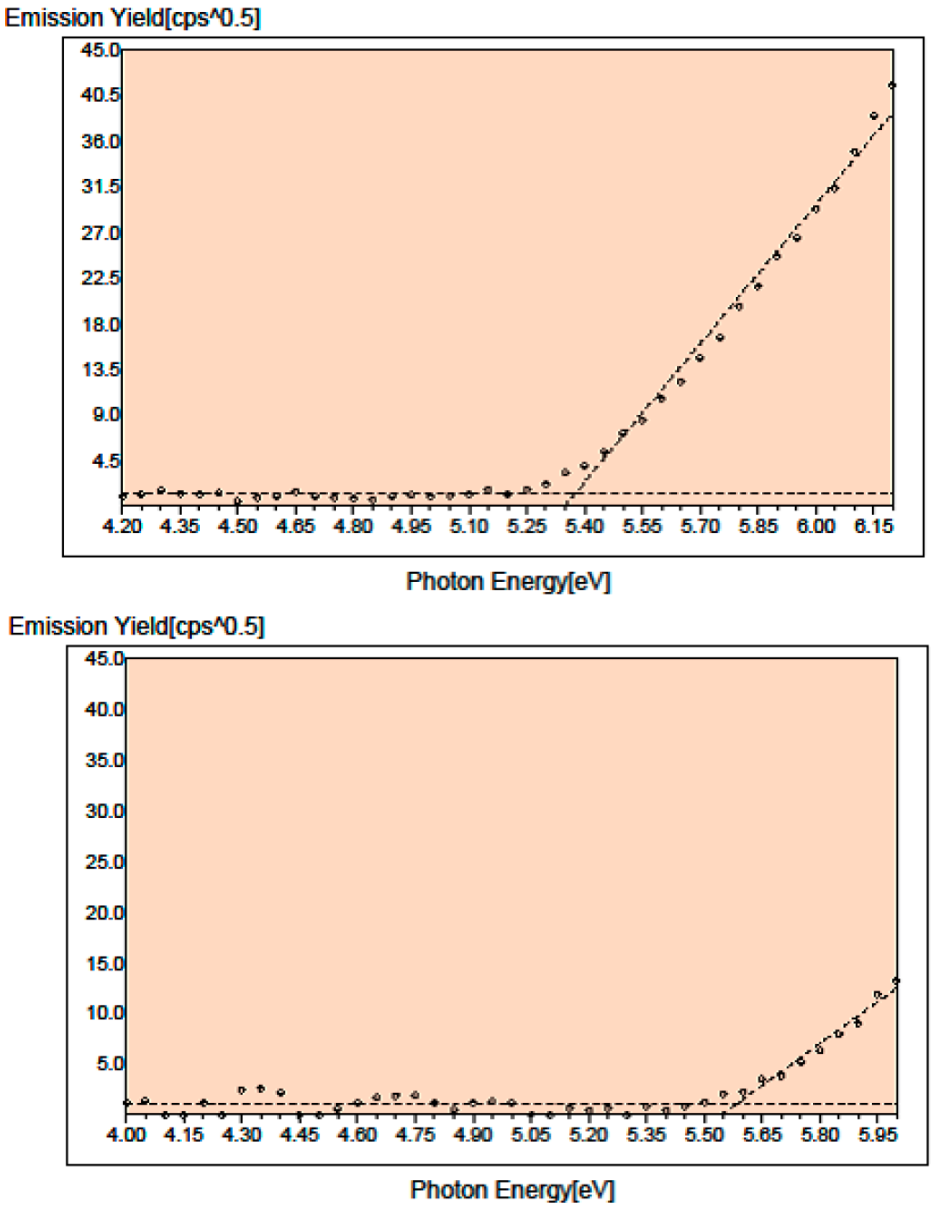

Figure S1. PESA spectra of thin films of **AS2** (upper) and **AS1** (lower). The dashed-lines show the fits to extract ionisation potentials which correspond to the HOMO energy levels.

Table S1. Comparative optoelectronic properties of **AS2** and **AS1**

Material	Absorption (Solution) λ_{abs} [a] /(nm)	Extinction Coefficient (ε/($M^{-1}\cdot cm^{-1}$)	Absorption (Film) λ_{abs} [b]/onset /(nm)	Energy Levels [c] (HOMOs/LUMOs) /(eV)		$E_{bandgap}$/eV [d]	
				Theoretical	Experimental	Theoretical	Experimental
AS2	459	59,057	497/640	5.28/2.83	5.38/3.45	2.45	1.93
AS1	436	49,125	470/570	5.34/2.55	5.56/3.39	2.79	2.17

[a] UV–Vis absorption in chloroform solution; [b] Longest wavelength of UV–Vis absorption maxima for as-casted films from chloroform solutions; [c] Theoretical energy levels were calculated using the Gaussian 09 suite of programs and the B3LYP/6-311+G(d,p)//B3LYP/6-31G(d) level of theory. Experimental energy levels were measured/calculated using a combination of PESA and the optical absorption; [d] Optical band gaps were calculated/measured under similar conditions reported for c.

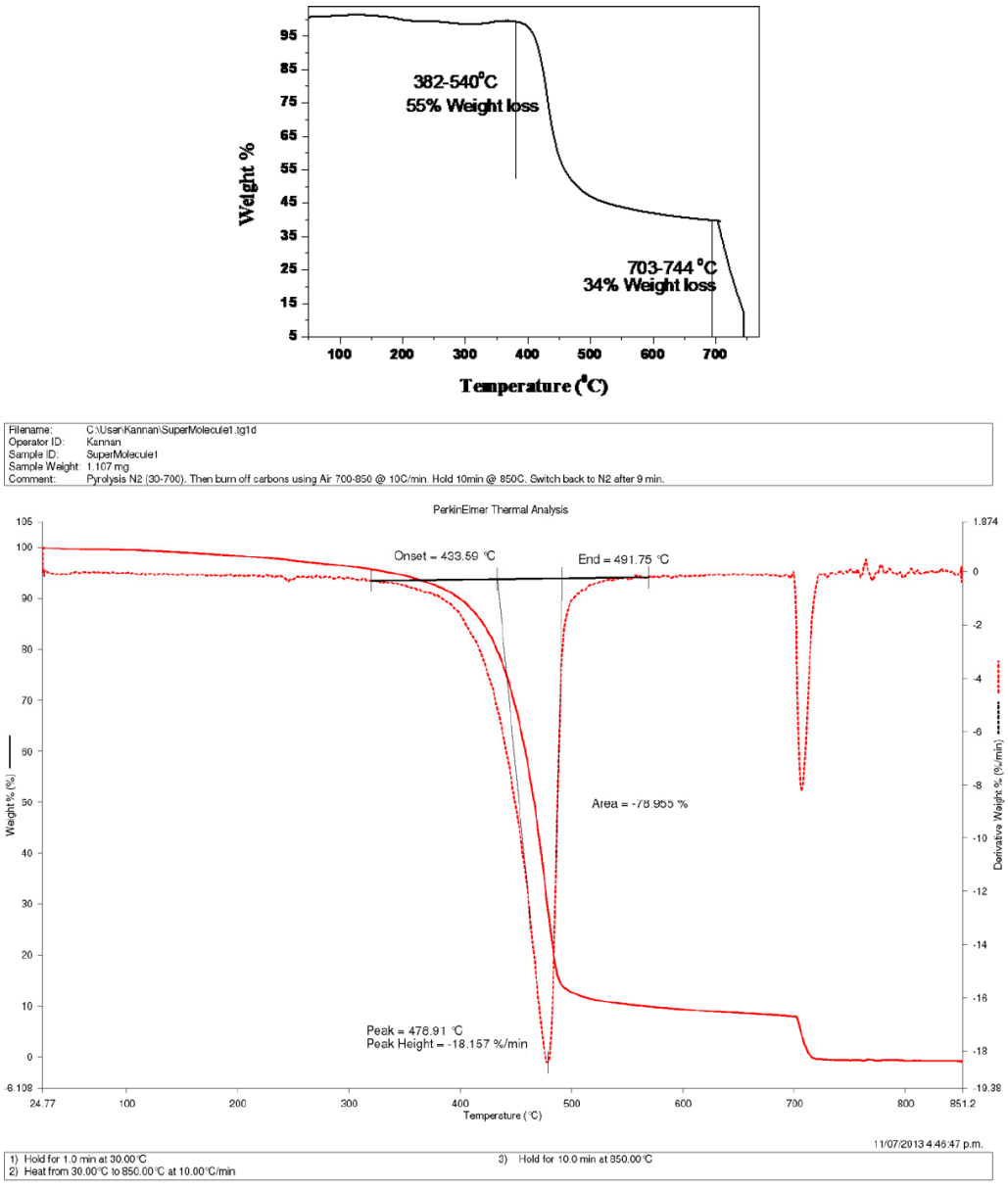

Figure S2. TGA curves of **AS2** (upper) and **AS1** (lower).

Spectra of AS1

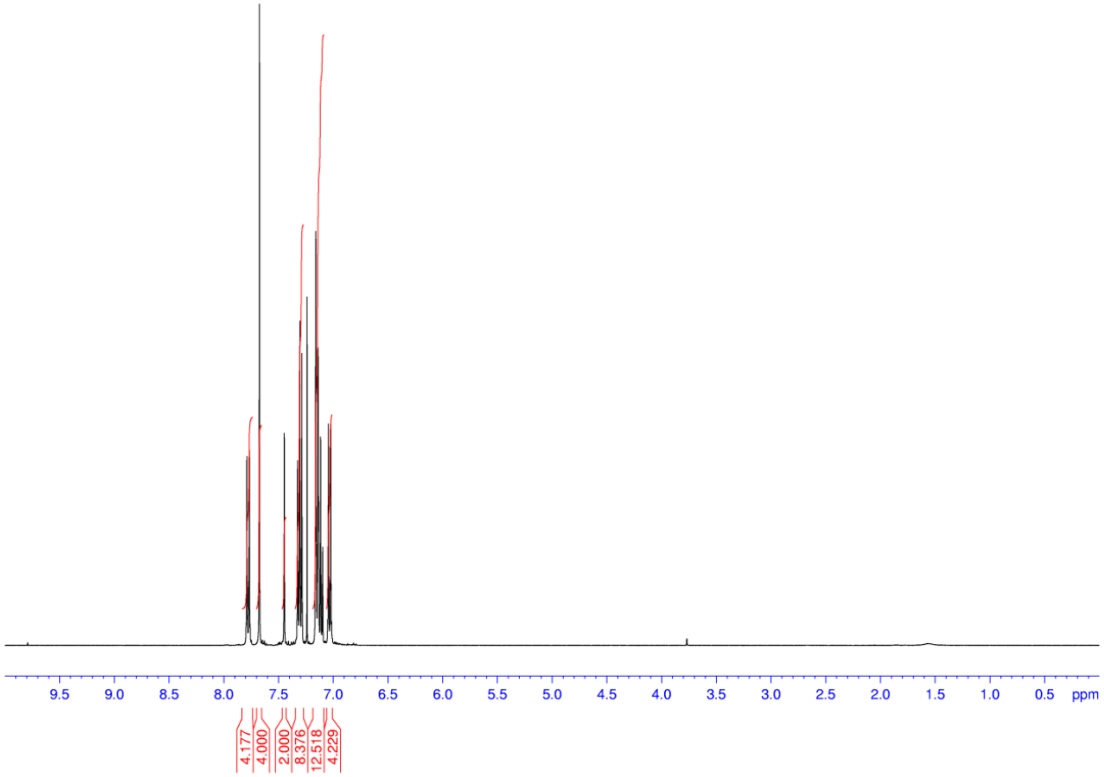

Figure S3. ^{1}H-NMR spectrum in $CDCl_3$.

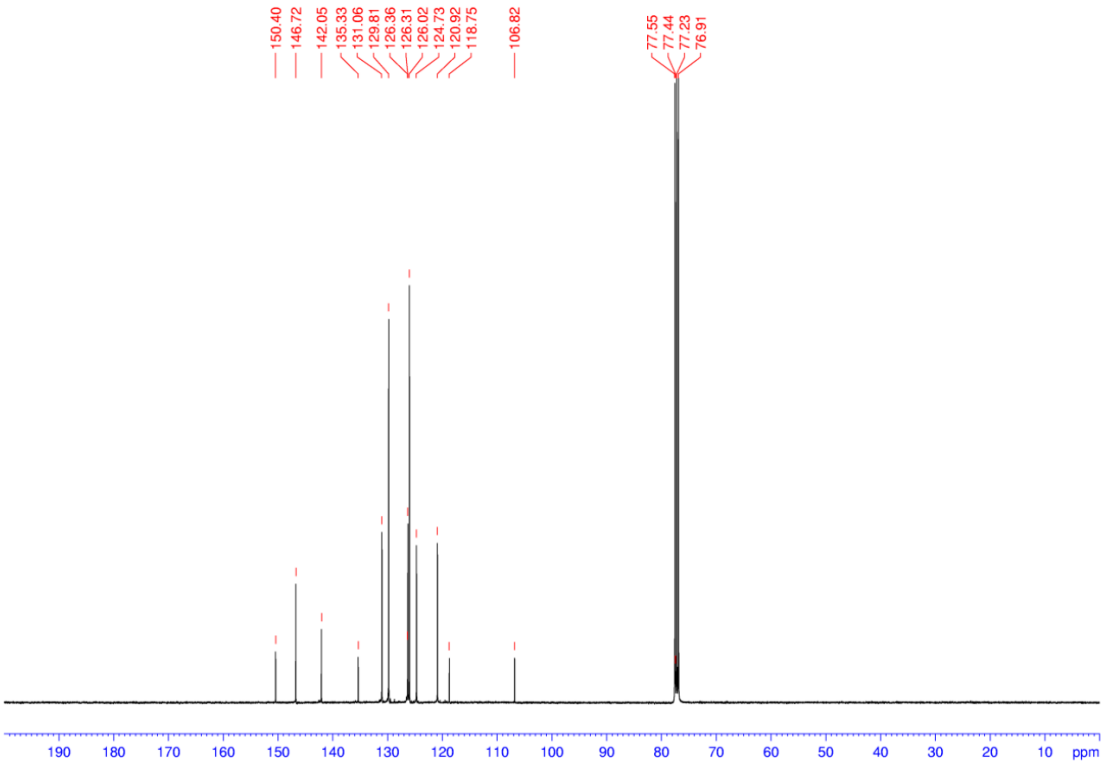

Figure S4. ^{13}C-NMR spectrum in $CDCl_3$.

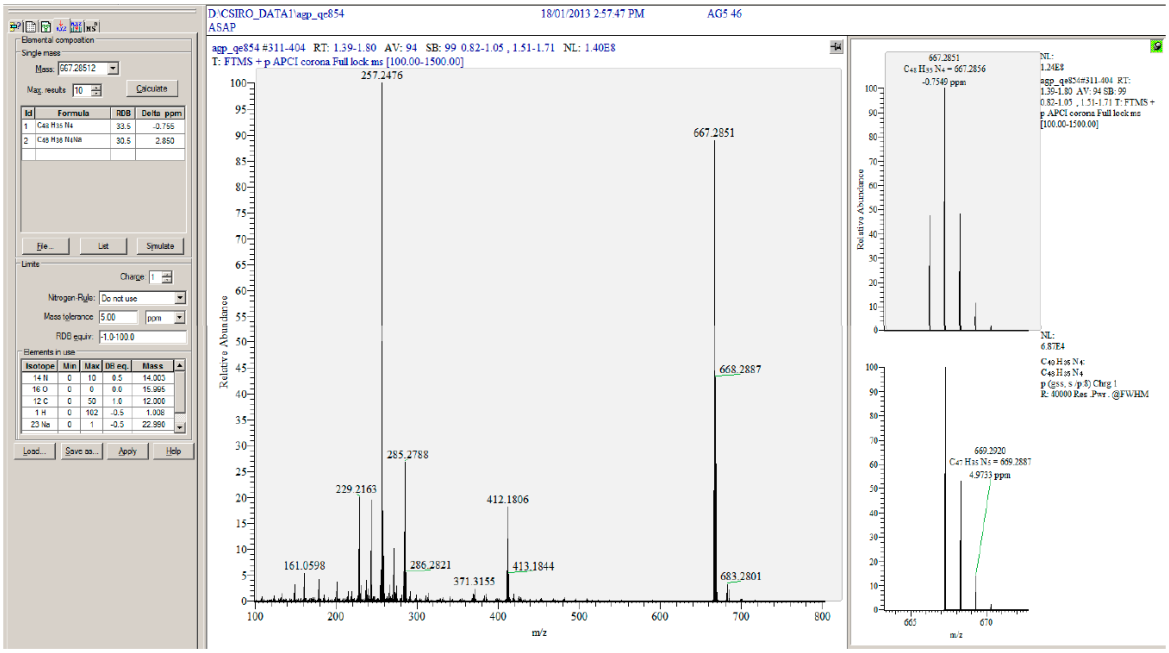

Figure S5. HRMS spectrum.

Spectra of Intermediate 1

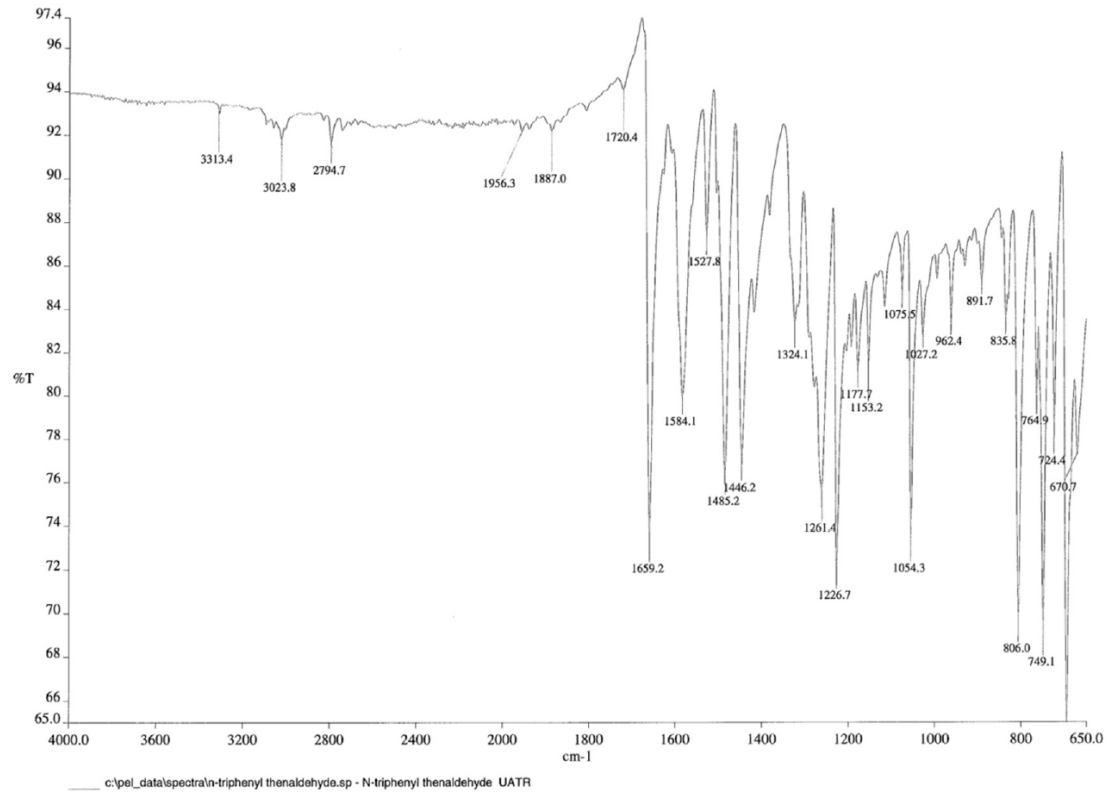

Figure S6. IR spectrum.

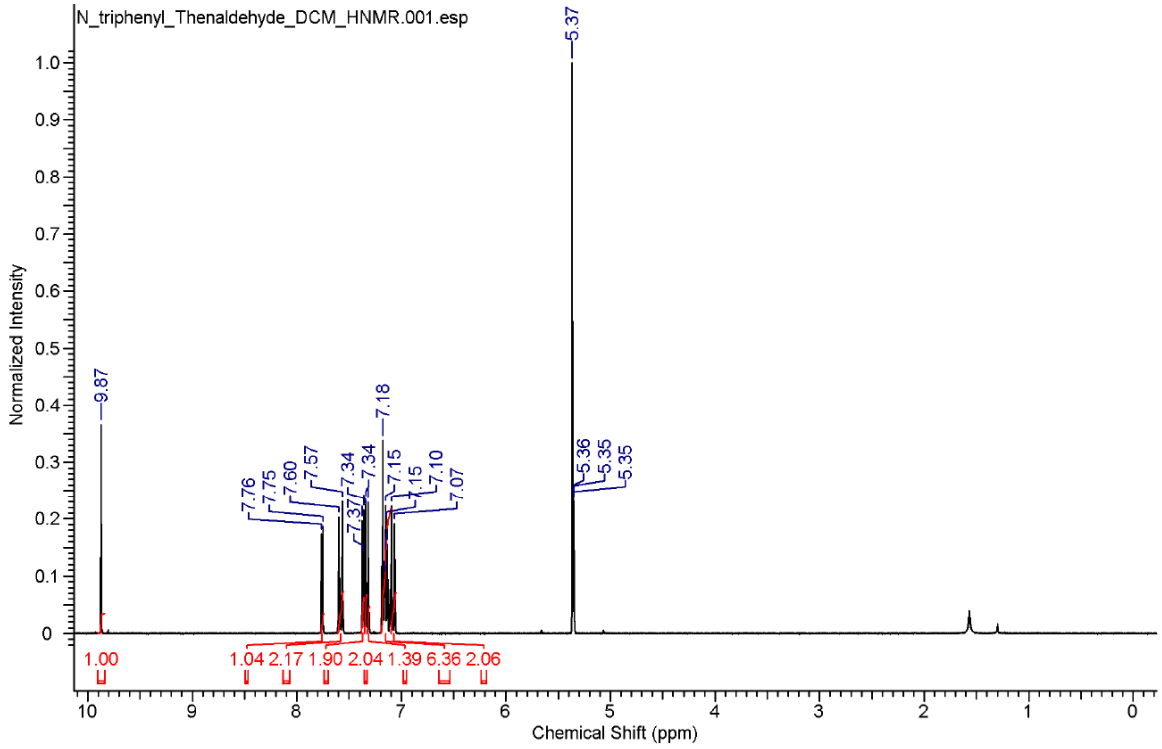

Figure S7. ^{1}H-NMR spectrum in CD_2Cl_2.

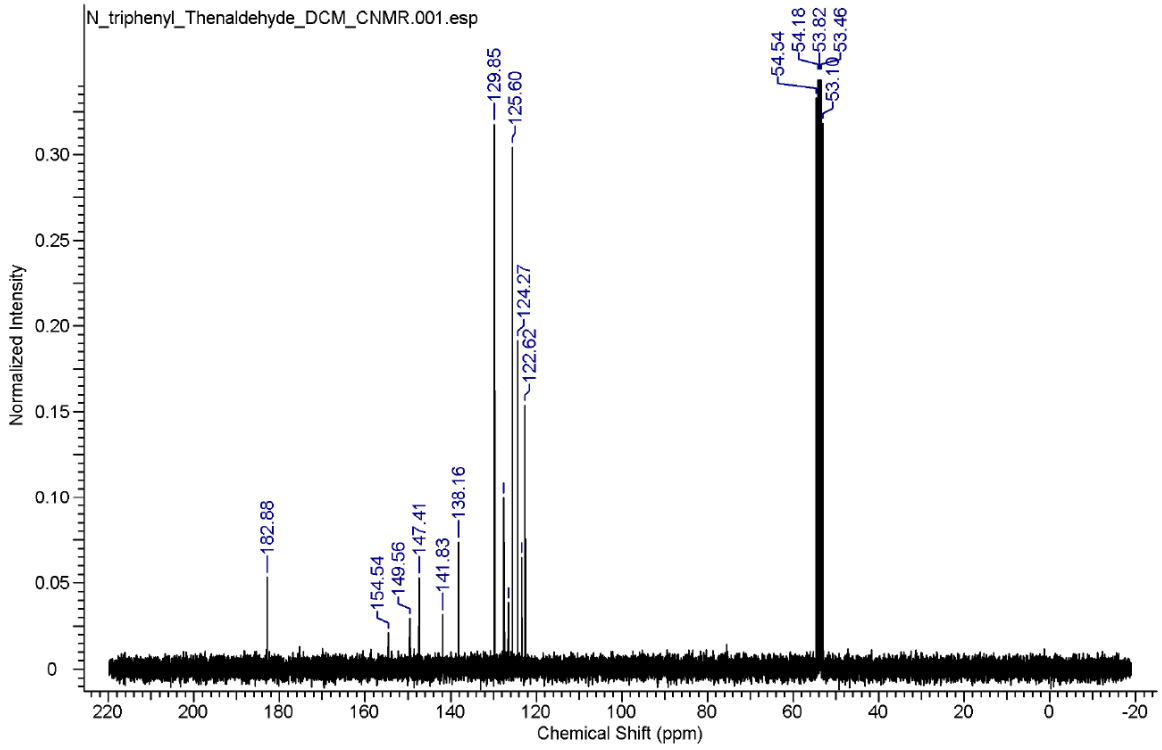

Figure S8. ^{13}C-NMR spectrum in CD_2Cl_2.

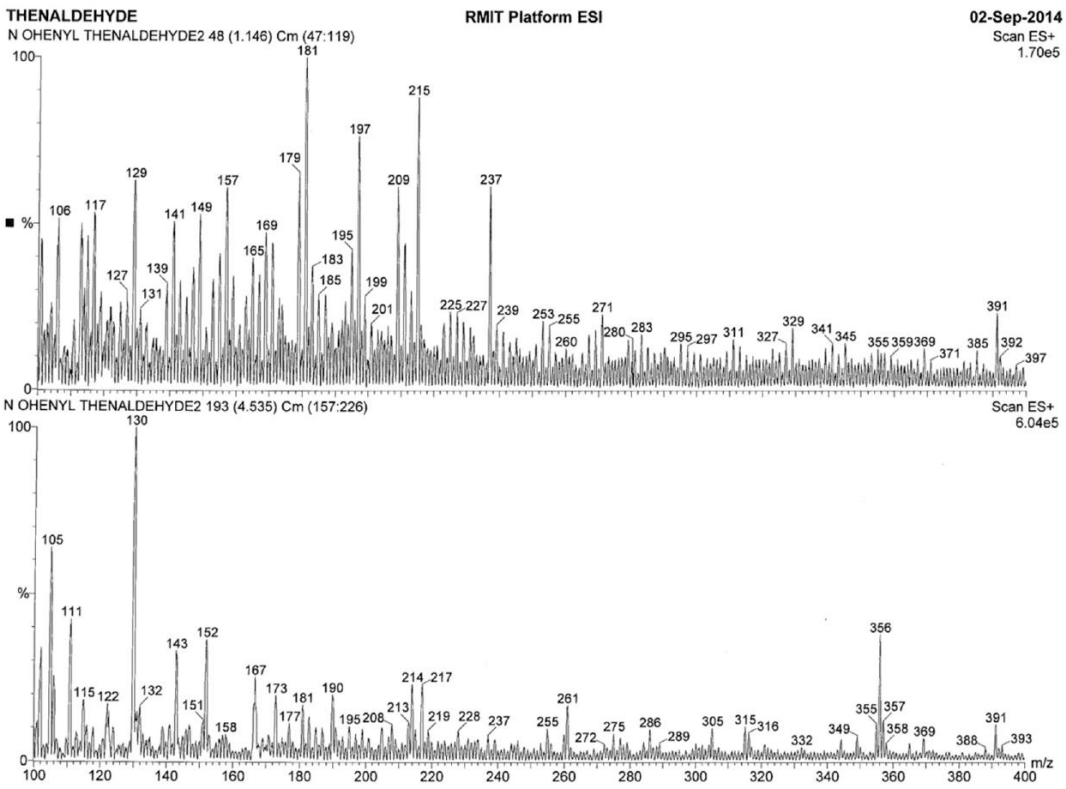

Figure S9. LRMS spectrum.

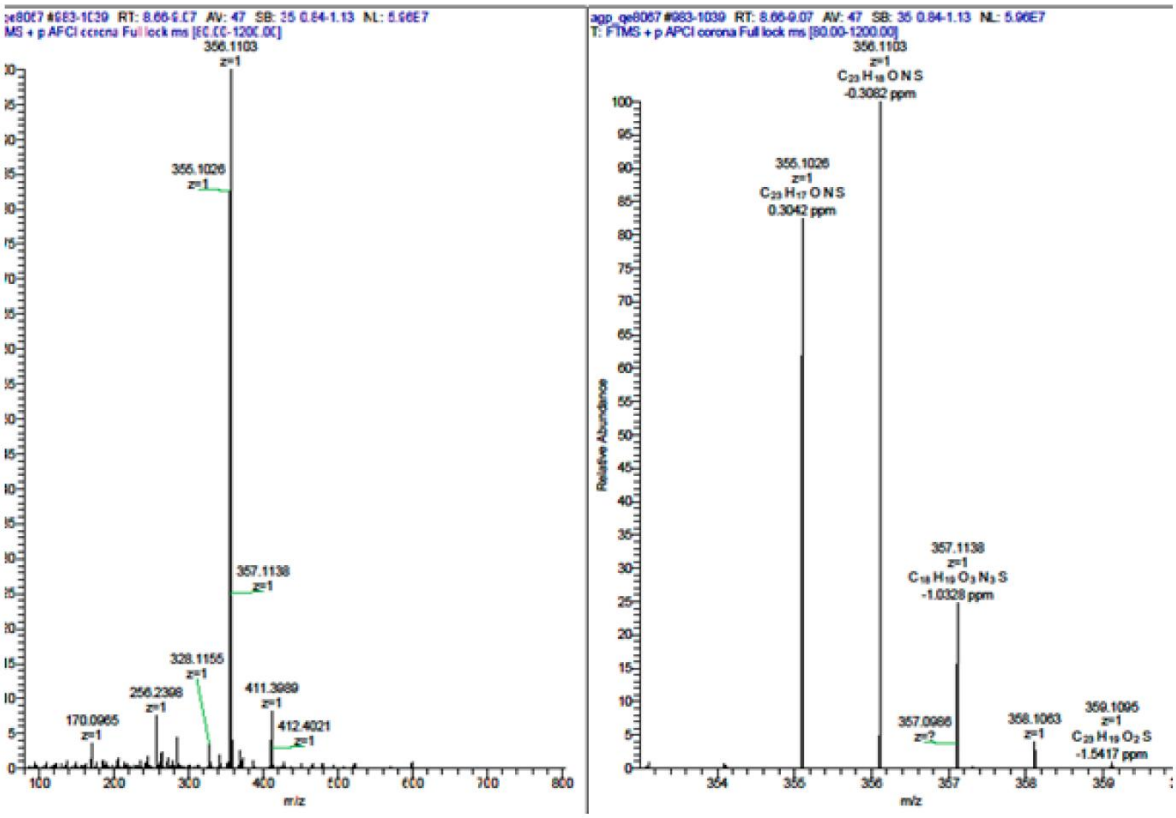

Figure S10. HRMS spectrum.

Spectra of AS2

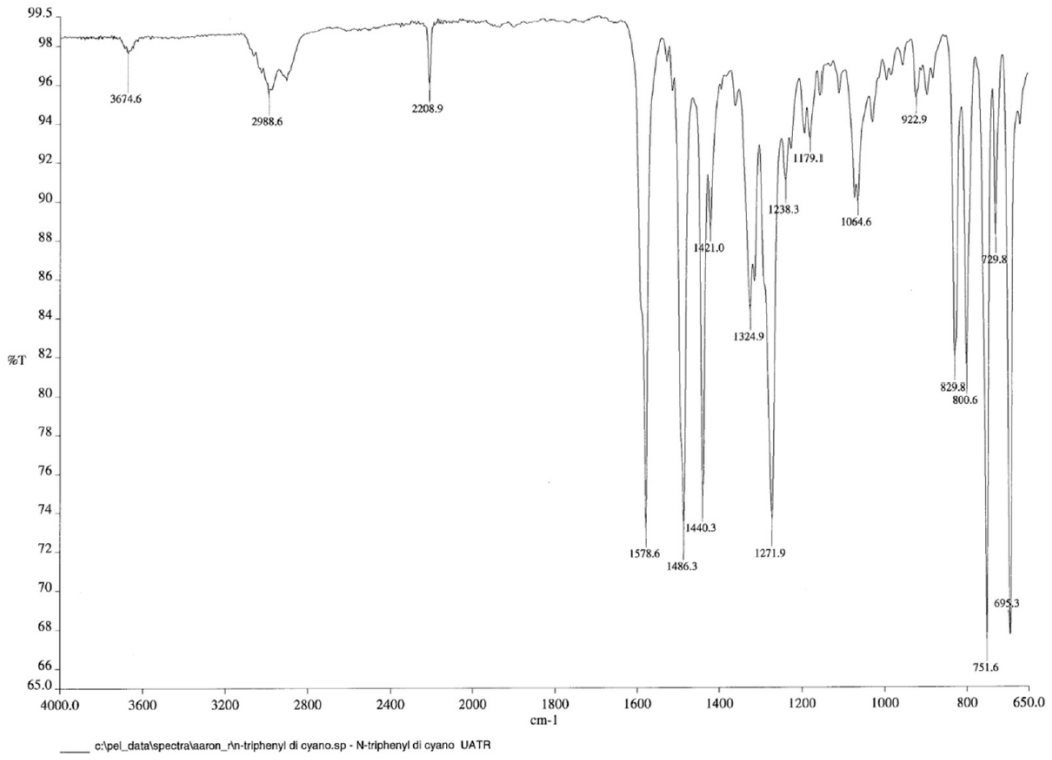

Figure S11. IR spectrum.

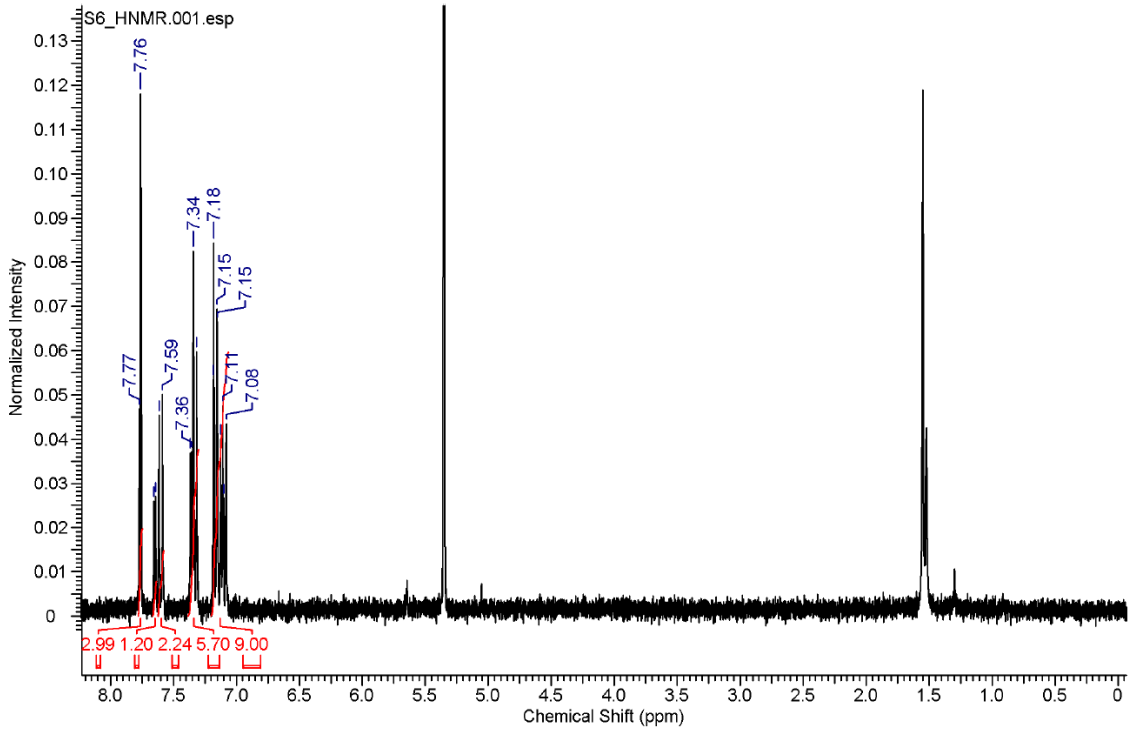

Figure S12. ^{1}H-NMR spectrum in CD_2Cl_2.

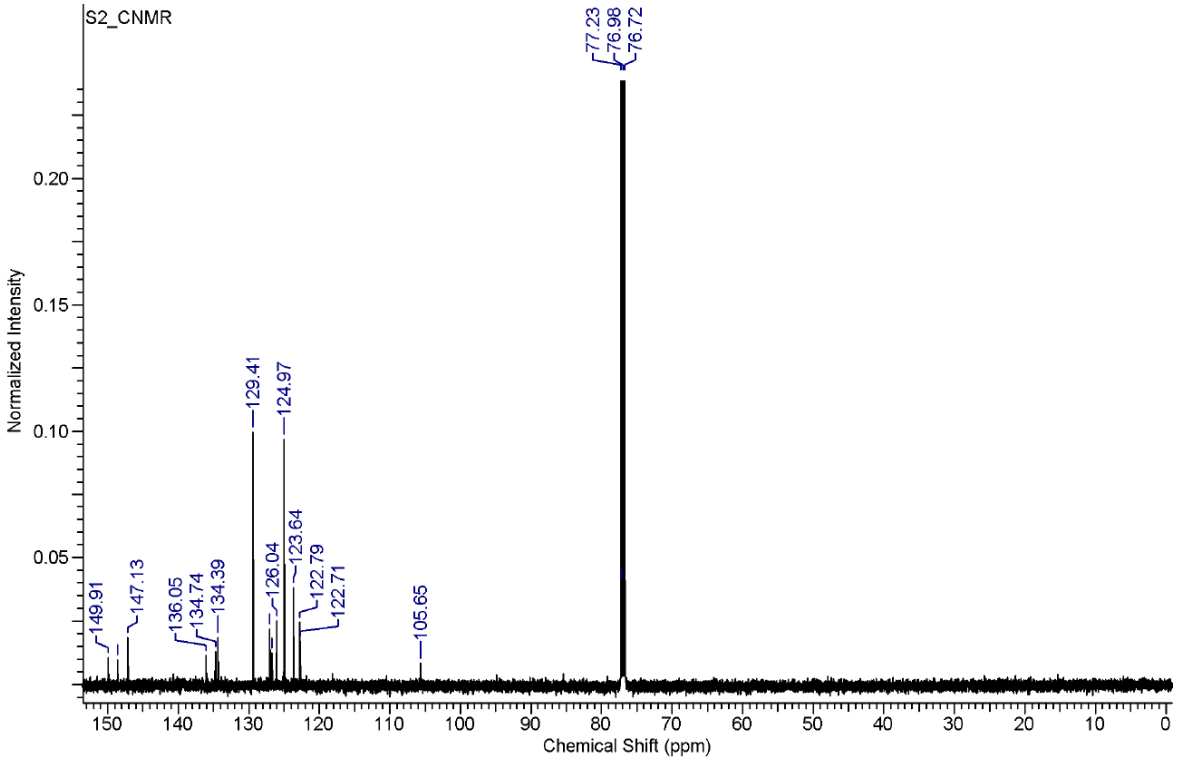

Figure S13. ^{13}C-NMR spectrum in $CDCl_3$.

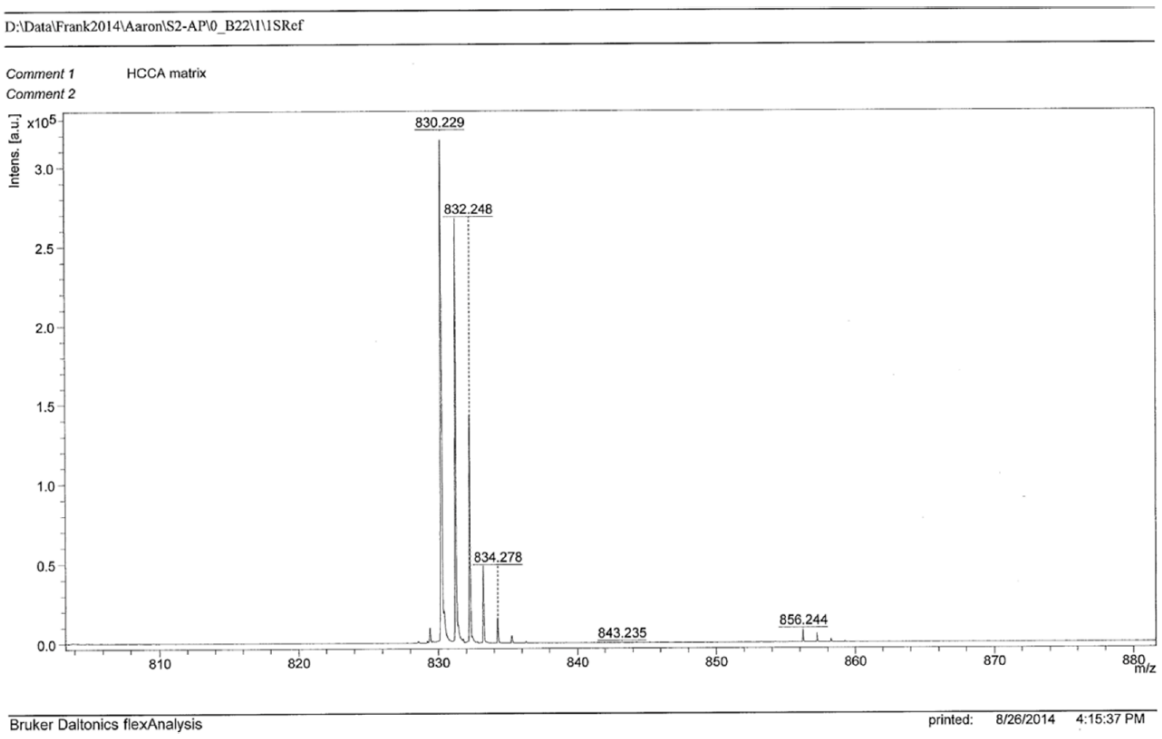

Figure S14. LRMS (MALDI-TOF) spectrum.

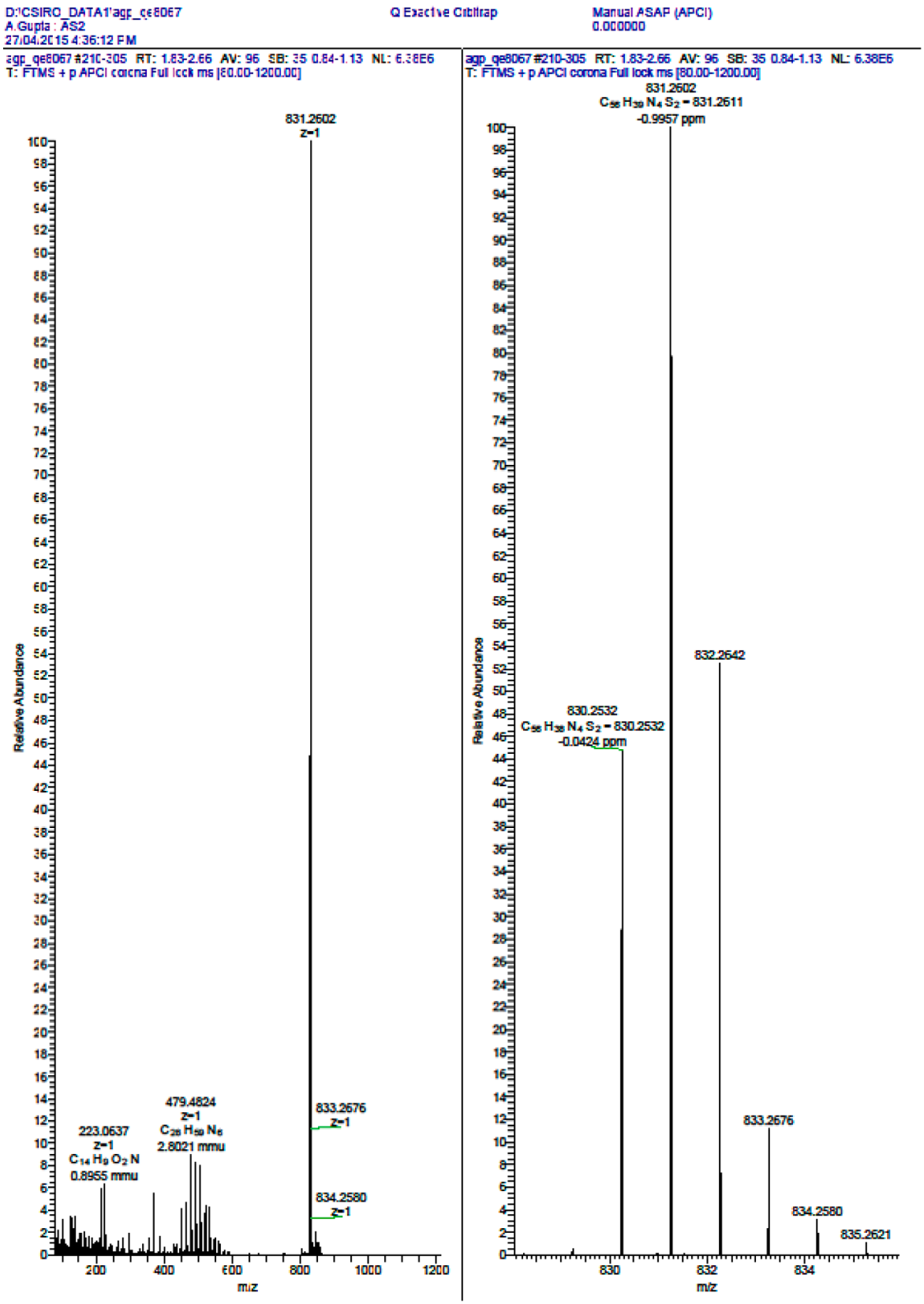

Figure S15. HRMS spectrum.

Check CIF of AS2

checkCIF/PLATON report

Structure factors have been supplied for datablock(s) shelxl

THIS REPORT IS FOR GUIDANCE ONLY. IF USED AS PART OF A REVIEW PROCEDURE FOR PUBLICATION, IT SHOULD NOT REPLACE THE EXPERTISE OF AN EXPERIENCED CRYSTALLOGRAPHIC REFEREE.

No syntax errors found. CIF dictionary Interpreting this report

Datablock: shelxl

```
Bond precision:  C-C = 0.0038 A          Wavelength=0.71073

Cell:          a=7.1570(19)      b=12.326(3)      c=14.492(4)
               alpha=82.712(6)   beta=89.825(7)   gamma=86.756(6)
Temperature:   200 K

                Calculated                Reported
Volume          1266.1(6)                 1266.1(6)
Space group     P -1                      P -1
Hall group      -P 1                      -P 1
Moiety formula  C56 H38 N4 S2, 2(C H Cl3)  C56 H38 N4 S2, 2(C H Cl3)
Sum formula     C58 H40 Cl6 N4 S2         C58 H40 Cl6 N4 S2
Mr              1069.76                   1069.76
Dx,g cm-3       1.403                     1.403
Z               1                         1
Mu (mm-1)       0.466                     0.464
F000            550.0                     550.0
F000'           551.29
h,k,lmax        10,18,22                  10,18,22
Nref            9484                      9484
Tmin,Tmax       0.889,0.984               0.889,0.984
Tmin'           0.873

Correction method= # Reported T Limits: Tmin=0.889 Tmax=0.984
AbsCorr = MULTI-SCAN

Data completeness= 1.000          Theta(max)= 32.950

R(reflections)= 0.0682( 5479)     wR2(reflections)= 0.2391( 9484)

S = 1.017                 Npar= 316
```

```
The following ALERTS were generated. Each ALERT has the format
      test-name_ALERT_alert-type_alert-level.
Click on the hyperlinks for more details of the test.
```

Figure S16. *Cont.*

Alert level C

```
PLAT244_ALERT_4_C Low   'Solvent' Ueq as Compared to Neighbors of         C29 Check
PLAT790_ALERT_4_C Centre of Gravity not Within Unit Cell: Resd.  #          1 Note
             C56 H38 N4 S2
```

Alert level G

```
PLAT066_ALERT_1_G Predicted and Reported Tmin&Tmax Range Identical          ? Check
PLAT072_ALERT_2_G SHELXL First  Parameter in WGHT Unusually Large.       0.12 Report
PLAT804_ALERT_5_G Number of ARU-Code Packing Problem(s) in PLATON           1 Info
```

```
   0 ALERT level A = Most likely a serious problem - resolve or explain
   0 ALERT level B = A potentially serious problem, consider carefully
   2 ALERT level C = Check. Ensure it is not caused by an omission or oversight
   3 ALERT level G = General information/check it is not something unexpected

   1 ALERT type 1 CIF construction/syntax error, inconsistent or missing data
   1 ALERT type 2 Indicator that the structure model may be wrong or deficient
   0 ALERT type 3 Indicator that the structure quality may be low
   2 ALERT type 4 Improvement, methodology, query or suggestion
   1 ALERT type 5 Informative message, check
```

It is advisable to attempt to resolve as many as possible of the alerts in all categories. Often the minor alerts point to easily fixed oversights, errors and omissions in your CIF or refinement strategy, so attention to these fine details can be worthwhile. In order to resolve some of the more serious problems it may be necessary to carry out additional measurements or structure refinements. However, the purpose of your study may justify the reported deviations and the more serious of these should normally be commented upon in the discussion or experimental section of a paper or in the "special_details" fields of the CIF. checkCIF was carefully designed to identify outliers and unusual parameters, but every test has its limitations and alerts that are not important in a particular case may appear. Conversely, the absence of alerts does not guarantee there are no aspects of the results needing attention. It is up to the individual to critically assess their own results and, if necessary, seek expert advice.

Publication of your CIF in IUCr journals

A basic structural check has been run on your CIF. These basic checks will be run on all CIFs submitted for publication in IUCr journals (*Acta Crystallographica*, *Journal of Applied Crystallography*, *Journal of Synchrotron Radiation*); however, if you intend to submit to *Acta Crystallographica Section C* or *E*, you should make sure that full publication checks are run on the final version of your CIF prior to submission.

Publication of your CIF in other journals

Please refer to the *Notes for Authors* of the relevant journal for any special instructions relating to CIF submission.

PLATON version of 29/01/2015; check.def file version of 29/01/2015

Figure S16. *Cont.*

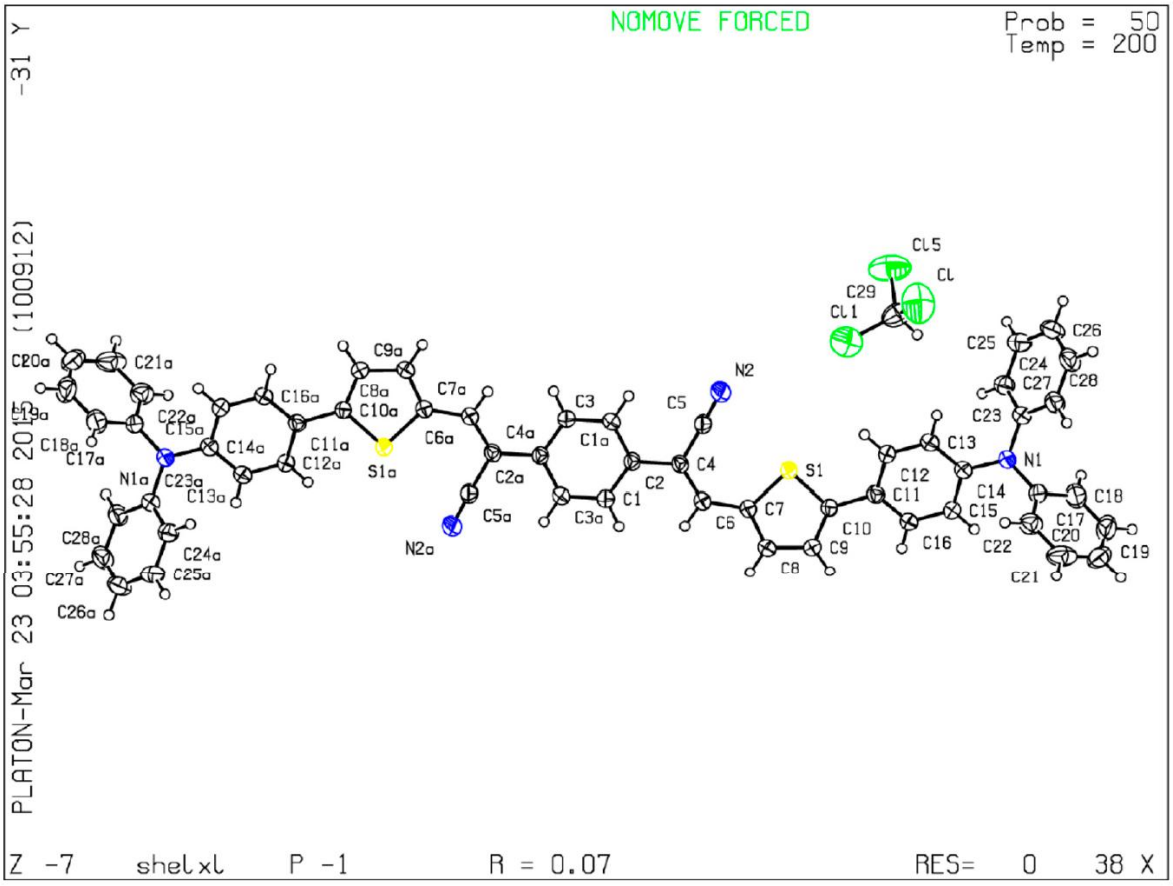

Figure S16. CIF of AS2.

Check CIF of aldehyde (1)

checkCIF/PLATON report

Structure factors have been supplied for datablock(s) shelxl

THIS REPORT IS FOR GUIDANCE ONLY. IF USED AS PART OF A REVIEW PROCEDURE FOR PUBLICATION, IT SHOULD NOT REPLACE THE EXPERTISE OF AN EXPERIENCED CRYSTALLOGRAPHIC REFEREE.

No syntax errors found. CIF dictionary Interpreting this report

Datablock: shelxl

```
Bond precision:  C-C = 0.0041 A          Wavelength=0.71073

Cell:            a=19.916(3)     b=6.6680(9)        c=13.4336(16)
                 alpha=90        beta=96.613(3)     gamma=90
Temperature:     200 K

                 Calculated                  Reported
Volume           1772.1(4)                   1772.1(4)
Space group      P 21/c                      P 21/c
Hall group       -P 2ybc                     -P 2ybc
Moiety formula   C23 H17 N O S               C23 H17 N O S
Sum formula      C23 H17 N O S               C23 H17 N O S
Mr               355.44                      355.43
Dx,g cm-3        1.332                       1.332
Z                4                           4
Mu (mm-1)        0.194                       0.194
F000             744.0                       744.0
F000'            744.77
h,k,lmax         23,7,15                     23,7,15
Nref             2883                        2883
Tmin,Tmax        0.982,0.988                 0.982,0.988
Tmin'            0.945

Correction method= # Reported T Limits: Tmin=0.982 Tmax=0.988
AbsCorr = MULTI-SCAN

Data completeness= 1.000          Theta(max)= 24.294

R(reflections)= 0.0412( 2029)     wR2(reflections)= 0.1274( 2883)

S = 0.949                  Npar= 235
```

The following ALERTS were generated. Each ALERT has the format
test-name_ALERT_alert-type_alert-level.
Click on the hyperlinks for more details of the test.

Figure S17. *Cont.*

Alert level C

```
CRYSC01_ALERT_1_C No recognised colour has been given for crystal colour.
THETM01_ALERT_3_C  The value of sine(theta_max)/wavelength is less than 0.590
           Calculated sin(theta_max)/wavelength =    0.5789
PLAT230_ALERT_2_C Hirshfeld Test Diff for    C15    --  C16     ..        6.0 su
PLAT340_ALERT_3_C Low Bond Precision on  C-C Bonds ..............     0.0041 Ang.
```

Alert level G

```
PLAT066_ALERT_1_G Predicted and Reported Tmin&Tmax Range Identical          ? Check
```

```
   0 ALERT level A = Most likely a serious problem - resolve or explain
   0 ALERT level B = A potentially serious problem, consider carefully
   4 ALERT level C = Check. Ensure it is not caused by an omission or oversight
   1 ALERT level G = General information/check it is not something unexpected

   2 ALERT type 1 CIF construction/syntax error, inconsistent or missing data
   1 ALERT type 2 Indicator that the structure model may be wrong or deficient
   2 ALERT type 3 Indicator that the structure quality may be low
   0 ALERT type 4 Improvement, methodology, query or suggestion
   0 ALERT type 5 Informative message, check
```

It is advisable to attempt to resolve as many as possible of the alerts in all categories. Often the minor alerts point to easily fixed oversights, errors and omissions in your CIF or refinement strategy, so attention to these fine details can be worthwhile. In order to resolve some of the more serious problems it may be necessary to carry out additional measurements or structure refinements. However, the purpose of your study may justify the reported deviations and the more serious of these should normally be commented upon in the discussion or experimental section of a paper or in the "special_details" fields of the CIF. checkCIF was carefully designed to identify outliers and unusual parameters, but every test has its limitations and alerts that are not important in a particular case may appear. Conversely, the absence of alerts does not guarantee there are no aspects of the results needing attention. It is up to the individual to critically assess their own results and, if necessary, seek expert advice.

Publication of your CIF in IUCr journals

A basic structural check has been run on your CIF. These basic checks will be run on all CIFs submitted for publication in IUCr journals (*Acta Crystallographica*, *Journal of Applied Crystallography*, *Journal of Synchrotron Radiation*); however, if you intend to submit to *Acta Crystallographica Section C* or *E*, you should make sure that full publication checks are run on the final version of your CIF prior to submission.

Publication of your CIF in other journals

Please refer to the *Notes for Authors* of the relevant journal for any special instructions relating to CIF submission.

PLATON version of 29/01/2015; check.def file version of 29/01/2015

Figure S17. *Cont.*

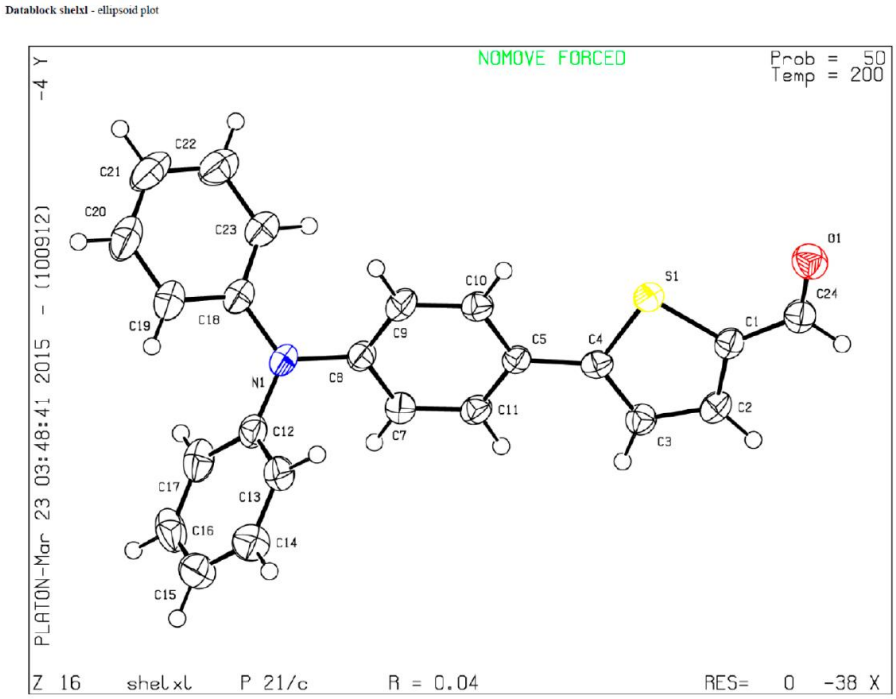

Figure S17. CIF of aldehyde (**1**).

Table S1. Fractional Atomic Coordinates (×10⁴) and Equivalent Isotropic Displacement Parameters (Å² × 10³) for AS1. U_{eq} is defined as 1/3 of of the trace of the orthogonalised U_{IJ} tensor.

Atom	*x*	*y*	*z*	U(eq)
C1	5752.3(12)	4716(4)	3672.2(17)	30.3(6)
C2	5829.3(13)	2697(4)	3808.0(18)	35.1(6)
C3	5223.0(12)	1696(4)	3891.0(18)	32.6(6)
C4	4675.4(12)	2960(4)	3813.6(16)	28.2(6)
C5	3966.4(12)	2440(4)	3880.9(16)	27.0(6)
C7	3111.3(13)	−74(4)	4010.9(19)	35.4(7)
C8	2621.7(12)	1390(4)	4097.2(18)	32.0(6)
C9	2810.6(13)	3393(4)	4052.0(19)	36.7(7)
C10	3470.5(13)	3895(4)	3938.4(18)	33.4(6)
C11	3768.0(13)	449(4)	3913.5(18)	32.8(6)
C12	1931.8(13)	−686(4)	5047(2)	34.9(6)
C13	2309.2(13)	−395(4)	5974(2)	38.9(7)
C14	2289.5(16)	−1798(5)	6724(2)	52.8(8)
C15	1904.4(16)	−3467(5)	6581(3)	55.4(9)
C16	1535.0(16)	−3794(4)	5665(3)	55.1(9)
C17	1546.8(14)	−2421(4)	4886(2)	46.0(8)
C18	1375.7(13)	1828(4)	3883(2)	36.0(6)
C19	800.6(13)	1790(5)	4385(2)	45.0(7)
C20	228.3(15)	2830(5)	4004(3)	57.1(9)
C21	217.0(16)	3932(5)	3133(3)	61.4(10)
C22	782.5(15)	3966(5)	2634(2)	52.8(8)
C23	1354.5(14)	2913(4)	3002(2)	40.9(7)
C24	6278.6(14)	6183(4)	3599.4(19)	36.0(6)
N1	1964.5(10)	769(3)	4274.5(16)	38.5(6)
O1	6199.3(9)	7976(3)	3532.4(13)	43.4(5)
S1	4917.2(3)	5401.6(10)	3636.0(5)	32.8(2)

Table S2. Anisotropic Displacement Parameters ($Å^2 \times 10^3$) for AS1. The Anisotropic displacement factor exponent takes the form: $-2\pi^2[h^2a^{*2}U_{11}+2hka^*b^*U_{12}+\ldots]$.

Atom	U_{11}	U_{22}	U_{33}	U_{23}	U_{13}	U_{12}
C1	27.6(14)	40.5(17)	22.5(13)	−1.1(11)	1.5(10)	1.3(12)
C2	30.0(14)	38.3(17)	36.8(15)	−2.4(12)	3.2(11)	6.9(12)
C3	31.3(14)	31.4(16)	35.1(15)	−2.0(11)	4.1(11)	1.3(12)
C4	33.2(14)	32.1(15)	18.8(13)	−1.1(11)	1.2(10)	3.0(12)
C5	26.8(13)	34.0(16)	20.1(12)	0.6(11)	2.2(10)	2.5(11)
C7	32.1(15)	34.9(16)	39.2(16)	1.7(12)	4.2(12)	−0.5(12)
C8	25.9(14)	39.4(17)	30.5(14)	3.3(12)	2.1(11)	2.2(12)
C9	28.2(14)	41.6(18)	40.3(16)	−0.9(13)	3.8(12)	7.7(12)
C10	34.3(15)	30.8(15)	34.8(15)	1.0(12)	3.7(11)	3.5(12)
C11	30.6(14)	34.3(16)	33.5(15)	1.4(12)	4.4(11)	7.2(12)
C12	26.2(14)	35.1(16)	44.3(16)	−0.8(13)	7.7(12)	2.2(12)
C13	34.5(16)	37.9(17)	44.3(17)	0.4(14)	4.1(12)	−5.1(13)
C14	49.5(19)	58(2)	51.3(19)	8.5(16)	7.3(14)	2.9(16)
C15	51(2)	49(2)	70(2)	16.5(17)	19.0(17)	6.8(16)
C16	45.0(19)	28.5(17)	97(3)	−4.8(18)	29.9(19)	−6.8(14)
C17	32.9(16)	47(2)	58.3(19)	−14.6(16)	6.7(13)	−4.7(13)
C18	28.7(15)	37.2(16)	41.1(16)	−6.8(13)	−0.3(12)	2.4(12)
C19	30.7(16)	49.4(19)	54.9(19)	−6.4(15)	4.8(13)	−0.5(13)
C20	30.1(16)	58(2)	83(2)	−10.1(19)	5.0(16)	4.4(15)
C21	38.0(19)	54(2)	87(3)	−3.1(19)	−15.8(17)	12.0(15)
C22	45(2)	48(2)	61(2)	−1.3(16)	−10.7(16)	5.2(15)
C23	34.1(15)	43.2(17)	44.0(17)	−4.7(14)	−1.5(12)	3.9(13)
C24	34.1(15)	43.5(18)	30.1(15)	−0.7(13)	2.7(11)	−0.6(13)
N1	23.0(12)	47.9(15)	43.7(14)	8.6(11)	0.7(10)	2.8(10)
O1	45.2(12)	41.5(13)	43.0(12)	0.3(9)	2.5(9)	−4.7(10)
S1	30.1(4)	34.4(4)	33.6(4)	3.1(3)	2.5(3)	3.0(3)

Table S3. Bond Lengths for **AS1**.

Atom	Atom	Length/Å	Atom	Atom	Length/Å
C1	C2	1.365(4)	C12	C13	1.392(4)
C1	C24	1.445(4)	C12	N1	1.428(3)
C1	S1	1.720(2)	C13	C14	1.379(4)
C2	C3	1.396(4)	C14	C15	1.353(4)
C3	C4	1.373(3)	C15	C16	1.377(5)
C4	C5	1.467(3)	C16	C17	1.392(4)
C4	S1	1.722(3)	C18	C23	1.384(4)
C5	C11	1.387(4)	C18	C19	1.395(4)
C5	C10	1.393(3)	C18	N1	1.417(3)
C7	C11	1.374(3)	C19	C20	1.381(4)
C7	C8	1.394(4)	C20	C21	1.379(5)
C8	C9	1.391(4)	C21	C22	1.376(5)
C8	N1	1.419(3)	C22	C23	1.380(4)
C9	C10	1.382(4)	C24	O1	1.208(3)
C12	C17	1.391(4)			

Table S4. Bond Angles for **AS1**.

Atom	Atom	Atom	Angle/°	Atom	Atom	Atom	Angle/°
C2	C1	C24	127.3(2)	C13	C12	N1	119.4(2)
C2	C1	S1	111.1(2)	C14	C13	C12	120.1(3)
C24	C1	S1	121.6(2)	C15	C14	C13	121.2(3)
C1	C2	C3	113.4(2)	C14	C15	C16	119.5(3)
C4	C3	C2	112.8(2)	C15	C16	C17	120.9(3)
C3	C4	C5	127.7(2)	C12	C17	C16	119.1(3)
C3	C4	S1	111.02(19)	C23	C18	C19	118.5(2)
C5	C4	S1	121.25(18)	C23	C18	N1	121.4(2)
C11	C5	C10	117.3(2)	C19	C18	N1	120.1(3)
C11	C5	C4	120.5(2)	C20	C19	C18	120.0(3)
C10	C5	C4	122.2(2)	C21	C20	C19	121.0(3)
C11	C7	C8	120.8(3)	C22	C21	C20	119.2(3)
C9	C8	C7	118.3(2)	C21	C22	C23	120.4(3)
C9	C8	N1	123.2(2)	C22	C23	C18	121.0(3)
C7	C8	N1	118.5(2)	O1	C24	C1	125.8(3)
C10	C9	C8	120.2(2)	C18	N1	C8	122.1(2)
C9	C10	C5	121.8(3)	C18	N1	C12	120.2(2)
C7	C11	C5	121.6(2)	C8	N1	C12	116.1(2)
C17	C12	C13	119.1(3)	C1	S1	C4	91.70(12)
C17	C12	N1	121.5(3)				

Table S5. Torsion Angles for **AS1**.

A	B	C	D	Angle/°	A	B	C	D	Angle/°
C24	C1	C2	C3	177.4(2)	C23	C18	C19	C20	−0.4(4)
S1	C1	C2	C3	−0.5(3)	N1	C18	C19	C20	179.8(3)
C1	C2	C3	C4	0.3(3)	C18	C19	C20	C21	−0.7(5)
C2	C3	C4	C5	−179.0(2)	C19	C20	C21	C22	0.9(5)
C2	C3	C4	S1	0.0(3)	C20	C21	C22	C23	−0.1(5)
C3	C4	C5	C11	−8.2(4)	C21	C22	C23	C18	−0.9(5)
S1	C4	C5	C11	172.89(18)	C19	C18	C23	C22	1.2(4)
C3	C4	C5	C10	170.3(2)	N1	C18	C23	C22	−179.0(3)
S1	C4	C5	C10	−8.7(3)	C2	C1	C24	O1	−175.8(3)
C11	C7	C8	C9	1.9(4)	S1	C1	C24	O1	1.8(4)
C11	C7	C8	N1	−175.1(2)	C23	C18	N1	C8	28.6(4)
C7	C8	C9	C10	−0.9(4)	C19	C18	N1	C8	−151.6(3)
N1	C8	C9	C10	176.0(2)	C23	C18	N1	C12	−165.9(2)
C8	C9	C10	C5	−1.0(4)	C19	C18	N1	C12	13.9(4)
C11	C5	C10	C9	1.8(4)	C9	C8	N1	C18	36.5(4)
C4	C5	C10	C9	−176.7(2)	C7	C8	N1	C18	−146.6(2)
C8	C7	C11	C5	−1.1(4)	C9	C8	N1	C12	−129.5(3)
C10	C5	C11	C7	−0.8(4)	C7	C8	N1	C12	47.3(3)
C4	C5	C11	C7	177.7(2)	C17	C12	N1	C18	64.0(3)
C17	C12	C13	C14	−1.1(4)	C13	C12	N1	C18	−118.0(3)
N1	C12	C13	C14	−179.2(2)	C17	C12	N1	C8	−129.7(3)
C12	C13	C14	C15	−0.4(5)	C13	C12	N1	C8	48.3(3)
C13	C14	C15	C16	1.3(5)	C2	C1	S1	C4	0.41(19)
C14	C15	C16	C17	−0.7(5)	C24	C1	S1	C4	−177.6(2)
C13	C12	C17	C16	1.7(4)	C3	C4	S1	C1	−0.26(19)
N1	C12	C17	C16	179.7(2)	C5	C4	S1	C1	178.83(19)
C15	C16	C17	C12	−0.8(4)					

Table S6. Fractional Atomic Coordinates (×10⁴) and Equivalent Isotropic Displacement Parameters (Å² × 10³) for **AS2**. U_{eq} is defined as 1/3 of of the trace of the orthogonalised U_{IJ} tensor.

Atom	*x*	*y*	*z*	U(eq)
Cl	7297(2)	8374.8(13)	4936.0(9)	108.9(5)
Cl1	5445.2(18)	9262.2(9)	3228.2(8)	86.0(3)
Cl5	8022(3)	10543.6(11)	4045.7(12)	121.1(5)
S1	2804.4(8)	7696.3(5)	1111.9(4)	31.81(15)
N1	10844(3)	5259.8(17)	2946.1(17)	43.8(5)
N2	55(3)	9454(2)	2006.3(17)	50.1(6)
C1	-4197(3)	9256.6(19)	-540.2(17)	34.6(5)
C2	-3211(3)	9486.8(17)	235.6(15)	28.8(4)
C3	-4060(3)	10242.3(19)	770.1(16)	33.9(5)
C4	-1349(3)	8959.6(17)	485.5(15)	29.2(4)
C5	-550(3)	9224(2)	1335.1(17)	34.5(5)
C6	-381(3)	8274.0(18)	-23.9(16)	32.1(4)
C7	1397(3)	7689.8(18)	144.0(16)	31.1(4)
C8	2247(3)	7027.6(19)	-454.4(18)	37.2(5)
C9	3978(3)	6536.4(19)	-137.8(18)	36.7(5)
C10	4469(3)	6812.1(17)	715.9(15)	29.0(4)
C11	6161(3)	6445.9(17)	1281.1(16)	30.6(4)
C12	6292(3)	6674.8(19)	2197.7(17)	35.6(5)
C13	7829(4)	6300(2)	2744.1(18)	38.5(5)
C14	9294(3)	5680.9(19)	2394.7(17)	36.1(5)
C15	9185(3)	5474(2)	1468.7(18)	38.6(5)
C16	7644(3)	5854.4(19)	925.7(17)	34.9(5)
C17	11744(3)	4241.5(19)	2801.9(17)	36.7(5)
C18	13673(4)	4151(3)	2685(2)	52.1(7)
C19	14551(5)	3157(4)	2576(2)	70.1(11)
C20	13539(7)	2244(3)	2582(2)	74.2(12)
C21	11637(7)	2323(3)	2676(2)	67.7(10)
C22	10725(4)	3324(2)	2796(2)	48.7(6)
C23	11500(3)	5811(2)	3678.0(17)	36.2(5)
C24	11505(4)	6945(2)	3570.8(18)	39.9(5)
C25	12169(4)	7464(2)	4288(2)	47.2(6)
C26	12870(4)	6869(3)	5096(2)	52.8(7)
C27	12874(4)	5751(3)	5196(2)	52.5(7)
C28	12179(4)	5213(2)	4497(2)	43.7(6)
C29	7506(6)	9217(3)	3893(3)	66.2(9)

Table S7. Anisotropic Displacement Parameters ($Å^2 \times 10^3$) for **AS2**. The Anisotropic displacement factor exponent takes the form: $-2\pi^2[h^2a^{*2}U_{11}+2hka^*b^*U_{12}+\ldots]$.

Atom	U_{11}	U_{22}	U_{33}	U_{23}	U_{13}	U_{12}
Cl	102.2(9)	135.6(12)	77.8(8)	28.8(7)	13.5(7)	−5.0(8)
Cl1	102.7(8)	76.1(6)	78.3(7)	−0.5(5)	1.5(6)	−16.6(6)
Cl5	156.3(14)	89.1(8)	131.6(13)	−53.0(9)	17.4(10)	−39.3(9)
S1	31.6(3)	35.2(3)	28.4(3)	−6.3(2)	−4.1(2)	4.4(2)
N1	45.1(11)	39.0(11)	48.6(13)	−17.1(9)	−20.6(10)	11.3(9)
N2	47.1(12)	65.4(15)	38.6(12)	−17.0(11)	−9(1)	12.4(11)
C1	35.3(11)	37.7(11)	31.7(11)	−10.9(9)	−4.2(9)	5.3(9)
C2	29.1(9)	28.7(9)	27.9(10)	−1.4(8)	−1.8(8)	0.8(7)
C3	35.3(11)	37.6(11)	29.4(11)	−8.6(9)	−6.4(9)	2.4(9)
C4	30.3(9)	29.2(9)	27.1(10)	−0.7(8)	−4.0(8)	−0.8(8)
C5	33.1(10)	38.6(11)	31.0(11)	−4.4(9)	−1.7(8)	4.8(9)
C6	32.2(10)	32.6(10)	31.7(11)	−5.9(8)	−6.1(8)	1.3(8)
C7	31.9(10)	30.9(10)	30.3(11)	−4.9(8)	−5.5(8)	1.7(8)
C8	40.3(12)	36.8(11)	35.8(12)	−11.5(9)	−11(1)	3.7(9)
C9	37.4(11)	35.5(11)	38.5(12)	−13.7(9)	−7.5(9)	7.1(9)
C10	30.9(10)	26.8(9)	29.1(10)	−3.4(8)	−4.2(8)	1.1(7)
C11	32.7(10)	27.7(9)	31.7(11)	−4.1(8)	−3.7(8)	−2.3(8)
C12	35.4(11)	35.9(11)	36.1(12)	−10.0(9)	−6.2(9)	6.7(9)
C13	42.4(12)	41.0(12)	33.1(12)	−11.2(10)	−9(1)	5.5(10)
C14	36.7(11)	34.3(11)	37.9(12)	−9.2(9)	−9.6(9)	2.4(9)
C15	35.6(11)	39.2(12)	42.3(13)	−14.6(10)	−7.5(10)	8.4(9)
C16	37.3(11)	36.7(11)	31.5(11)	−9.3(9)	−6.3(9)	2.6(9)
C17	41.2(12)	34.6(11)	33.8(12)	−6.5(9)	−8.0(9)	6.7(9)
C18	42.6(14)	67.9(19)	45.4(16)	−9.4(14)	−4.4(12)	4.7(13)
C19	58.9(19)	102(3)	48.4(18)	−22.2(19)	−6.5(15)	37(2)
C20	108(3)	67(2)	45.2(18)	−20.7(16)	−21.9(19)	47(2)
C21	120(3)	37.2(14)	46.0(17)	−7.0(12)	−14.3(19)	−2.0(17)
C22	57.4(16)	41.5(13)	47.6(16)	−5.6(11)	−3.5(13)	−5.2(12)
C23	36.5(11)	37.2(11)	35.8(12)	−9.9(9)	−7.0(9)	1.5(9)
C24	44.3(13)	40.0(12)	36.0(12)	−7.9(10)	−2.4(10)	−1.7(10)
C25	52.8(15)	45.8(14)	46.3(15)	−16.3(12)	0.9(12)	−8.1(12)
C26	51.9(16)	66.7(19)	44.9(16)	−24.5(14)	−7.0(12)	−8.0(14)
C27	51.5(15)	68.7(19)	36.6(14)	−6.9(13)	−10.7(12)	2.5(14)
C28	44.6(13)	42.2(13)	43.5(14)	−3.5(11)	−10.9(11)	−0.1(11)
C29	82(2)	59.1(19)	57(2)	−10.7(16)	19.0(17)	1.0(17)

Table S8. Bond Lengths for **AS2**.

Atom	Atom	Length/Å	Atom	Atom	Length/Å
Cl	C29	1.733(4)	C10	C11	1.480(3)
Cl1	C29	1.758(4)	C11	C16	1.389(3)
Cl5	C29	1.738(4)	C11	C12	1.397(3)
S1	C10	1.716(2)	C12	C13	1.380(3)
S1	C7	1.730(2)	C13	C14	1.394(3)
N1	C14	1.405(3)	C14	C15	1.401(3)
N1	C17	1.417(3)	C15	C16	1.382(3)
N1	C23	1.425(3)	C17	C22	1.381(4)
N2	C5	1.140(3)	C17	C18	1.390(4)
C1	C3 [1]	1.383(3)	C18	C19	1.371(5)
C1	C2	1.397(3)	C19	C20	1.372(6)
C2	C3	1.397(3)	C20	C21	1.366(6)
C2	C4	1.475(3)	C21	C22	1.393(4)
C3	C1 [1]	1.383(3)	C23	C24	1.386(3)
C4	C6	1.352(3)	C23	C28	1.390(4)
C4	C5	1.441(3)	C24	C25	1.386(4)
C6	C7	1.432(3)	C25	C26	1.380(4)
C7	C8	1.381(3)	C26	C27	1.367(5)
C8	C9	1.400(3)	C27	C28	1.388(4)
C9	C10	1.376(3)			

[1] 1 – X, 2 – Y, –Z.

Table S9. Bond Angles for **AS2**.

Atom	Atom	Atom	Angle/°	Atom	Atom	Atom	Angle/°
C10	S1	C7	92.58(10)	C12	C13	C14	120.7(2)
C14	N1	C17	119.77(19)	C13	C14	C15	118.2(2)
C14	N1	C23	121.57(19)	C13	C14	N1	121.8(2)
C17	N1	C23	118.61(19)	C15	C14	N1	120.0(2)
C3 [1]	C1	C2	121.3(2)	C16	C15	C14	120.7(2)
C1	C2	C3	117.25(19)	C15	C16	C11	121.2(2)
C1	C2	C4	121.8(2)	C22	C17	C18	119.2(3)
C3	C2	C4	120.97(19)	C22	C17	N1	120.5(2)
C1 [1]	C3	C2	121.4(2)	C18	C17	N1	120.2(2)
C6	C4	C5	119.67(19)	C19	C18	C17	120.2(3)
C6	C4	C2	124.7(2)	C18	C19	C20	120.5(3)
C5	C4	C2	115.61(19)	C21	C20	C19	120.1(3)
N2	C5	C4	178.5(3)	C20	C21	C22	120.2(3)
C4	C6	C7	130.6(2)	C17	C22	C21	119.8(3)
C8	C7	C6	124.4(2)	C24	C23	C28	119.6(2)
C8	C7	S1	109.62(16)	C24	C23	N1	120.4(2)
C6	C7	S1	125.96(17)	C28	C23	N1	120.0(2)
C7	C8	C9	114.1(2)	C23	C24	C25	119.4(2)
C10	C9	C8	112.6(2)	C26	C25	C24	121.0(3)
C9	C10	C11	128.6(2)	C27	C26	C25	119.4(2)
C9	C10	S1	111.14(16)	C26	C27	C28	120.7(3)
C11	C10	S1	120.25(16)	C27	C28	C23	119.9(3)
C16	C11	C12	118.1(2)	Cl	C29	Cl5	112.8(2)
C16	C11	C10	121.4(2)	Cl	C29	Cl1	110.7(2)
C12	C11	C10	120.5(2)	Cl5	C29	Cl1	109.2(2)
C13	C12	C11	121.1(2)				

[1] 1 – X, 2 – Y, –Z.

Table S10. Torsion Angles for **AS2**.

A	B	C	D	Angle/°	A	B	C	D	Angle/°
C3[1]	C1	C2	C3	0.1(4)	C17	N1	C14	C15	−32.7(4)
C3[1]	C1	C2	C4	−179.8(2)	C23	N1	C14	C15	149.9(3)
C1	C2	C3	C1[1]	−0.1(4)	C13	C14	C15	C16	−1.4(4)
C4	C2	C3	C1[1]	179.8(2)	N1	C14	C15	C16	178.0(2)
C1	C2	C4	C6	4.2(4)	C14	C15	C16	C11	−0.3(4)
C3	C2	C4	C6	−175.7(2)	C12	C11	C16	C15	1.9(4)
C1	C2	C4	C5	−176.3(2)	C10	C11	C16	C15	−177.2(2)
C3	C2	C4	C5	3.8(3)	C14	N1	C17	C22	−52.5(4)
C5	C4	C6	C7	2.3(4)	C23	N1	C17	C22	125.1(3)
C2	C4	C6	C7	−178.3(2)	C14	N1	C17	C18	128.9(3)
C4	C6	C7	C8	−178.5(3)	C23	N1	C17	C18	−53.5(4)
C4	C6	C7	S1	1.6(4)	C22	C17	C18	C19	−0.8(4)
C10	S1	C7	C8	−0.8(2)	N1	C17	C18	C19	177.8(3)
C10	S1	C7	C6	179.2(2)	C17	C18	C19	C20	−0.1(5)
C6	C7	C8	C9	−179.6(2)	C18	C19	C20	C21	1.5(5)
S1	C7	C8	C9	0.3(3)	C19	C20	C21	C22	−2.1(5)
C7	C8	C9	C10	0.5(3)	C18	C17	C22	C21	0.2(4)
C8	C9	C10	C11	178.8(2)	N1	C17	C22	C21	−178.4(3)
C8	C9	C10	S1	−1.0(3)	C20	C21	C22	C17	1.3(5)
C7	S1	C10	C9	1.03(19)	C14	N1	C23	C24	−38.4(4)
C7	S1	C10	C11	−178.84(19)	C17	N1	C23	C24	144.1(3)
C9	C10	C11	C16	9.1(4)	C14	N1	C23	C28	143.1(3)
S1	C10	C11	C16	−171.08(18)	C17	N1	C23	C28	−34.4(4)
C9	C10	C11	C12	−170.0(2)	C28	C23	C24	C25	−0.8(4)
S1	C10	C11	C12	9.9(3)	N1	C23	C24	C25	−179.3(3)
C16	C11	C12	C13	−1.7(4)	C23	C24	C25	C26	1.8(4)
C10	C11	C12	C13	177.4(2)	C24	C25	C26	C27	−1.3(5)
C11	C12	C13	C14	0.0(4)	C25	C26	C27	C28	−0.1(5)
C12	C13	C14	C15	1.6(4)	C26	C27	C28	C23	1.1(5)
C12	C13	C14	N1	−177.9(2)	C24	C23	C28	C27	−0.7(4)
C17	N1	C14	C13	146.8(3)	N1	C23	C28	C27	177.9(3)
C23	N1	C14	C13	−30.7(4)					

3.0 A diketopyrrolopyrrole and benzothiadiazole based small molecule electron acceptor: design, synthesis, characterization and photovoltaic properties

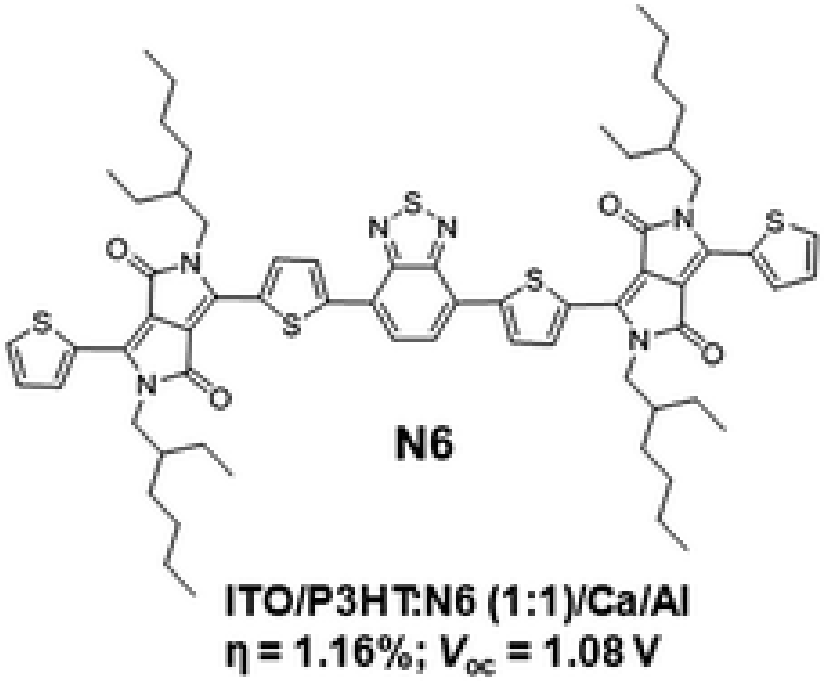

Journal article published in *RSC Adv.* **2014**, *4*, 57635-57638 presented as **Chapter 3**.

RSC Advances

COMMUNICATION

View Article Online
View Journal | View Issue

Cite this: *RSC Adv.*, 2014, **4**, 57635

Received 3rd September 2014
Accepted 30th October 2014

DOI: 10.1039/c4ra09668a

www.rsc.org/advances

A diketopyrrolopyrrole and benzothiadiazole based small molecule electron acceptor: design, synthesis, characterization and photovoltaic properties†

Aaron M. Raynor,[a] Akhil Gupta,*[ab] Hemlata Patil,[a] Ante Bilic[c] and Sheshanath V. Bhosale*[a]

A novel solution-processable electron acceptor based on diketopyrrolopyrrole and benzothiadiazole building blocks was designed and synthesized, which exhibited excellent solubility and thermal stability, and afforded 1.16% power conversion efficiency with high open-circuit voltage (1.08 V) when tested with the classical poly(3-hexylthiophene) electron donor in bulk-heterojunction solar cells. The open-circuit voltage reported here (~1.1 V) is among the highest values for a single bulk-heterojunction device.

Research into organic-based bulk-heterojunction (BHJ) solar cells has surged in the past decade. These organic cells have huge potential for the fabrication of low-cost, flexible and light weight photovoltaic devices.[1] From the materials perspective, more research has been focused on the design and development of donor materials.[2] Donor functionalities such as the archetypal polymer poly(3-hexylthiophene) (P3HT), conjugated polymers and small molecules have been investigated in conjunction with fullerenes and their soluble derivatives, such as [6,6]-phenyl-C_{61}-butyric acid methyl ester ($PC_{61}BM$), as electron acceptor materials.[3] Power conversion efficiencies (PCEs) have exceeded the 10% mark for polymer donors and fullerene acceptors.[4] The latter are the choice of dominant electron acceptor materials in BHJ research as they provide high electron mobility, large electron affinity, excellent solubility and the ability to form a favourable nanoscale network with donor materials.[5] However, these high performing fullerene acceptors are afflicted by a number of potential disadvantages, such as weak absorption in the visible spectrum and restricted electronic tuning *via* structural modification. Also, a large electron affinity can result in a low open-circuit voltage (V_{oc}).[6] These inadequacies with fullerenes provide a strong stimulus to develop non-fullerene electron acceptors which can exert broad absorption, good solubility, high charge carrier mobility and matching energy levels with those of donors.

Recently, non-fullerene electron acceptors have been developed[7] and PCEs exceeding 2% and 4% have been reported using conventional P3HT and non-P3HT donors, respectively.[8] This progress is inspiring, however, there still remain a plethora of incentives to develop new electron acceptors that will not only overcome the insufficiencies associated with fullerenes but will also exhibit properties such as strong optical absorption, photochemical stability and excellent solubility. One of the common strategies to tailor properties of electron acceptors is to introduce/accumulate electron-withdrawing building blocks and to make an elongated conjugated system. Functionalities such as diketopyrrolopyrrole (DPP), naphthalenediimide (NDI) and perylene diimide (PDI) not only serve this purpose, but also demonstrate good thermal and chemical stability at molecular level. Furthermore, attachment of alkyl chains on the nitrogen atoms of such functionalities not only enhances the solubility, but also helps to generate excellent films without crystallization. Such stated reasons encourage us to pursue research for the development of new electron acceptors based on DPP functionality. The present work is in continuation of our efforts on the development of small molecular chromophores for organic solar cells.[9]

Herein we design, theoretically calculate, synthesize and characterize a DPP-based chromophore (**N6**, Fig. 1) where bulky peripheral DPP substituents are connected through a small-sized benzo[*c*][1,2,5]thiadiazole (BTD) functionality used as a central core.

We envisioned that the connection of DPP and BTD functionalities can provide highly conjugated chromophore with good planarity, high chemical and thermal stability, and with adequate solubility. **N6** was applied in solution-processable BHJ devices as an electron acceptor along with the classical polymer

[a]*School of Applied Sciences, RMIT University, GPO Box 2476, Melbourne, Victoria 3001, Australia. E-mail: sheshanath.bhosale@rmit.edu.au; Tel: +61 3 9925 2680*

[b]*Medicinal Chemistry, Monash Institute of Pharmaceutical Sciences, Monash University, Parkville, Victoria 3052, Australia. E-mail: akhil.gupta@monash.edu; Tel: +61 3 9903 9599*

[c]*CSIRO Manufacturing, Virtual Nanoscience Lab, Parkville, Victoria 3052, Australia*

† Electronic supplementary information (ESI) available: Synthetic details & characterization, DFT diagrams, PESA spectrum, TGA, DSC and IPCE spectra of **N6**. See DOI: 10.1039/c4ra09668a

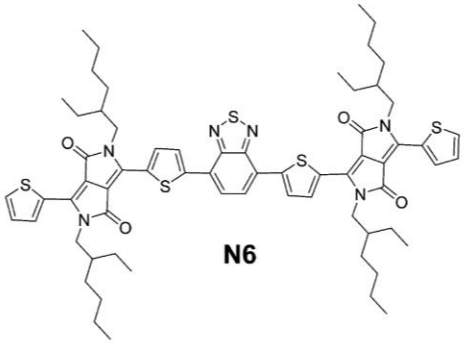

Fig. 1 Molecular structure of the investigated non-fullerene electron acceptor **N6**.

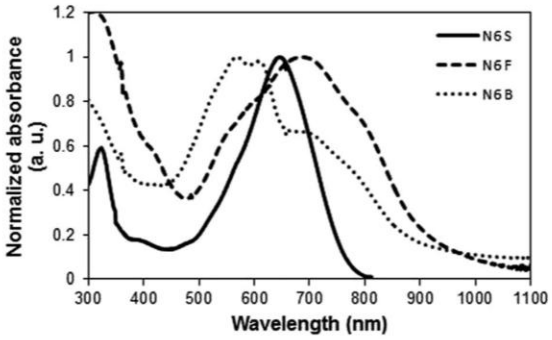

Fig. 2 UV-vis absorption spectra of pristine film (**N6 F**; dashed black curve), 1 : 1 blend with P3HT (**N6 B**; dotted black curve) and in chloroform solution (**N6 S**; solid black curve).

donor P3HT. Solution-processable BHJ devices based on P3HT : **N6** (1 : 1 w/w) exhibited PCEs as high as 1.16% with high V_{oc} of 1.08 V; and the V_{oc} of ~1.1 V is among the highest value reported for solution-processed fullerene-free small molecular organic solar cells.[10] **N6** is the first non-fullerene electron acceptor in the literature with BTD as a core and DPP as arms.

Compound **N6** was successfully synthesized in 70% yield *via* one step Suzuki coupling reaction between commercially available bis-boronic acid pinacol ester derivative of BTD, 2,1,3-benzothiadiazole-4,7-bis(boronic acid pinacol ester) (**1**), and 3-(5-bromothien-2-yl)-2,5-bis(2-ethylhexyl)-6-(thien-2-yl)pyrrolo-[3,4-*c*]pyrrole-1,4(2*H*,5*H*)-dione (**2**) using tetrakis(triphenylphosphine)palladium(0) [$Pd(PPh_3)_4$] as catalyst (See Scheme 1). **N6** was fully characterized by high resolution mass spectrometry (HRMS), ^{1}H NMR and ^{13}C NMR spectroscopic techniques. **N6** was found to be highly soluble in a variety of solvents such as chloroform, dichlorobenzene and toluene (for instance, >20 mg mL^{-1} in *o*-dichlorobenzene). High solubility of organic semiconducting chromophores is an essential feature for the fabrication of solution-processable BHJ devices and **N6** fulfils this criterion.

The normalized optical absorption spectra of **N6** in chloroform solution and in thin solid film are shown in Fig. 2. In solution, **N6** exhibits strong absorption with a maximum extinction coefficient of 54 916 M^{-1} cm^{-1} at 645 nm (8.47×10^{-6} M). As a thin film, **N6** showed a very broad absorption throughout the visible region (400–1000 nm) and tailing into the near infra-red region (panchromatic absorbance). Thin film absorption is red-shifted by around 40 nm when compared with its solution spectrum. Thin films of blends of P3HT with **N6** (in a ratio of 1 : 1 w/w) show quenching of the photoluminescence (Fig. S1, ESI†), a finding that is consistent with literature reported non-fullerene electron acceptors and indicates that an effective photo-induced charge transfer occurred between **N6** and P3HT in the blend film.[8]

Density functional theory (DFT) calculations using the Gaussian 09 suite of programs[10] and B3LYP/6-311+G(d,p)//B3LYP/6-31G(d) level of theory indicated that orbital densities are evenly distributed over the whole molecular backbone (Fig. S2, ESI†), a finding that is consistent with literature reported non-fullerene acceptor materials.[8] The highest occupied molecular orbital (HOMO) energy of **N6** was estimated using Photo Electron Spectroscopy in Air (PESA) (Fig. S3, ESI†) and the lowest unoccupied molecular orbital (LUMO) energy was calculated by adding the optical bandgap to the HOMO value. The optical bandgap, estimated from the tangent of the edge of longest wavelength in thin solid film, was 1.35 eV. The estimated HOMO and calculated LUMO energies were found to be −5.06 and −3.71 eV respectively. The difference between the HOMO of donor (P3HT; −4.80 eV from PESA) and the LUMO of **N6** (−3.71 eV) was found to be as large as ~1.10 eV, which is promising for achieving a high V_{oc} in solar cells. **N6** was further tested for its thermal stability so that it can endure rigid device fabricating conditions such as device annealing at a higher temperature. To check the thermal stability, we conducted thermogravimetry (TGA) and differential scanning calorimetry (DSC) analyses. Thermal analyses indicated that **N6** exhibits good thermal stability, a finding that supports temperature annealing of P3HT:**N6** devices at temperatures higher than 100 °C (Fig. S4, ESI†).

Once established that **N6** possesses promising optical and electrochemical properties, we tested its efficacy in solution-processable BHJ devices. **N6** was used as a non-fullerene electron acceptor (n-type) along with classical donor polymer P3HT (p-type). It is well known that BHJ architectures exert higher PCEs by maximising the surface area of interface between the p- and n-type materials in an active layer. The BHJ device structure used was ITO/PEDOT:PSS (38 nm)/active layer/Ca (20 nm)/Al

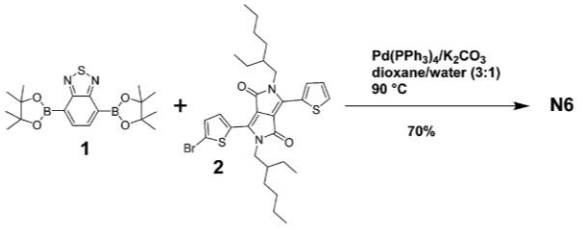

Scheme 1 Reaction strategy for the synthesis of **N6**.

(100 nm) where the active layer was a solution-processed blend of P3HT and **N6**, a 1 : 1 blend spin-casted from *o*-dichlorobenzene solution. We[8c] and others[10,11] have shown that thermal annealing of DPP-based small molecule semiconductors can be advantageous for molecular reorganization, high V_{oc} and superior device efficiency. Consideration of such factors allowed us to anneal our active films at 120 °C for 5 min and the devices were fabricated. BHJ devices showed significant performance and the device parameters, V_{oc}, short circuit current density (J_{sc}), fill factor (FF) and PCE, reached 1.08 V, 2.06 mA cm^{-2}, 0.52 and 1.16%, respectively. These fabricated devices yielded very high V_{oc}, a finding that is consistent with the measured optical band gap between the LUMO of **N6** and the HOMO of P3HT. It is notable that all the devices (a total of ten devices were made) afforded $V_{oc} > 1$ V and the device parameters reported herein are for the best performing device. $V_{oc} > 1$ V is not only the highest V_{oc} among the DPP-based small molecular acceptor semiconductors, but also amongst the highest for single-junction solution-processable BHJ devices. Although the PCEs with the use of non-fullerene electron acceptors have approached 4%,[8] the DPP-based acceptors still lag in design and efficiency. Having said the latter, **N6**-based devices yielded PCE among the top values reported in literature for the DDP-based chromophores, thus providing strong support and incentive for the present research. However, the PCE for the studied devices was low compared to the fullerene-based devices.[12] The lower performance was primarily due to the low short-circuit current and fill factor, which in turn were lower due to charge recombinations and lower electron mobility of the acceptor materials in the active layer. Representative current–voltage (*J*–*V*) curve is shown in the Fig. 3.

The analysis of the incident-photon-to-current conversion efficiency (IPCE) measurement of the blend film with a donor–acceptor weight ratio of 1 : 1 is shown in Fig. S5, ESI.† The blend film of best photovoltaic device showed broad IPCE spectrum from 400 to 1000 nm with an IPCE maximum of ~16% at 560 nm. This suggests that both donor and acceptor components in the BHJ blend made a considerable contribution to the IPCE and J_{sc}. Even though the IPCE value is moderate, it is an interesting outcome in view of using **N6** with low band-gap conjugated donors such that charge generation could be achieved over a broad range of wavelengths, typically over the whole visible region tailing into the near infra-red region.

To examine the physical microstructure of the blend surface, we used atomic force microscopy (AFM) in tapping mode. The actual surface morphology of the blend film of P3HT : **N6** (1 : 1 w/w) is shown in Fig. 4. The blend appears to have bush-like morphology with larger crystalline domains and better phase separation with surface roughness of ~3.2 nm. Physically, the blend films were observed as smooth and with no cracks when spin-casted from *o*-dichlorobenzene (3000 rpm s^{-1} for 1 min) followed by annealing at 120 °C for 5 min. These processing conditions to generate blend film are in good agreement with the AFM morphology as the use of low-boiling solvents, such as chloroform, resulted in very poor photovoltaic performance. Also, the finding that the BHJ devices comprising **N6** as an acceptor perform better with high-boiling solvent is significant from a processing point of view. Blend film of P3HT : **N6** (1 : 1 w/w) was analyzed for the measurement of hole and electron mobilities using the transistor technique. Hole and electron mobilities of the order of 10^{-5} cm^2 V^{-1} s^{-1} and 10^{-6} cm^2 V^{-1} s^{-1} were observed respectively. Electron mobility, in particular, was low which accounted for lower J_{sc} and hence moderate PCE. Hole mobility indicated that the presence of **N6** doesn't disrupt the hole-rich P3HT, an observation consistent with the blend film morphology.

Although the material reported in this study achieved a high V_{oc} with moderate, albeit promising, PCE in solution-processable BHJ devices, there is still an appreciable room to explore device strategies to enhance PCE. The performance can be improved by either using effective interlayer, such as metal oxide interlayer, which can facilitate the efficient charge extraction or by devising processing methods, such as using solvent additives and solvent annealing techniques. Working towards some of these strategies is the subject of on-going work in our laboratories. The discovery of such materials exhibiting promising optoelectronic properties opens up the way to develop such motifs (based on the central BTD functionality) and paves the way for such materials to be used for other organic electronic applications such as organic field-effective transistors.

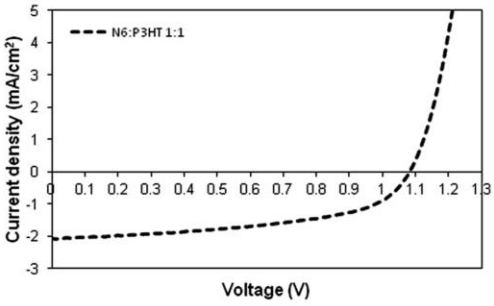

Fig. 3 Current–voltage curve for the best device based on **N6** and P3HT (1 : 1 w/w) under simulated sunlight (AM1.5, 1000 W m^{-2}). Device structure is: ITO/PEDOT:PSS (38 nm)/active layer/Ca (20 nm)/Al (100 nm). The active layer was ~52 nm thick.

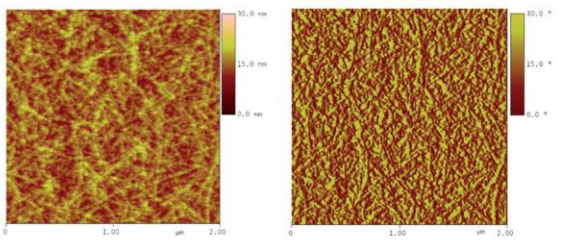

Fig. 4 AFM image for thin film of P3HT:**N6** blend annealed at 120 °C for 5 min (10 mg P3HT, 10 mg **N6** in 1 mL *o*-dichlorobenzene, 3000 rpm s^{-1} for 1 min).

In summary, a novel non-fullerene electron acceptor, **N6**, with BTD as a central core and DPP as arms was designed, synthesized and characterized. **N6** possesses excellent solubility, thermal and chemical stability, strong panchromatic absorbance, and appropriate energy levels matching with those of classical donor polymer P3HT. The solution-processable BHJ devices based on P3HT:**N6** blend after annealing at 120 °C for 5 min gave a PCE of 1.16% and a very high V_{oc} of ~1.10 V, which are among the highest values reported for solution-processable photovoltaic devices using DPP-based non-fullerene acceptors. Our work clearly demonstrates that small molecule acceptors, such as **N6**, with promising optoelectronic properties have an excellent prospect to be at the forefront of non-fullerene acceptor research and enriches the library of acceptors to provide numerous possibilities for donor–acceptor blending recipes to seek high device performance.

Acknowledgements

S.V.B. acknowledges financial support from the Australian Research Council, Australia under a Future Fellowship Scheme (FT110100152). The RMIT University, Melbourne VIC 3001 and CSIRO Manufacturing, Clayton is acknowledged for providing support through a visiting fellow position (A.G.). H.P. and A.G. acknowledge the assistance of Dr Jegadesan Subbiah from Bio21 Institute, University of Melbourne VIC 3010 for providing support and guidance during the fabrication of BHJ devices.

Notes and references

1 (*a*) S. Günes, H. Neugebauer and N. S. Sariciftci, *Chem. Rev.*, 2007, **107**, 1324–1338; (*b*) B. C. Thompson and J. M. J. Frechet, *Angew. Chem., Int. Ed.*, 2008, **47**, 58–77.

2 (*a*) Y. Lin, Y. Li and X. Zhan, *Chem. Soc. Rev.*, 2012, **41**, 4245–4272; (*b*) Y. Li, *Acc. Chem. Res.*, 2012, **45**, 723–733; (*c*) J. Roncali, *Acc. Chem. Res.*, 2009, **42**, 1719–1730.

3 (*a*) A. Gupta, S. E. Watkins, A. D. Scully, T. B. Singh, G. J. Wilson, L. J. Rozanski and R. A. Evans, *Synth. Met.*, 2011, **161**, 856–863; (*b*) C. J. Brabec, S. Gowrisanker, J. J. M. Halls, D. Laird, S. Jia and S. P. Williams, *Adv. Mater.*, 2010, **22**, 3839–3856; (*c*) B. Walker, C. Kim and T.-Q. Nguyen, *Chem. Mater.*, 2011, **23**, 470–482; (*d*) Y. Li, Q. Guo, Z. Li, J. Pei and W. Tian, *Energy Environ. Sci.*, 2010, **3**, 1427–1436; (*e*) A. Mishra and P. Bäuerle, *Angew. Chem., Int. Ed.*, 2012, **51**, 2020–2067.

4 J. B. You, L. T. Dou, K. Yoshimura, T. Kato, K. Ohya, T. Moriarty, K. Emery, C. C. Chen, J. Gao, G. Li and Y. Yang, *Nat. Commun.*, 2013, **4**, 1446–1455.

5 Y. He and Y. Li, *Phys. Chem. Chem. Phys.*, 2011, **13**, 1970–1983.

6 R. Y. C. Shin, P. Sonar, P. S. Siew, Z. K. Chen and A. Sellinger, *J. Org. Chem.*, 2009, **74**, 3293–3298.

7 (*a*) P. Sonar, J. P. Fong Lim and K. L. Chan, *Energy Environ. Sci.*, 2011, **4**, 1558–1574; (*b*) J. E. Anthony, *Chem. Mater.*, 2011, **23**, 583–590; (*c*) A. Facchetti, *Mater. Today*, 2013, **16**, 123–132.

8 (*a*) J. T. Bloking, X. Han, A. T. Higgs, J. P. Kastrop, L. Pandey, J. E. Norton, C. Risko, C. E. Chen, J.-L. Brédas, M. D. McGehee and A. Sellinger, *Chem. Mater.*, 2011, **23**, 5484–5490; (*b*) Y. Lin, Y. Li and X. Zhan, *Adv. Energy Mater.*, 2013, **3**, 724–728; (*c*) H. Patil, A. Gupta, A. Bilic, S. V. Bhosale and S. V. Bhosale, *Tetrahedron Lett.*, 2014, **55**, 4430–4432; (*d*) Y. Zhou, L. Ding, K. Shi, Y.-Z. Dai, N. Ai, J. Wang and J. Pei, *Adv. Mater.*, 2012, **24**, 957–961; (*e*) T. Zhou, T. Jia, B. Kang, F. Li, M. Fahlman and Y. Wang, *Adv. Energy Mater.*, 2011, **1**, 431–439; (*f*) X. Zhang, Z. Lu, L. Ye, C. Zhan, J. Hou, S. Zhang, B. Jiang, Y. Zhao, J. Huang, S. Zhang, Y. Liu, Q. Shi, Y. Liu and J. Yao, *Adv. Mater.*, 2013, **25**, 5791–5797; (*g*) Y. Lin, Y. Wang, J. Wang, J. Hou, Y. Li, D. Zhu and X. Zhan, *Adv. Mater.*, 2014, **26**, 5137–5142; (*h*) Y. Lin, J. Wang, S. Dai, Y. Li, D. Zhu and X. Zhan, *Adv. Energy Mater.*, 2014, **4**, 1400420; (*i*) P. Cheng, L. Ye, X. Zhao, J. Hou, Y. Li and X. Zhan, *Energy Environ. Sci.*, 2014, **7**, 1351–1356.

9 (*a*) A. Gupta, A. Ali, A. Bilic, M. Gao, K. Hegedus, B. Singh, S. E. Watkins, G. J. Wilson, U. Bach and R. A. Evans, *Chem. Commun.*, 2012, **48**, 1889–1891; (*b*) A. Gupta, V. Armel, W. Xiang, G. Fanchini, S. E. Watkins, D. R. MacFarlane, U. Bach and R. A. Evans, *Tetrahedron*, 2013, **69**, 3584–3592; (*c*) R. J. Kumar, Q. I. Churches, J. Subbiah, A. Gupta, A. Ali, R. A. Evans and A. B. Holmes, *Chem. Commun.*, 2013, **49**, 6552–6554; (*d*) A. Gupta, A. Ali, T. B. Singh, A. Bilic, U. Bach and R. A. Evans, *Tetrahedron*, 2012, **68**, 9440–9447; (*e*) H. Patil, W. X. Zu, A. Gupta, V. Chellappan, A. Bilic, P. Sonar, A. Rananaware, S. V. Bhosale and S. V. Bhosale, *Phys. Chem. Chem. Phys.*, 2014, **16**, 23837–23842.

10 Y. Lin, P. Cheng, Y. Li and X. Zhan, *Chem. Commun.*, 2012, **48**, 4773–4775.

11 O. V. Mikhnenko, J. Lin, Y. Shu, J. E. Anthony, P. W. M. Blom, T.-Q. Nguyen and M. A. Loi, *Phys. Chem. Chem. Phys.*, 2012, **14**, 14196–14201.

12 J. Subbiah, D. Y. Kim, M. Hartel and F. So, *Appl. Phys. Lett.*, 2010, **96**, 063303.

Experimental Section

1.1. *Materials*

All the reagents and chemicals used, unless otherwise specified, were purchased from Sigma-Aldrich Co. The solvents used for reactions were obtained from Merck Speciality Chemicals (Sydney, Australia) and were used as such. 2,1,3-Benzothiadiazole-4,7-bis(boronic acid pinacol ester) and 3-(5-bromothien-2-yl)-2,5-bis(2-ethylhexyl)-6-(thien-2-yl)pyrrolo[3,4-*c*]pyrrole-1,4(2*H*,5*H*)-dione were purchased from Luminescence Technology Corporation, Taiwan and were used as such.

1.2. *Instruments and characterization*

Unless otherwise specified, all ^{1}H and ^{13}C NMR spectra were recorded using a Bruker AV400 spectrometer at 400 MHz and 100.6 MHz, respectively, or a Bruker AV200 spectrometer at 200 MHz and 50 MHz, respectively. Chemical shifts (δ) are measured in parts per million (ppm). Thin Layer Chromatography (TLC) was performed using 0.25 mm thick plates precoated with Merck Kieselgel 60 F_{254} silica gel, and visualised using ultraviolet (UV) light (254 nm and 365 nm). Melting points were measured using a Gallenkamp MPD350 digital melting point apparatus and are uncorrected. High resolution mass spectra (atmospheric-pressure chemical ionization (APCI)) experiments were carried out on a Thermo Scientific Q-Exactive FTMS, ionizing by APCI from an ASAP probe.[S1]

All UV-vis absorption spectra were recorded on a Hewlett Packard HP 8453 Diode array UV-visible spectrophotometer. Thin films were spin-coated from *o*-dichlorobenzene (*o*-DCB) at a spin speed of 3000 rpm for 1 min onto cleaned glass slides. **N6** was spin-coated from solutions at a concentration of 17 mg/mL. P3HT: **N6** blend solutions were prepared in the same manner as for devices, i.e. P3HT (17 mg) and **N6** (17 mg) in a total volume of 1 mL. Films were annealed at 120 °C for 5 min. Fluorescence spectra were recorded using a Perkin-Elmer LS50B fluorimeter. Photoelectron Spectroscopy in Air (PESA) measurements were recorded using a Riken Keiki AC-2 PESA spectrometer with a power setting of 5 nW and a power number of 0.5. Samples for PESA were prepared on glass substrates.

1.3 Device fabrication and characterization of photovoltaic devices, and experimental details for the preparation of thin-film transistors have been reported in our previous work.[S2]

Section 2: Synthetic Details

N6 was synthesized as per the following procedure:

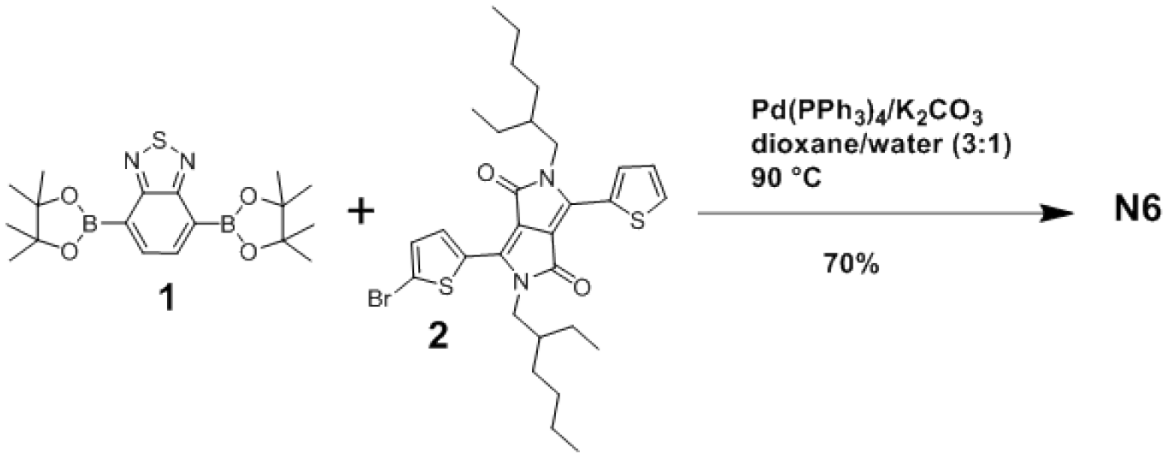

S

cheme 1 Synthetic strategy for **N6**

6,6'-(benzo[c][1,2,5]thiadiazole-4,7-diylbis(thiophene-5,2-diyl))bis(2,5-bis(2-ethylhexyl)-3-(thiophen-2-yl)-2,5-dihydropyrrolo[3,4-c]pyrrole-1,4-dione) (**N6**):

2,1,3-Benzothiadiazole-4,7-bis(boronic acid pinacol ester) (**1**) (120 mg, 0.31 mmol) was taken in a solvent mixture of doixane:water (3:1) (10.0 mL) in a 100 mL round bottom flask followed by the addition of potassium carbonate (128 mg, 0.93 mmol) and tetrakis(triphenylphosphine)palladium(0) (115 mg, 1 mmol) at room temperature. The resulting solution was stirred for 20 min followed by the addition of 3-(5-bromothien-2-yl)-2,5-bis(2-ethylhexyl)-6-(thien-2-yl)pyrrolo[3,4-*c*]pyrrole-1,4(2*H*,5*H*)-dione (**2**) (0.56 mmol, 338 mg) at room temperature. The yellow coloured reaction mixture was heated to 90 °C and stirred overnight. Solvent was evaporated under reduced pressure and the residue was purified by silica gel chromatography (hexane:dichloromethane 9:1) to get 258 mg (70.4%) of **N6** as a bluish-black powder. ^{1}H NMR (400 MHz, CD_2Cl_2): δ 9.10–9.09 (m, 2H), 8.91–8.89 (m, 2H), 8.19–8.18 (m, 2H), 8.03 (s, 2H), 7.66–7.64 (m, 2H), 7.28–7.26 (m, 2H), 4.15-3.98 (m, 8H), 2.03–1.93 (m, 2H), 1.90–1.81 (m, 2H), 1.45–1.21 (m, 32H), 0.96–0.85 (m, 24H); ^{13}C NMR (400 MHz, CD_2Cl_2): δ 161.69, 161.60, 152.38, 140.18, 139.88, 136.16, 135.30, 131.95, 130.86, 130.15, 129.10, 128.41, 128.04, 126.01, 125.70, 108.76, 108.39, 46.04, 45.88, 39.68, 39.30, 30.51, 30.31, 28.69, 28.50, 23.37, 23.22, 14.06, 13.95, 10.47, 10.37; HRMS (APCI): M^+, found 1180.4830. $C_{66}H_{80}N_6O_4{}^{32}S_5$ requires 1180.4839

IH NMR

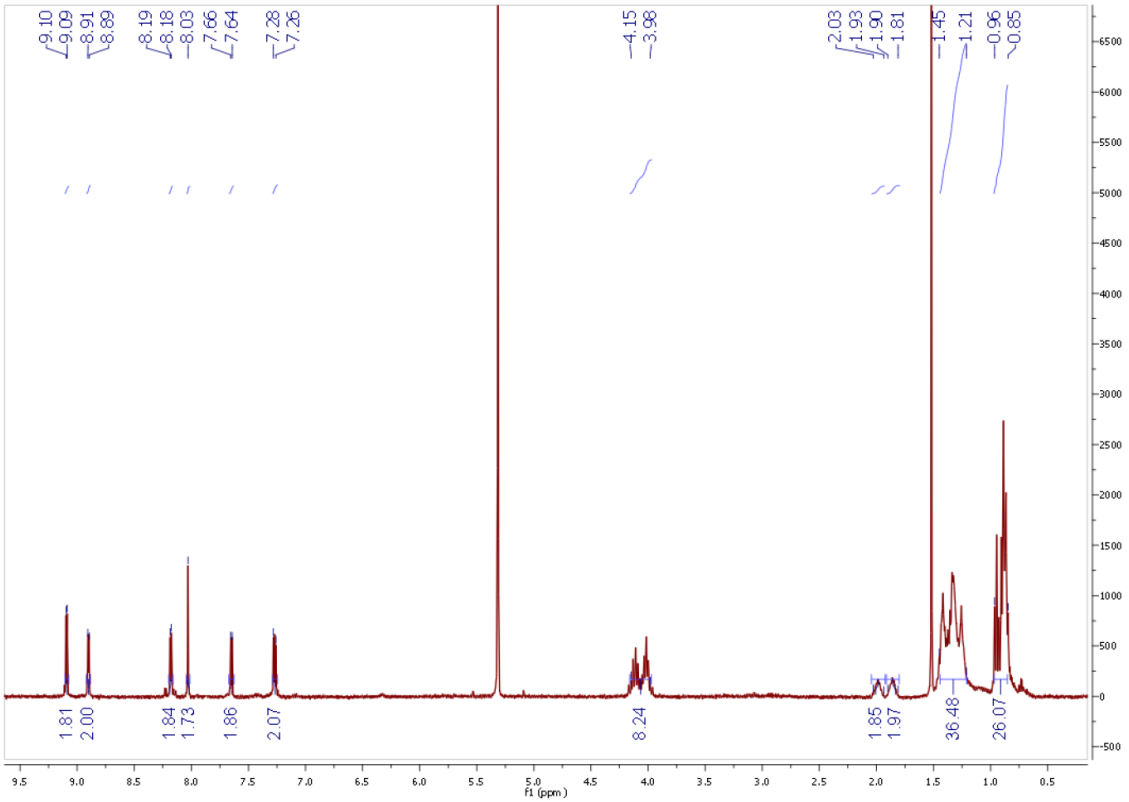

13C NMR

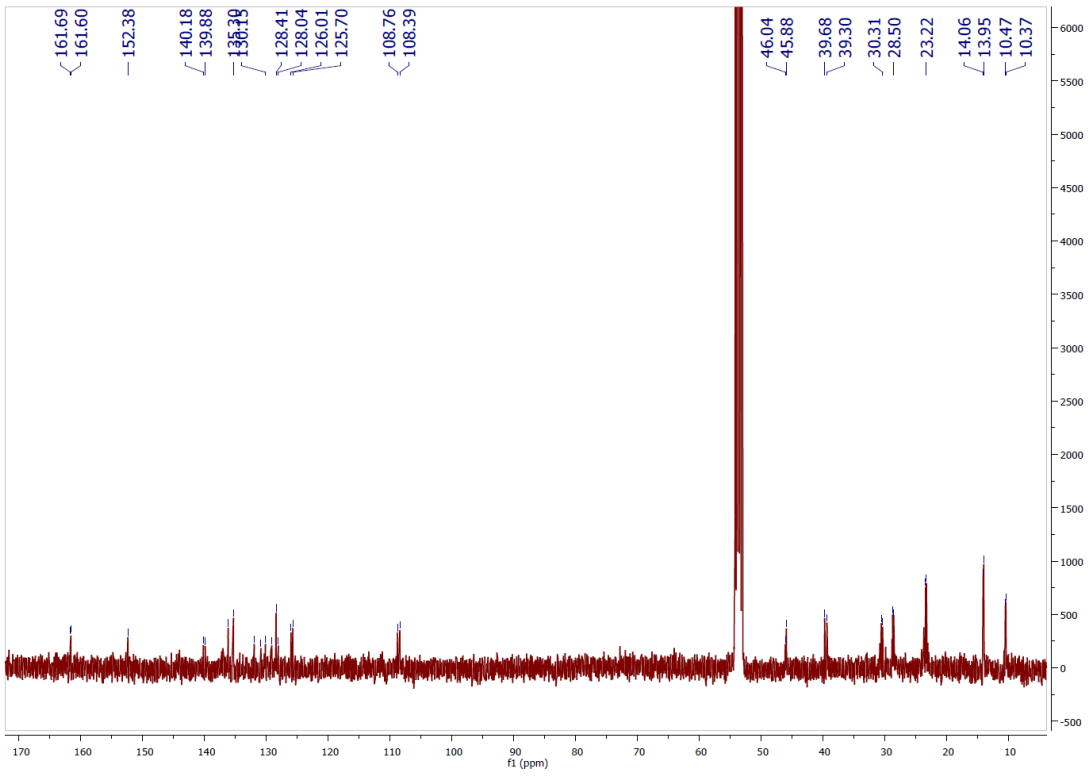

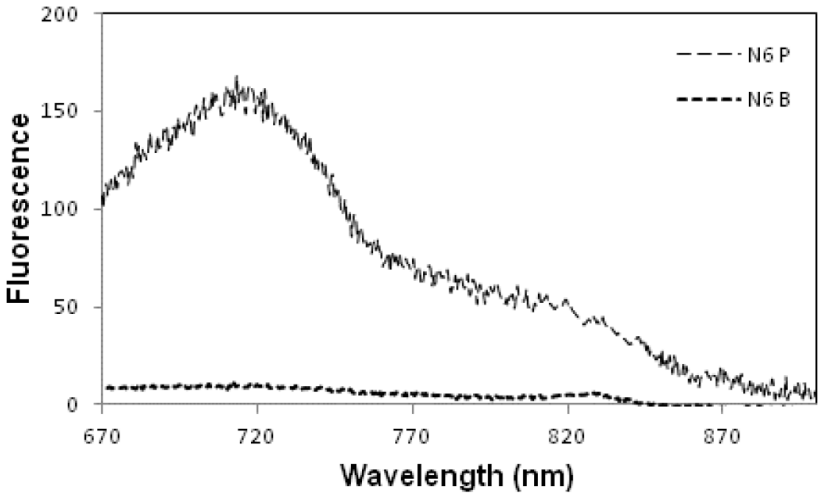

Fig. S1 Fluorescence spectra of pristine film of **N6** (**N6 P**) along with its blend with P3HT [as-cast; **N6 B**), spin-coated from *o*-dichlorobenzene (λ_{exc} = 600 nm).

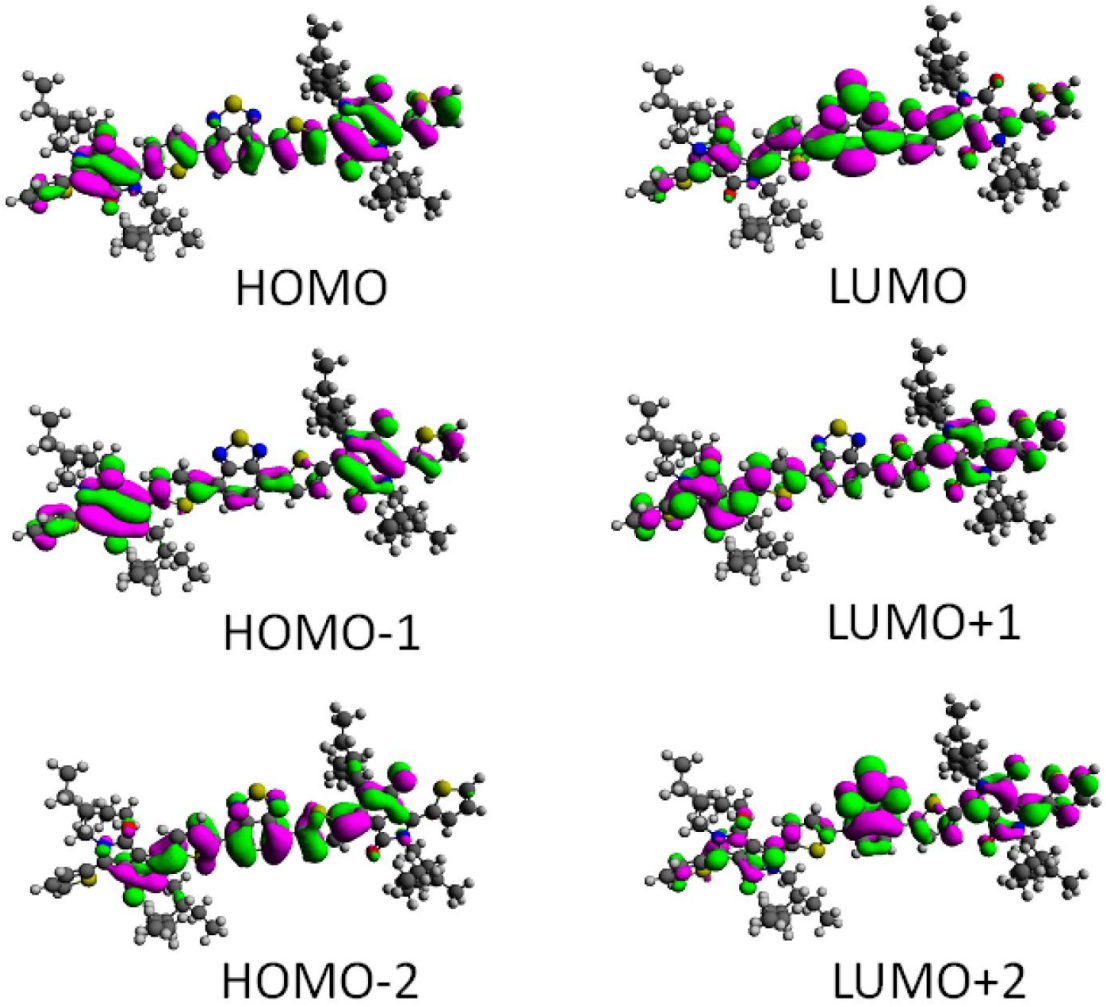

Fig. S2 Orbital density distribution for frontier molecular orbitals of **N6**. Density functional theory calculations were performed using the Gaussian 09 suite of programs and B3LYP/6-311+G(d,p)//B3LYP/6-31G(d) level of theory.

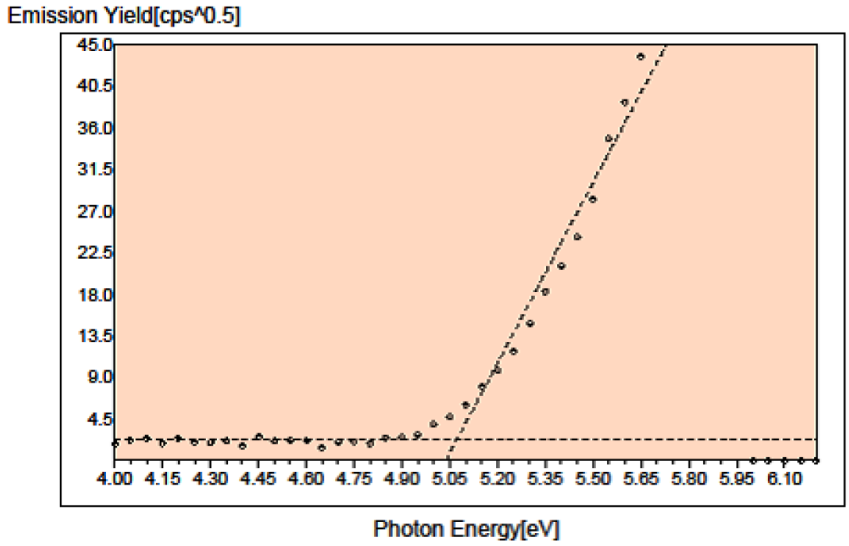

Fig. S3 PESA spectrum of thin film of **N6** from *o*-DCB. The dashed-lines show the fits to extract ionisation potential (-5.06 eV) which corresponds to the HOMO energy level.

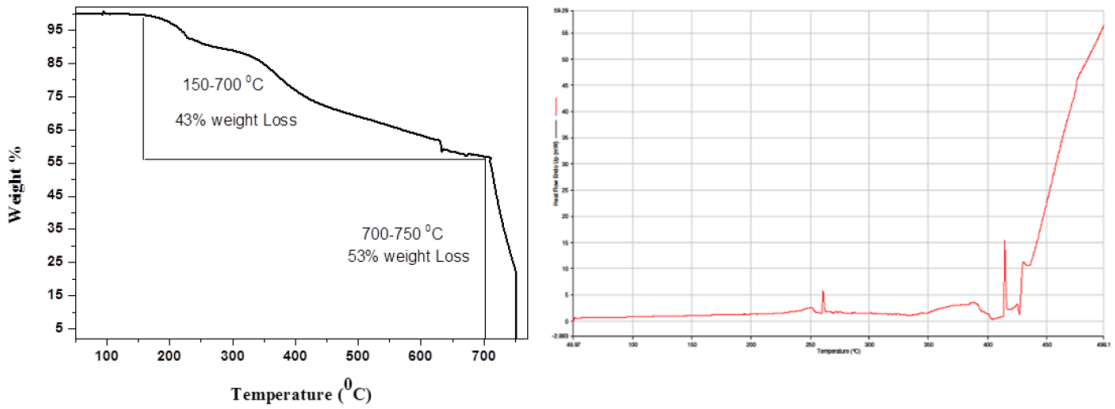

Fig. S4 TGA (left) and DSC (right) curves showing thermal stability of **N6**.

4.0 A non-fullerene electron acceptor based on central carbazole and terminal diketopyrrolopyrrole functionalities for efficient, reproducible and solution-processable bulk-heterojunction devices

ITO/P3HT:N7 (1:1.2)Ca/Al

η = 2.30%; V_{oc} = 1.17 V

Journal article published in *RSC Adv.* **2016**, *6*, 28103–28109 presented as **Chapter 4**.

RSC Advances

PAPER

View Article Online
View Journal | View Issue

Cite this: *RSC Adv.*, 2016, **6**, 28103

A non-fullerene electron acceptor based on central carbazole and terminal diketopyrrolopyrrole functionalities for efficient, reproducible and solution-processable bulk-heterojunction devices†

Aaron M. Raynor,[a] Akhil Gupta,*[ab] Hemlata Patil,[a] Di Ma,[c] Ante Bilic,[d] Trevor J. Rook[a] and Sheshanath V. Bhosale*[a]

Received 19th January 2016
Accepted 8th March 2016

DOI: 10.1039/c6ra01558a

www.rsc.org/advances

A novel, solution-processable non-fullerene electron acceptor, 6,6′-((9-(heptadecan-9-yl)-9*H*-carbazole-2,7-diyl)bis(thiophene-5,2-diyl))bis(2,5-bis(2-ethylhexyl)-3-(thiophen-2-yl)-2,5-dihydropyrrolo[3,4-*c*]pyrrole-1,4-dione) (coded as **N7**), based on central carbazole and terminal diketopyrrolopyrrole building blocks was designed, synthesized and characterized. **N7** displayed excellent solubility, thanks to its design allowing incorporation of numerous lipophilic chains, thermal stability, and afforded a 2.30% power conversion efficiency with a high open-circuit voltage (1.17 V) when tested with the conventional donor polymer poly(3-hexylthiophene) in solution-processable bulk-heterojunction devices. To our knowledge, not only is **N7** the first reported chromophore based on carbazole and diketopyrrolopyrrole functionalities but the open-circuit voltage reported here is among the highest values for a single junction bulk-heterojunction device that has been fabricated using a simple device architecture, with reproducible outcomes and with no special treatment.

Introduction

The development of renewable energy resources is one of mankind's long standing desires to fulfil the energy needs of modern society. It can be dated back to Becquerel's 1839 work when he observed the photovoltaic effect while studying liquid electrolytes.[1] However, Tang's 1989 work[2] instigated a momentum that organic solar cells can in fact be a reality in the near future. Since then many approaches have been investigated for harvesting solar energy. Among them organic, or otherwise termed as bulk-heterojunction, solar cells[3] and dye-sensitized solar cells[4] are the most studied strategies. In regards to bulk-heterojunction (BHJ) devices, two types of developments have attracted considerable attention over the past two decades; one being the design and development of novel materials and other is the development and improvement of device fabrication strategies. Both of these developments are equally important given the fact that BHJ devices promise multiple advantages such as light weight, low cost and flexibility.[5–7]

Typically, BHJ devices are an interwoven network of organic donor and acceptor domains which are formed during device fabrication *via* solution processing. Conventionally, semiconducting donor polymers, such as poly(3-hexylthiophene) (P3HT), and acceptors, such as solvent-dissolvable fullerene derivatives, [6,6]-phenyl-C_{61}-butyric acid methyl ester ($PC_{61}BM$) and its C_{71} analogue ($PC_{71}BM$), have been used to acquire an understanding of material design and device morphology.[5–7] As a result, conjugated polymers and small molecules as alternative donors, and non-fullerene functionalities as alternate acceptors have been developed over time. Power conversion efficiencies (PCEs) have exceeded or approached 10% with the use of polymeric and small molecular donors with fullerene acceptors, respectively.[8,9] The latter are the choice of dominant acceptors as they provide high electron mobility, large electron affinity, excellent solubility and an ability to form a favourable nanoscale network with versatile donor semiconducting components.[10] Even though the fullerenes are favourable accepting counterparts, they are afflicted with a number of potential disadvantages such as restricted electronic tuning *via* structural modification and weak absorption in the visible spectrum. Moreover, a large electron affinity can result in low open-circuit voltage (V_{oc}).[11] Such disadvantages with fullerenes provide a strong incentive that research must be carried on the design and development of non-fullerene acceptors which can

[a]*School of Applied Sciences, RMIT University, GPO Box 2476, Melbourne, Victoria 3001, Australia. E-mail: sheshanath.bhosale@rmit.edu.au; Tel: +61 3 9925 2680*

[b]*Institute for Frontier Materials, Deakin University, Waurn Ponds, Victoria 3216, Australia. E-mail: akhilgk15@gmail.com; Tel: +61 3 9903 9599*

[c]*College of Material Science and Engineering, Beijing University of Chemical Technology, Beijing 100029, China*

[d]*Virtual Nanoscience Lab, CSIRO Manufacturing, Parkville, Victoria 3052, Australia*

† Electronic supplementary information (ESI) available: ^{1}H and ^{13}C, PESA and theoretical optical absorption spectra. See DOI: 10.1039/c6ra01558a

exert efficient absorption over visible spectrum, excellent solubility, high charge carrier mobility and matching energy levels with those of potential donors.

In recent years, the study of design and development of non-fullerene acceptors has gone through something of a renaissance. Reviews by Sonar *et al.* and Lin *et al.* highlight the key examples of their development,[12,13] and recent reports from Hwang *et al.* and Zhong *et al.*, along with others, demonstrated over 8% PCEs with the use of low-band gap polymer donors.[14–23] We have also seen significant changes in our understanding of the area which has led to major advances in our ability to control and predict the outcome of a thoughtfully designed chromophore.[24–26] Although the efforts exerted by various research groups in the development of non-fullerene acceptors are appreciative and tireless, one must consider their principal suitability with easily synthesizable and scalable or commercially available donors in order to make these acceptors viable for practical applications. Such requirements indeed pose a substantial challenge to an organic chemist who must think in advance to devise a strategy not only to draw potential structures on plain paper but also to synthesize them in an efficient and timely manner. The design of most efficient non-fullerene acceptors teaches us that the target chromophore must be highly conjugated through a combination of donor and acceptor building blocks. We, and others, have been successful in demonstrating this strategy *via* designing a number of potential electron acceptors where such materials have manifested promising device performance.[14–26] We realised that functionalities such as diketopyrrolopyrrole (DPP) and naphthalenediimide (NDI) are great allies when used as terminal acceptors in conjunction with central conjugated blocks.[24,27,28]

The use of DPP in particular provides higher V_{oc}, allows tuning of solubility *via* incorporating lipophilic chains on nitrogen atoms, demonstrates good thermal and chemical stability at molecular level and generates a target with facile and easily scalable synthetic protocols. Such advantages are likely responsible for spurring an intensified interest in designing of chromophores based on terminal DPP-units and are an inspiration to pursue research on the development of new electron acceptors based on DPP functionality. Fig. 1 provides an overview of recent research where target chromophores have been developed based on terminal DPPs along with central conjugated units. Fig. 1 further demonstrates our current work where we have designed a new target chromophore based on terminal DPPs and central carbazole (CBZ) functionality.

Herein we report the synthesis, detailed theoretical calculations and characterization of the optoelectronic and photovoltaic properties of a novel small molecule, non-fullerene electron acceptor, 6,6′-((9-(heptadecan-9-yl)-9*H*-carbazole-2,7-diyl)bis(thiophene-5,2-diyl))bis(2,5-bis(2-ethylhexyl)-3-(thiophen-2-yl)-2,5-dihydropyrrolo[3,4-*c*]pyrrole-1,4-dione) (coded as **N7**), which was envisioned based on the connection of CBZ and DPP functionalities. **N7** turned out a highly conjugated chromophore with high chemical and thermal stability, and with excellent solubility. We were able to demonstrate that **N7**, when blended with P3HT in solution-processable BHJ solar cells, can deliver promising PCE, and the BHJ devices based on

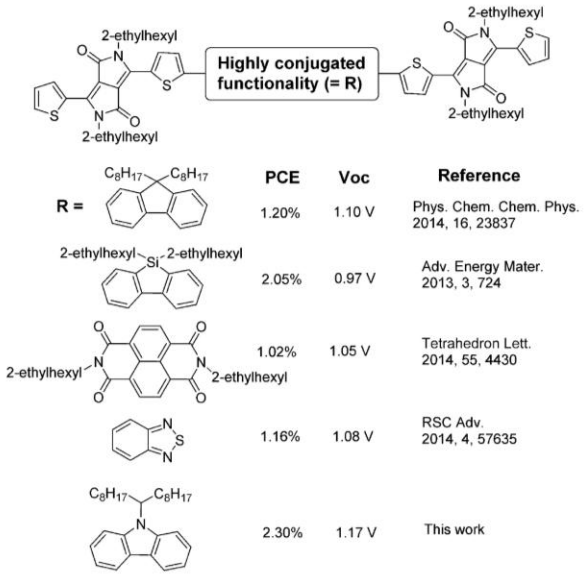

Fig. 1 Molecular structures of current and literature reported non-fullerene acceptors comprising central conjugated functionalities and terminal DPP-units.

a combination of CBZ and DPP building blocks perform better than the devices based on either fluorine : DPP[24] or dibenzosilole : DPP[29] combinations. Solution-processable BHJ devices based on the blend of P3HT : **N7** (1 : 1.2 w/w) exhibited PCEs as high as 2.30% with a high V_{oc} of 1.17 V; and the V_{oc} > 1.15 V is among the highest values reported for solution-processed fullerene-free small molecular organic solar cells. To our knowledge, there are no reports on the connected use of CBZ and DPP functionalities to generate a non-fullerene acceptor for solution-processable BHJ devices. It is vital to mention that we are highly interested to develop novel materials for organic electronics, organic solar cells in particular, and the present work is a continuation of our efforts on the design and development of small molecular chromophores for such applications.[30–33]

Experimental details

Materials

All the reagents and chemicals used, unless otherwise specified, were purchased from Sigma-Aldrich Co. The solvents used for reactions were obtained from Merck Specialty Chemicals (Sydney, Australia) and were used as received. All the substrates were purchased from Luminescence Technology Corporation, Taiwan, and were used as received.

Instruments and characterization, and device fabrication and characterization of photovoltaic devices have been reported previously.[26]

Design and synthesis

N7 was successfully synthesized in 61% yield *via* one step Suzuki coupling reaction between commercially available

bis-boronic acid pinacol ester derivative of CBZ, 9-(heptadecan-9-yl)-2,7-bis(4,4,5,5-tetramethyl-1,3,2-dioxaborolan-2-yl)-9*H*-carbazole and 3-(5-bromothien-2-yl)-2,5-bis(2-ethylhexyl)-6-(thien-2-yl)pyrrolo-[3,4-*c*]pyrrole-1,4(2*H*,5*H*)-dione using tetrakis(triphenylphosphine)palladium(0) [$Pd(PPh_3)_4$] as catalyst (Scheme 1). **N7** was fully characterized by high resolution mass spectrometry (HRMS), ^{1}H NMR and ^{13}C NMR spectroscopic techniques. As expected, **N7** was found to be highly soluble in a variety of common laboratory solvents such as dichloromethane, dichlorobenzene and chloroform; for instance 22 mg mL^{-1} in *o*-dichlorobenzene and 20 mg mL^{-1} in chloroform. High solubility of organic semiconducting chromophores is desirable for laboratory and industrial applications, and **N7** fulfils this criterion.

6,6′-((9-(Heptadecan-9-yl)-9*H*-carbazole-2,7-diyl)bis(thiophene-5,2-diyl))bis(2,5-bis(2-ethylhexyl)-3-(thiophen-2-yl)-2,5-dihydropyrrolo[3,4-*c*]pyrrole-1,4-dione) (N7). 9-(Heptadecan-9-yl)-2,7-bis(4,4,5,5-tetramethyl-1,3,2-dioxaborolan-2-yl)-9*H*-carbazole (202 mg, 0.31 mmol) was taken in toluene in a 100 mL round bottom flask followed by the addition of cesium carbonate (128 mg, 0.93 mmol) and tetrakis(triphenylphosphine)palladium(0) (58 mg, 0.05 mmol) at room temperature. The resulting solution was stirred under nitrogen blanketing for 20 min followed by the addition of 3-(5-bromothien-2-yl)-2,5-bis(2-ethylhexyl)-6-(thien-2-yl)pyrrolo[3,4-*c*]pyrrole-1,4(2*H*,5*H*)-dione (0.56 mmol, 338 mg) at room temperature. The yellow coloured reaction mixture was heated to reflux for 18 h, cooled down and diluted with ethyl acetate (15.0 mL) and water (25.0 mL). The reaction mixture was filtered through Celite and the organic layer was separated. Solvent was evaporated under reduced pressure and the residue was purified through silica gel chromatography (hexane : ethyl acetate 9.5 : 0.5) to get 271 mg (61%) of **N7** as a bluish-black powder. ^{1}H NMR (400 MHz, $CDCl_3$) δ 9.12–9.03 (m, 2H), 8.90–8.89 (m, 2H), 8.14–8.10 (m, 2H), 7.86 (s, 1H), 7.67 (s, 1H), 7.63–7.62 (m, 2H), 7.61–7.54 (m, 4H), 7.29–7.27 (m, 2H), 4.67–4.60 (m, 1H), 4.17–4.02 (m, 8H), 2.39–2.31 (m, 2H), 2.05–1.96 (m, 4H), 1.93–1.85 (m, 2H), 1.49–1.04 (m, 56H), 1.00–0.83 (m, 24H), 0.79–0.77 (m, 6H); ^{13}C NMR (126 MHz, $CDCl_3$) δ 162.02, 161.82, 151.36, 143.29, 140.54, 139.95, 137.55, 137.35, 131.39, 130.91, 130.48, 130.11, 124.29, 122.95, 121.39, 121.15, 109.19, 108.34, 108.08, 106.52, 56.95, 46.07, 39.27, 34.03, 31.87, 30.52, 30.38, 29.52, 29.43, 29.27, 28.52, 26.96, 23.73, 23.23, 22.71, 14.18, 10.67; HRMS (MALDI-TOF): *m*/*z*: calculated for $C_{89}H_{119}N_5O_4S_4$: 1449.81394 $[M]^+$; found 1449.81396. Elemental analysis calculated for $C_{89}H_{119}N_5O_4S_4$ (%): C 73.66, H 8.27, N 4.83, O 4.41, S 8.84; found: C 73.62, H 8.31, N 4.85, O 4.42, S 8.87 (for spectra please see Fig. S1 and S2 in the (ESI)†).

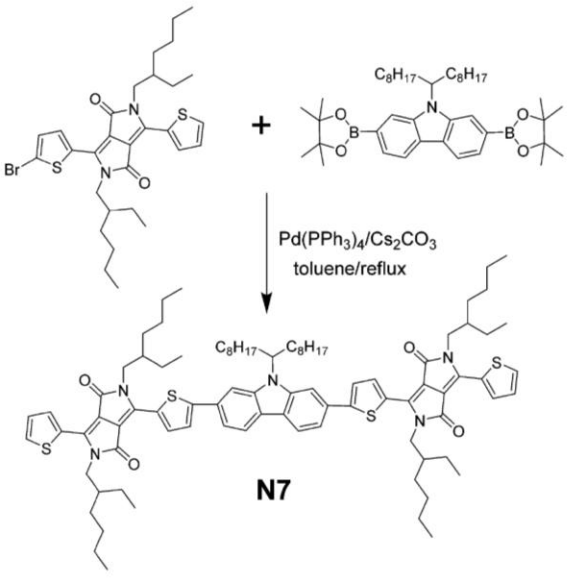

Scheme 1 Synthetic route to **N7**. Reagents and conditions: $Pd(PPh_3)_4$, toluene, Cs_2CO_3, inert atmosphere, 18 h, reflux; yield = 61%.

Results and discussion

Fig. 2 shows the normalized spectra of optical absorption of **N7** in chloroform solution (1.72×10^{-5} M) and in thin solid films. **N7** in solution exhibits strong absorption with the maximum extinction coefficient of 79 870 M^{-1} cm^{-1} at 599 nm. A thin film of **N7** shows significant absorption throughout the visible region (350–700 nm) with three peaks at 400, 580 and 615 nm, and the maximum peak red shifts 13 nm relative to that in solution. The optical band gap estimated from the absorption edge (680 nm using tangent method) of the thin film is 1.82 eV. The blend film absorption using a combination of CBZ/DPP indicated slight red shift when compared with either fluorene/DPP[24] or dibenzosilole/DPP[29] combinations, thus suggesting that there is an efficient charge transfer transition between donor and acceptor domains.

Density functional theory (DFT) calculations using the Gaussian 09 suite of programs[34] and the B3LYP/6-311+G(d,p)//B3LYP/6-31G(d) level of theory indicated that orbital densities are evenly distributed over the whole molecular backbone, a recent finding that is fairly usual with small-molecule non-fullerene acceptors[24,25] (Fig. 3). DFT calculations further indicated that dipole moment in case of **N7** (2.4930 Debye; field-independent basis) was larger than the dipole moment of

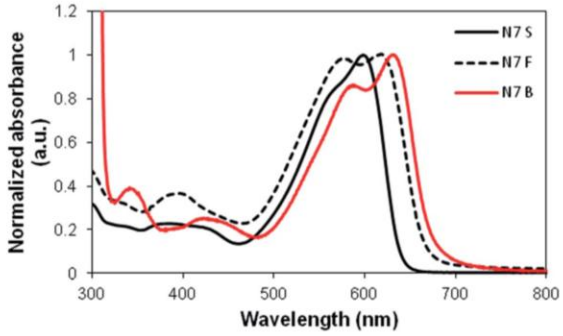

Fig. 2 UV-Vis absorption spectra of **N7** in chloroform solution (**N7** S; solid black curve), as a pristine as-casted film (**N7** F; dashed black curve) and as a blend with P3HT [1 : 1.2 P3HT : **N7** (**N7** B; solid red curve)].

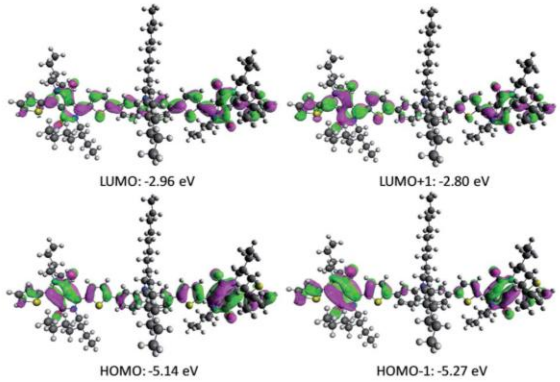

Fig. 3 Orbital density distribution for frontier molecular orbitals of **N7**. Density functional theory calculations were performed using the Gaussian 09 suite of programs and the B3LYP/6-311+G(d,p)//B3LYP/6-31G(d) level of theory.

fluorene/DPP combination (1.1862 Debye), thus indicating the suitability of CBZ : DPP combination in terms of efficient intramolecular charge transfer transition. Furthermore, the torsional angle between the two thiophene ring planes and carbazole plane was found to be ~25.8°, thus giving **N7** a non-planar structure overall (Fig. 4). The non-planarity in small molecular non-fullerene acceptors may be considered vital over their planar counterparts as is demonstrated by S. Holliday *et al.*[14] and H. Patil *et al.*[26] The theoretical optical absorption transition of **N7** is also shown in Fig. S3 (ESI†) which corroborates our experimental finding.

As such, the highest occupied molecular orbital (HOMO) and lowest unoccupied molecular orbital (LUMO) energy levels were estimated using a combination of photoelectron spectroscopy in air (PESA) and UV-Vis spectroscopy on thin films. The repetitive analyses of HOMO energy levels using pristine and blend films indicated that the average HOMO level resides around −5.56 eV. The LUMO energy level was calculated using absorption onset (680 nm) of thin film of **N7**. The optical band gap of **N7** matched the literature reports based on the combinations of either fluorene/DPP[24] or dibenzosilole/DPP.[29] This, again, is a confirmation that DPP-bound chromophores can indeed guarantee high V_{oc} of BHJ devices (Fig. 5 for energy level diagram and Fig. S4 (ESI†) for PESA curve).

Furthermore, **N7** was tested for its thermal stability so that it can bear rigid device fabricating conditions such as device annealing at a higher temperature (*e.g.* >100 °C). We conducted thermogravimetry analysis (TGA) and observed that **N7** indeed is a thermally stable chromophore, hence can endure annealing conditions at a higher temperature (Fig. 6 for TGA curve).

Once it was established that **N7** displayed promising opto-electronic properties and is a potential acceptor with energy levels matching with those of the classical electron donor P3HT, solution-processable BHJ devices were fabricated. The BHJ device architecture used was indium-tin oxide (ITO)/poly(3,4-ethylenedioxythiophene):polystyrene sulfonate (PEDOT:PSS, 38 nm)/active layer (~62 nm)/Ca (20 nm)/Al (100 nm) where the active layer was a 1 : 1.2 blend of P3HT : **N7**, respectively, spin-cast from *o*-dichlorobenzene on top of the PEDOT:PSS surface. It is vital to mention that we chose a simple device architecture to start with and to observe initial performance, stability, fabricating conditions and reproducibility of BHJ devices. Regarding the fabrication of small molecular non-fullerene acceptors, it is well established that thermal annealing of devices and use of high boiling solvent is preferred for optimal performance and to avoid formation of large-scale crystals on active surfaces, respectively. This principle was demonstrated by Kim *et al.*,[35] Lin *et al.*[36] and Patil *et al.*[37] Based on the literature findings and our own understanding of the BHJ device architecture we used *o*-dichlorobenzene as the processing solvent and annealed our active blend surfaces at 120 °C for 5 min. The optimized donor : acceptor weight ratio was found to be 1 : 1.2 where the BHJ device gave encouraging performance. The photovoltaic cell parameters; V_{oc}, short circuit current density (J_{sc}), fill factor (FF), and PCE, reached 1.17 V, 3.16 mA cm^{-2},

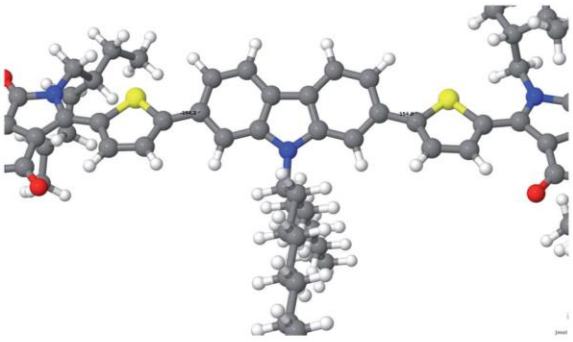

Fig. 4 Torsional angle of 154.2° or 25.8° between the two wings (from thiophene to the end) and the central CBZ block of **N7** from the minimum energy conformations calculated using the Gaussian 09 suite of programs and the B3LYP/6-311+G(d,p)//B3LYP/6-31G(d) level of theory.

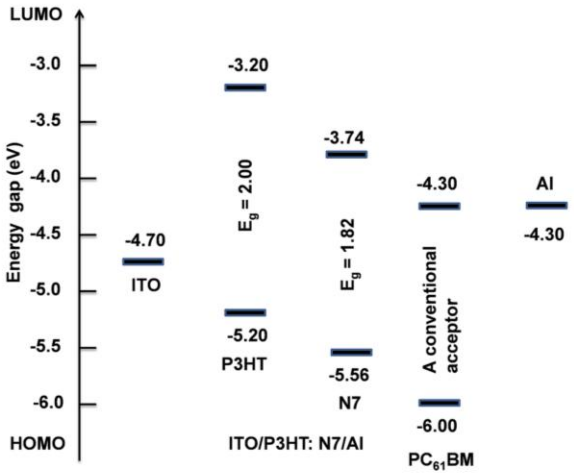

Fig. 5 Energy level diagram showing alignments of different components of BHJ device architecture.

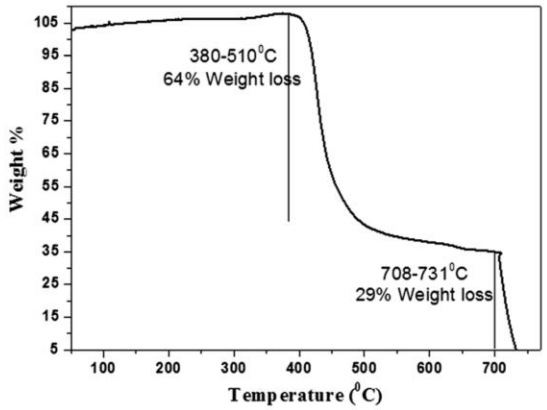

Fig. 6 TGA trace of **N7** under nitrogen atmosphere. Heating rate: 10 °C min^{-1} from room temperature to 800 °C.

0.62, and 2.30%, respectively. All the fabricated devices yielded very high V_{oc}, a finding that is consistent with the measured optical band gaps between the LUMO of **N7** and the HOMO of P3HT. V_{oc} approaching 1.20 V is among the highest voltages displayed by any DPP-based small molecular acceptor and is in fact amongst the highest for single-junction solution-processable BHJ devices. In contrast, the maximum PCE, V_{oc}, and J_{sc} reached 3.15%, 0.61 V and 8.46 mA cm^{-2}, respectively, for a device based on P3HT : $PC_{61}BM$ combination when fabricated under similar conditions, thus suggesting the reliability of our device strategy (Fig. S5, ESI†). Although the PCE values with the use of non-fullerene acceptors are surging, the DPP-based acceptors still linger in molecular design and device efficacy. Having said this, the PCE value reported here is among the top values reported in the literature for DDP-based chromophores, thereby providing strong support and incentive for the current research strategy. Representative current–voltage (*J*–*V*) curve is shown in Fig. 7.

The incident-photon-to-current conversion efficiency (IPCE) measurement of the blended film with a donor : acceptor weight ratio of 1 : 1.2 is shown in Fig. 8. The blended film of best photovoltaic device showed broad IPCE spectrum ranging

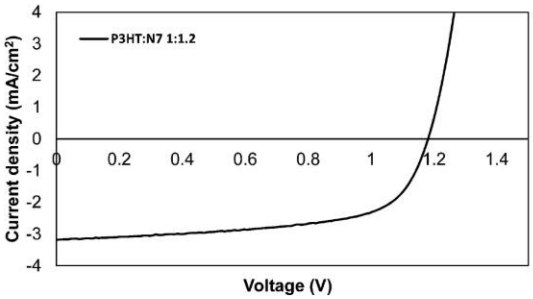

Fig. 7 Current–voltage curve for the best device based on P3HT and **N7** (1 : 1.2 w/w) under simulated sunlight (AM 1.5, 1000 W m^{-2}). Device structure was: ITO/PEDOT:PSS (38 nm)/active layer/Ca (20 nm)/Al (100 nm). The active layer was ~62 nm thick.

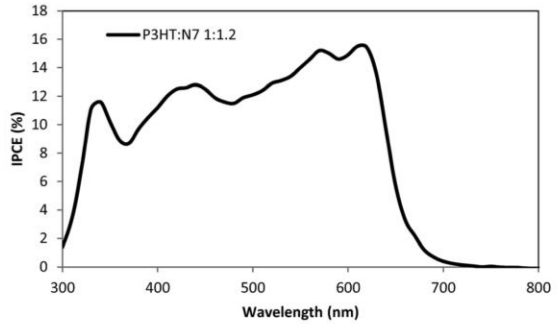

Fig. 8 IPCE spectrum of the best performing device described in Fig. 7.

from 300 to 700 nm, typically over the entire visible region, with an IPCE maximum of ~17% at 610 nm. Despite its moderate IPCE value, the broadness of this spectrum alludes that **N7** can be matched as an electron acceptor with a variety of electron donors, such as conjugated polymers and small molecules, in order to achieve charge generation over a broad range of wavelengths.

The physical microstructure of the blend surface was examined using atomic force microscopy (AFM) in tapping mode. The actual surface morphology of the blend film of P3HT : **N7** (1 : 1.2 w/w) is shown in Fig. 9. The active surface appears as a fine blend of donor and acceptor domains with a root-mean-square (RMS) roughness of 1.5 nm. Such an interpenetrating network of donor/acceptor components can be beneficial for exciton dissociation and charge-carrier transport, and can result in enhanced efficiency of photovoltaic devices.[5,6] The physical appearance of the blend surface was noted as being even and regular, and free from perceptible projections, lumps, or indentations. Clearly, the physical appearance matched the factual surface morphology and corroborated the fact that high

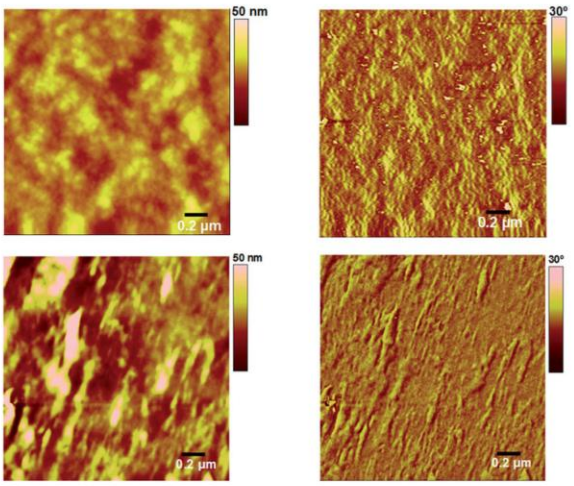

Fig. 9 AFM image of the P3HT : **N7** blend film annealed at 120 °C for 5 min (15 mg P3HT and 18 mg **N7** in 1 mL each of *o*-dichlorobenzene (upper) and chloroform (lower); film formation at 2500 rpm).

boiling solvents are preferable over low-boiling solvents such as chloroform. The chloroform blend film didn't show any nano-scale phase-separation and the surface roughness was too high (RMS roughness = 5.6 nm), which is disadvantageous for photovoltaic devices. Having said this, our attempts of fabrication using chloroform as a processing solvent resulted in very poor device results, which is attributed to either low film quality or an irregular intermixing of donor/acceptor components, thus verifying our AFM analysis and the literature principles.[35–37]

Though the research for non-fullerene electron acceptors is ever increasing, this work clearly demonstrates the possibility of achieving promising PCE in terms of material design, synthetic methodology and device efficacy. It further demonstrates that how crucial it is to carefully select a right building block not only to match with a suitable counterpart but also to achieve the desired optoelectronic and photovoltaic properties.

Conclusions

In summary, we have been successful to creating a small-molecular non-fullerene acceptor which was thoughtfully designed, synthesized and showed promising optoelectronic properties. Solution-processable BHJ devices displayed a propitious outcome, which is paramount for the advancement of research of non-fullerene acceptors. This work achieved one of the best efficiency outcomes with a very high V_{oc} of non-fullerene DPP-based electron acceptors and has provided an opportunity for judicious selection of various donor and acceptor building blocks for their union to seek high device performance.

Acknowledgements

S. V. B. (RMIT) acknowledges financial support from the Australian Research Council (ARC), Australia, under a Future Fellowship Scheme (FT110100152). A. G. is thankful to the IFM Alfred Deakin Fellowship Scheme at Deakin University, Waurn Ponds Victoria. The CSIRO Division of Materials Science and Engineering, Clayton, Victoria is acknowledged for providing support through a visiting fellow position for A. G.

Notes and references

1 E. Becquerel, *C. R. Acad. Sci.*, 1839, **9**, 561.
2 C. W. Tang, *Appl. Phys. Lett.*, 1986, **48**, 183.
3 G. Yu, J. Gao, J. C. Hummelen, F. Wudl and A. J. Heeger, *Science*, 1995, **270**, 1789.
4 W. Xiang, A. Gupta, M. K. Kashif, N. Duffy, A. Bilic, R. A. Evans, L. Spiccia and U. Bach, *ChemSusChem*, 2013, **6**, 256.
5 A. J. Heegar, *Adv. Mater.*, 2014, **26**, 10.
6 Y. Huang, E. J. Kramer, A. J. Heeger and G. C. Bazan, *Chem. Rev.*, 2014, **114**, 7006.
7 Y. Lin, Y. Li and X. Zhan, *Chem. Soc. Rev.*, 2012, **41**, 4245.
8 J. You, L. Dou, K. Yoshimura, T. Kato, K. Ohya, T. Moriarty, K. Emery, C.-C. Chen, J. Gao, G. Li and Y. Yang, *Nat. Commun.*, 2013, **4**, 1446.
9 B. Kan, Q. Zhang, M. Li, X. Wan, W. Ni, G. Long, Y. Wang, X. Yang, H. Feng and Y. Chen, *J. Am. Chem. Soc.*, 2014, **136**, 15529.
10 Y. He and Y. Li, *Phys. Chem. Chem. Phys.*, 2011, **13**, 1970.
11 R. Y. C. Shin, P. Sonar, P. S. Siew, Z. K. Chen and A. Sellinger, *J. Org. Chem.*, 2009, **74**, 3293.
12 P. Sonar, J. P. F. Lim and K. L. Chan, *Energy Environ. Sci.*, 2011, **4**, 1558.
13 Y. Lin and X. Zhan, *Mater. Horiz.*, 2014, **1**, 470.
14 S. Holliday, R. S. Ashraf, C. B. Nielsen, M. Kirkus, J. A. Rçhr, C.-H. Tan, E. C. Fregoso, A.-C. Knall, J. R. Durrant, J. Nelson and I. McCulloch, *J. Am. Chem. Soc.*, 2015, **137**, 898.
15 J. Zhao, Y. Li, H. Lin, Y. Liu, K. Jiang, C. Mu, T. Ma, J. Y. L. Lai, H. Hu, D. Yu and H. Yan, *Energy Environ. Sci.*, 2015, **8**, 520.
16 Y. Lin, Z.-G. Zhang, H. Bai, Y. Yao, Y. Li, D. Zhu and X. Zhan, *Energy Environ. Sci.*, 2015, **8**, 610.
17 Y. Lin, Z.-G. Zhang, H. Bai, Y. Li, D. Zhu and X. Zhan, *Adv. Mater.*, 2015, **27**, 1170.
18 X. Liu, Y. Xie, H. Zhao, X. Cai, H. Wu, S.-J. Su and Y. Cao, *New J. Chem.*, 2015, **39**, 8771.
19 X. Liu, Y. Xie, X. Cai, Y. Li, H. Wu, S.-J. Su and Y. Cao, *RSC Adv.*, 2015, **5**, 107566.
20 X. Liu, G. Luo, X. Cai, H. Wu, S.-J. Su and Y. Cao, *RSC Adv.*, 2015, **5**, 83155.
21 Y.-J. Hwang, H. Li, B. A. E. Courtright, S. Subramaniyan and S. A. Jenekhe, *Adv. Mater.*, 2016, **28**, 124.
22 Y. Zhong, *et al.*, *Nat. Commun.*, 2015, **6**, 8241.
23 S. Li, W. Liu, M. Shi, J. Mai, T.-K. Lau, J. Wan, X. Lu, C.-Z. Li and H. Chen, *Energy Environ. Sci.*, 2016, **9**, 604.
24 H. Patil, W. X. Zu, A. Gupta, V. Chellappan, A. Bilic, P. Sonar, A. Rananaware, S. V. Bhosale and S. V. Bhosale, *Phys. Chem. Chem. Phys.*, 2014, **16**, 23837.
25 A. M. Raynor, A. Gupta, H. Patil, A. Bilic and S. V. Bhosale, *RSC Adv.*, 2014, **4**, 57635.
26 H. Patil, A. Gupta, B. Alford, D. Ma, S. H. Privèr, A. Bilic, P. Sonar and S. V. Bhosale, *Asian J. Org. Chem.*, 2015, **4**, 1096.
27 A. Gupta, X. Wang, D. Srivani, B. Alford, V. Chellappan, A. Bilic, H. Patil, L. A. Jones, S. V. Bhosale, P. Sonar and S. V. Bhosale, *Asian J. Org. Chem.*, 2015, **4**, 800.
28 A. Gupta, R. V. Hangarge, X. Wang, B. Alford, V. Chellapan, L. A. Jones, A. Rananaware, A. Bilic, P. Sonar and S. V. Bhosale, *Dyes Pigm.*, 2015, **120**, 314.
29 Y. Lin, Y. Li and X. Zhan, *Adv. Energy Mater.*, 2013, **3**, 724.
30 A. Gupta, A. Ali, A. Bilic, M. Gao, K. Hegedus, B. Singh, S. E. Watkins, G. J. Wilson, U. Bach and R. A. Evans, *Chem. Commun.*, 2012, **48**, 1889.
31 A. Gupta, V. Armel, W. Xiang, G. Fanchini, S. E. Watkins, D. R. MacFarlane, U. Bach and R. A. Evans, *Tetrahedron*, 2013, **69**, 3584.
32 R. J. Kumar, Q. I. Churches, J. Subbiah, A. Gupta, A. Ali, R. A. Evans and A. B. Holmes, *Chem. Commun.*, 2013, **49**, 6552.
33 A. Gupta, A. Ali, T. B. Singh, A. Bilic, U. Bach and R. A. Evans, *Tetrahedron*, 2012, **68**, 9440.

34 M. J. Frisch, G. W. Trucks, H. B. Schlegel, G. E. Scuseria, M. A. Robb and J. R. Cheeseman, *et al.*, *Gaussian 09 revision D.01*, Gaussian Inc., Wallingford CT, 2013.
35 Y. Kim, C. E. Song, S.-J. Moon and E. Lim, *Chem. Commun.*, 2014, **50**, 8235.
36 Y. Lin, P. Cheng, Y. Li and X. Zhan, *Chem. Commun.*, 2012, **48**, 4773.
37 H. Patil, A. Gupta, A. Bilic, S. V. Bhosale and S. V. Bhosale, *Tetrahedron Lett.*, 2014, **55**, 4430.

Experimental Part

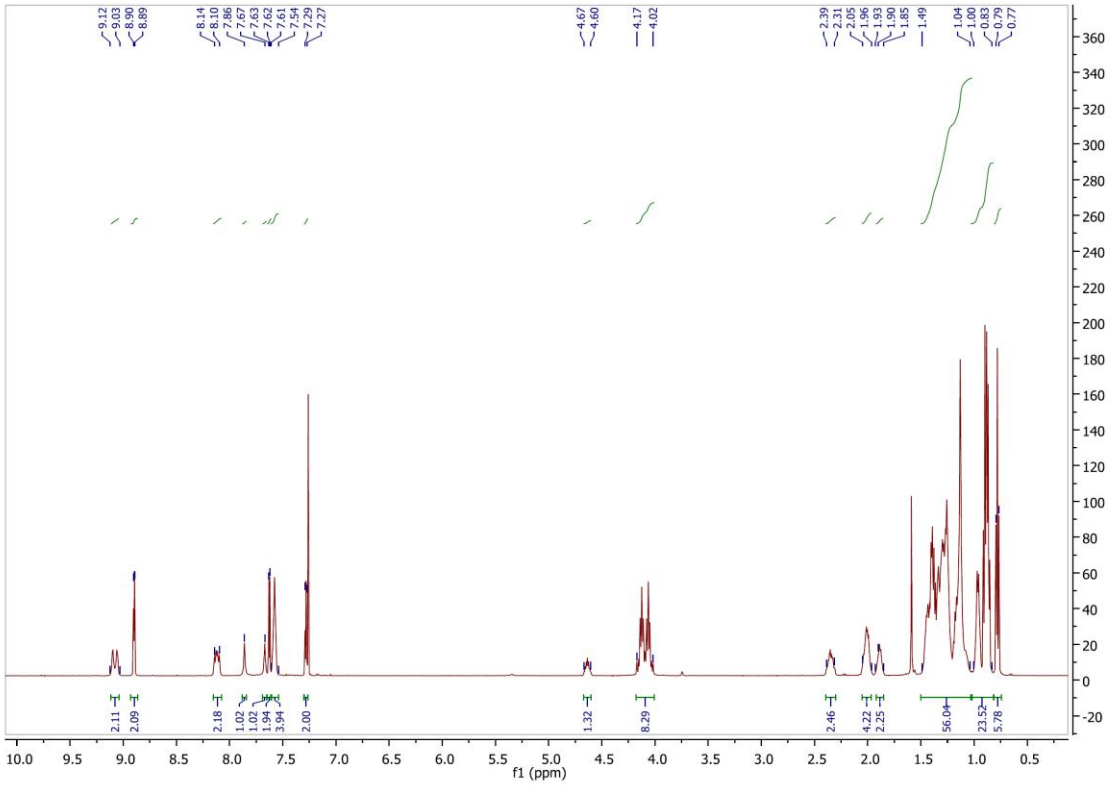

Fig. S1 ^{1}H NMR spectrum of **N7**.

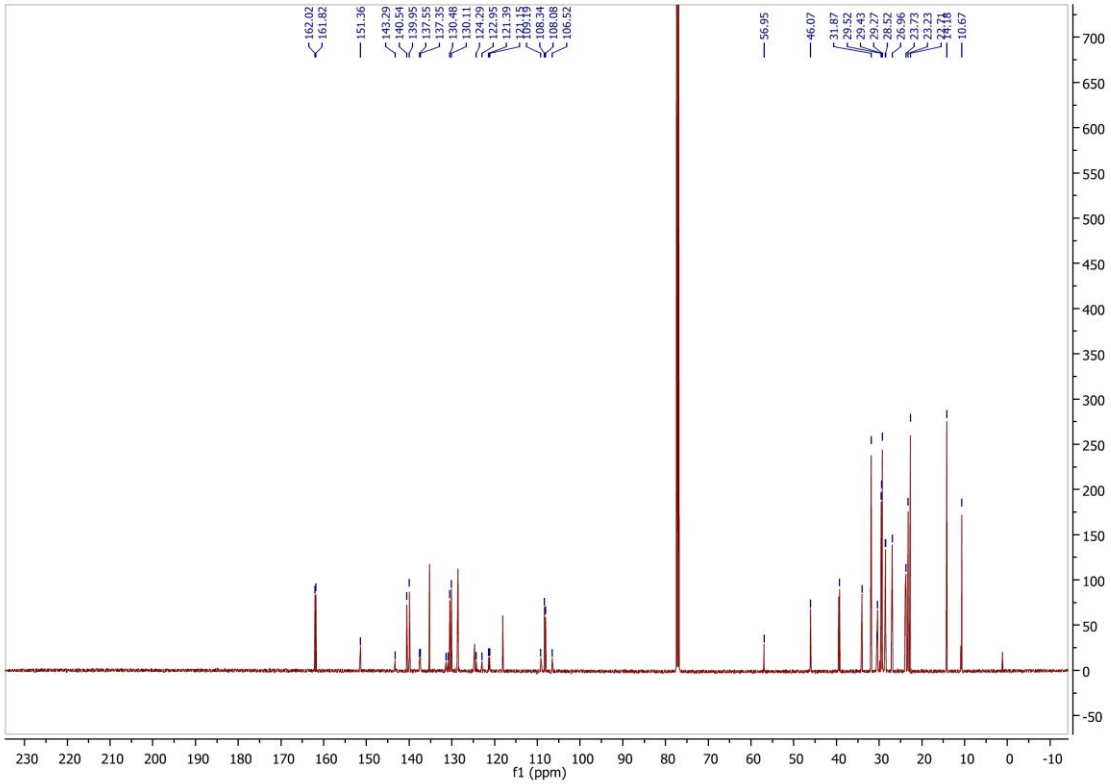

Fig. S2 ^{13}C NMR spectrum of **N7**.

The optical absorption transition for N7:

Excited State	1:	Singlet-A	1.9797 eV	626.29 nm	f=1.8137	<S**2>=0.000
Excited State	2:	Singlet-A	2.1368 eV	580.24 nm	f=0.0031	<S**2>=0.000
Excited State	3:	Singlet-A	2.2472 eV	551.73 nm	f=0.0899	<S**2>=0.000
Excited State	4:	Singlet-A	2.3141 eV	535.78 nm	f=0.4270	<S**2>=0.000
Excited State	5:	Singlet-A	2.7292 eV	454.29 nm	f=0.0113	<S**2>=0.000
Excited State	6:	Singlet-A	2.7908 eV	444.26 nm	f=0.2139	<S**2>=0.000
Excited State	7:	Singlet-A	2.9066 eV	426.56 nm	f=0.0004	<S**2>=0.000
Excited State	8:	Singlet-A	2.9540 eV	419.72 nm	f=0.0547	<S**2>=0.000
Excited State	9:	Singlet-A	2.9969 eV	413.71 nm	f=0.2561	<S**2>=0.000
Excited State	10:	Singlet-A	3.1167 eV	397.81 nm	f=0.0102	<S**2>=0.000

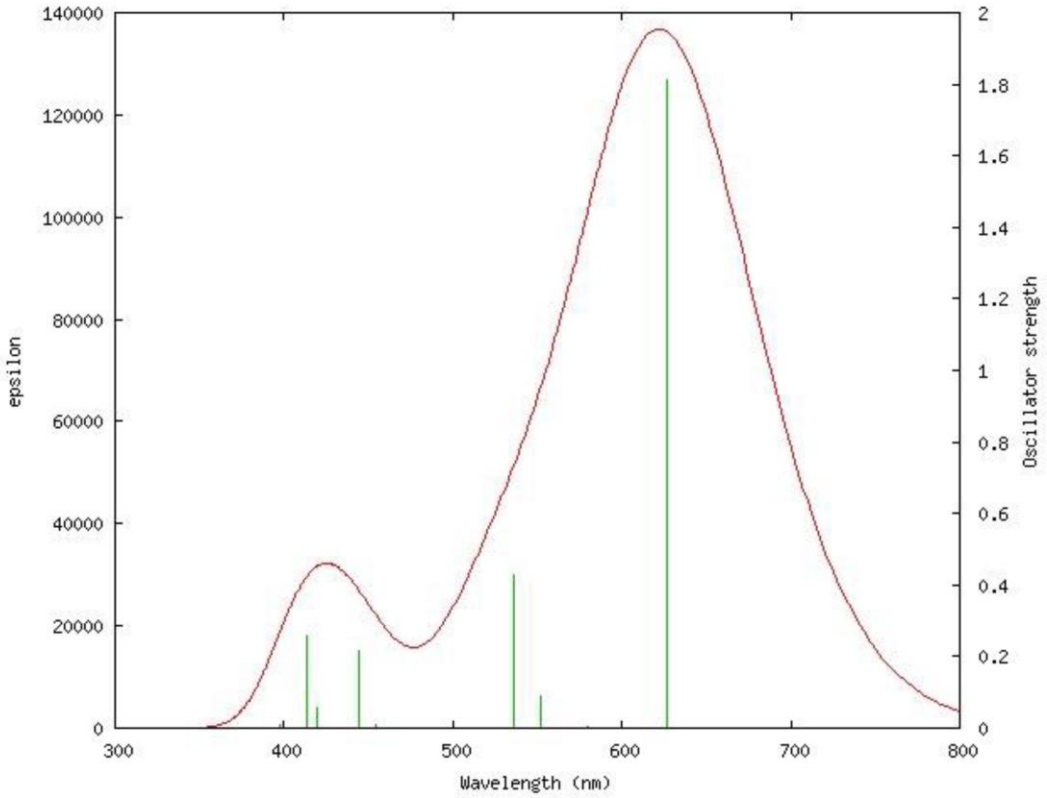

Fig. S3 Theoretical optical absorption transitions and spectrum of **N7**

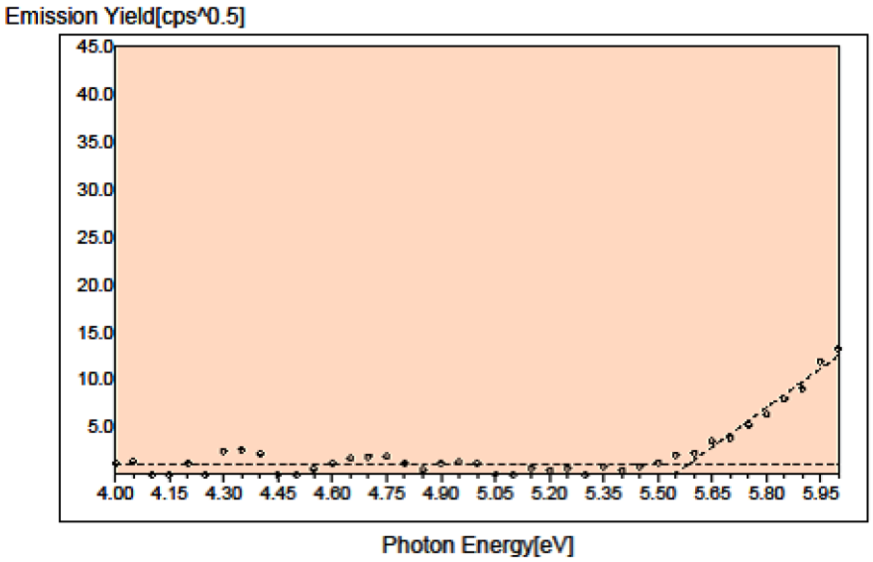

Fig. S4 PESA spectrum of thin film of **N7**. The dashed-lines show the fits to extract ionisation potential (-5.56 eV) which corresponds to the HOMO energy level.

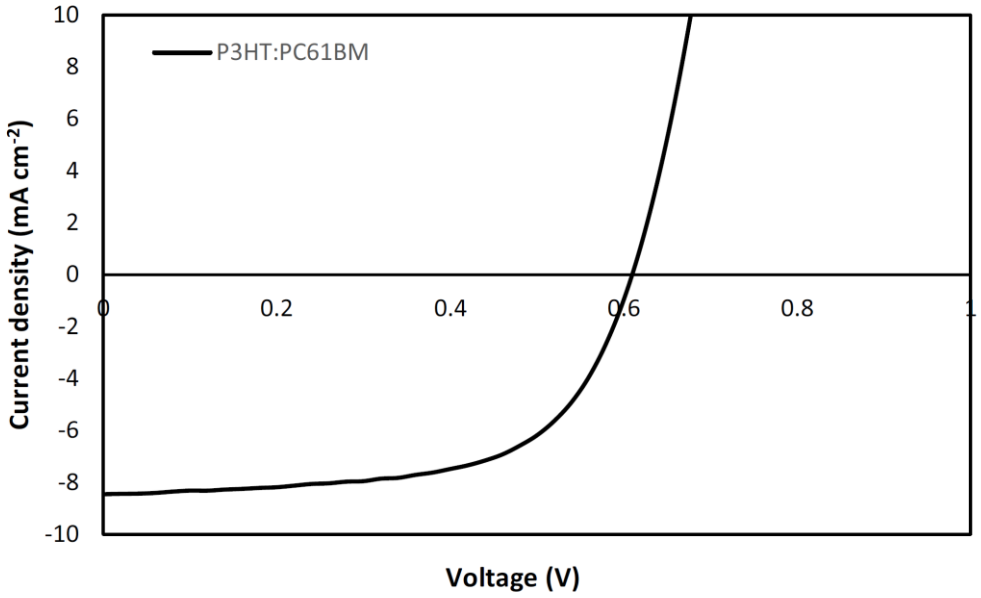

Fig. S5 P3HT:$PC_{61}BM$ device under similar conditions reported for P3HT:**N7**.

5.0 Class-A compounds

The class-A compounds were designed with the concept of having an acceptor-acceptor-acceptor compound with DPP at the core (Figure 1). Compounds of this nature typically have low laying HOMO/LUMO levels as well as the desired optical properties required form OPV chromophores.[1]These compounds have seen some success and have offered mixed results in terms of PCE[2], however they do yield relatively high V_{oc} considering the simplicity of the design. Sonar *et al.* reported on these type of compounds in 2010; since then they have rarely appeared in the literature.[2-3]

With comparability in mind four compounds were designed. Two of the compounds had cyano-bearing acceptor moieties, and the other two were rhodanine and barbituric acid homologues. These compounds were chosen in order to give insight into the role of ring size and cyano acceptor moieties within simple DPP acceptor chromophores.

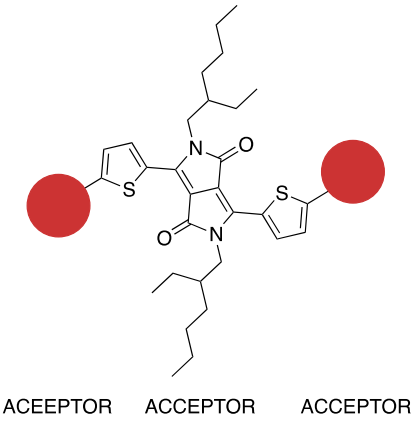

Figure 1. Generic Structure of class-A compounds

Synthesis of the class-A compounds was relatively straightforward. All compounds were synthesised from a DPP bis-aldehyde and the corresponding acceptor moiety (Figure 2) after refluxing in methanol overnight. This also allowed for simple isolation of the product by filtration, as it is insoluble in cold methanol.

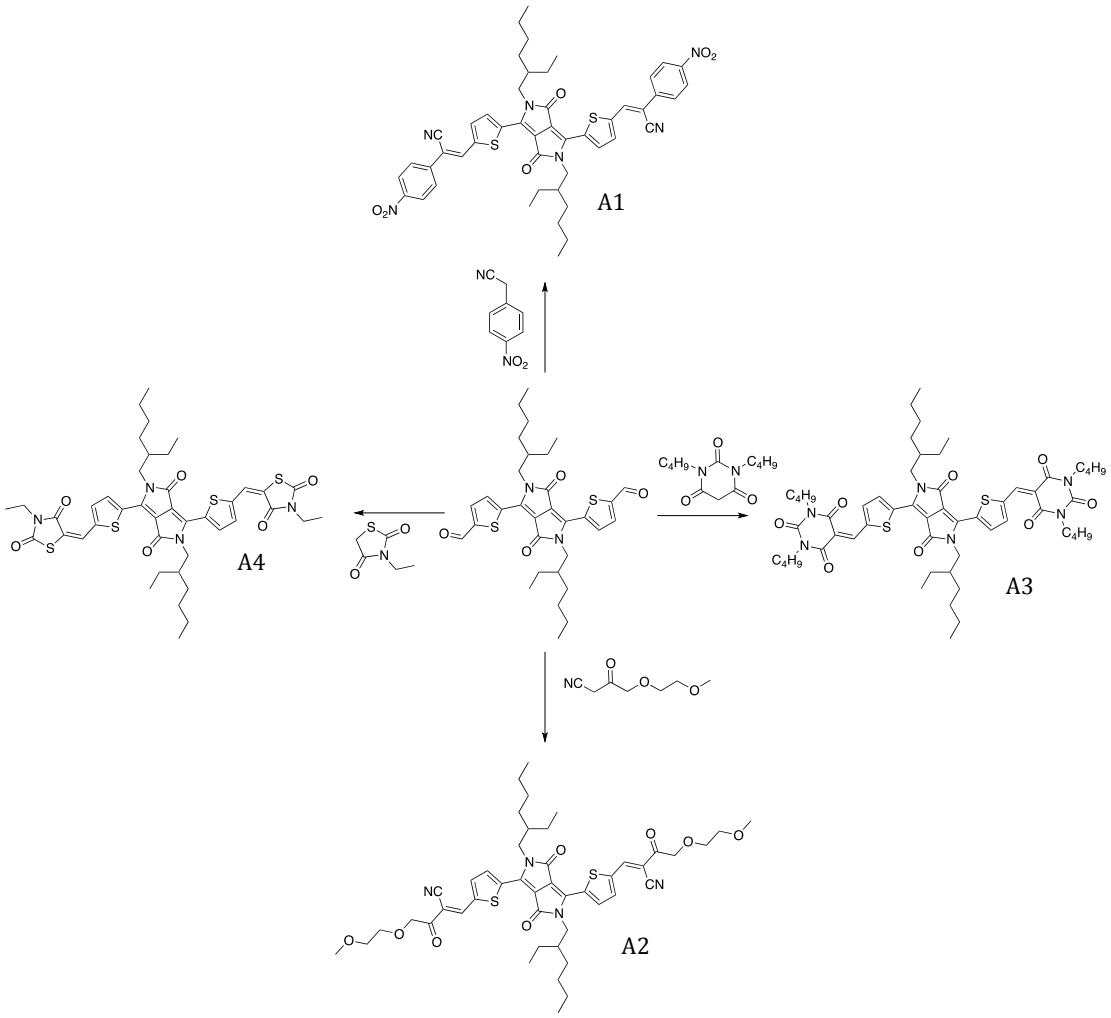

Figure 2. Class-A route of synthesis

The synthesis of the compounds appeared successful and ^{1}HNMR spectroscopy showed the presence of the desired compound with small amounts (estimated 10-15% *via* integration) of the mono condensed form, with one remaining unreactedcarbaldehyde group. Thin layer chromatography indicated it was possible to separate the components and traditional purification methods were employed including, flash chromatography, preparative thin layer chromatography and crystalisation. However, poor solubility meant that a

column or preparativeTLC plate could only be loaded with a small amount of material andonly very small (2 – 3mg) of "pure" disubstituted material was obtained. Dry loading was also attempted for flash chromatography, however the mixture just tailed as though it "leached" from the silica as opposed to desorbing resulting in constant overlap of both the desired compound and the mono-condensed impurity. Other, non-standard methods such as bulb-to-bulb distillation andderivatisation of the mono-aldehyde impurity to alter its solubility and retention time were also trialed, however these attempts were ultimately unsuccessful.

As all Class-A compounds exhibited only slight solubility in common laboratory solvents (DCM, $CHCl_3$, toluene etc.) both purification and full characterisation (in particular ^{13}CNMR) was not possible to a satisfactory degree. Obtaining ^{1}HNMR spectra was possible but required hundreds of scans and gave interpretable, albeit poor quality, spectra. As is clear from the ^{1}H NMR spectrum below (of A3, see supplementary data for all class-A compounds) a clear distinguishable peak for the carbaldehyde proton at approximately 10ppmwas present.

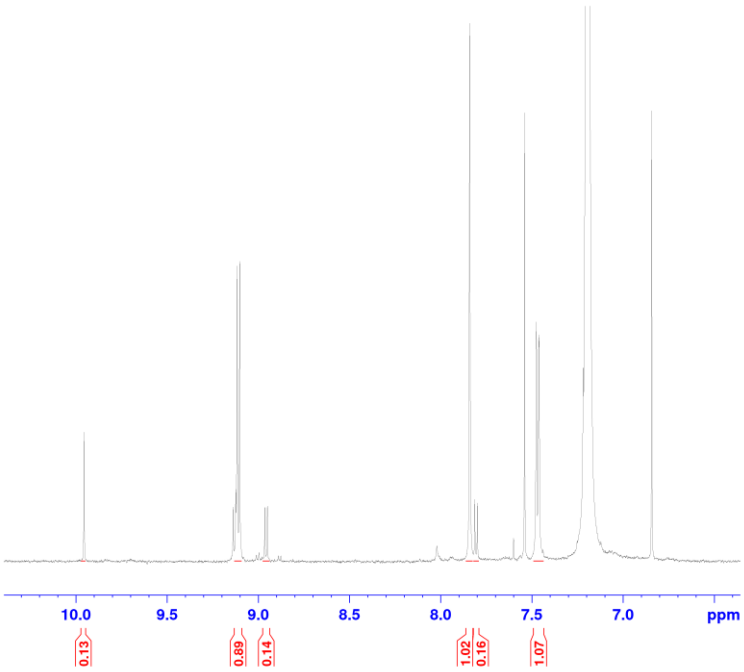

Figure 3. ^{1}H NMR of A3

Although pure samples of the class-A compounds could be obtained, it was only in small (2 – 3mg at a time) quantities. The barbituric acid derivative,could be purified (Figure 4) by washing the sample with hot hexanes as the mono-condensed compound was slightly more soluble. However, some of the desired compound was also lost.

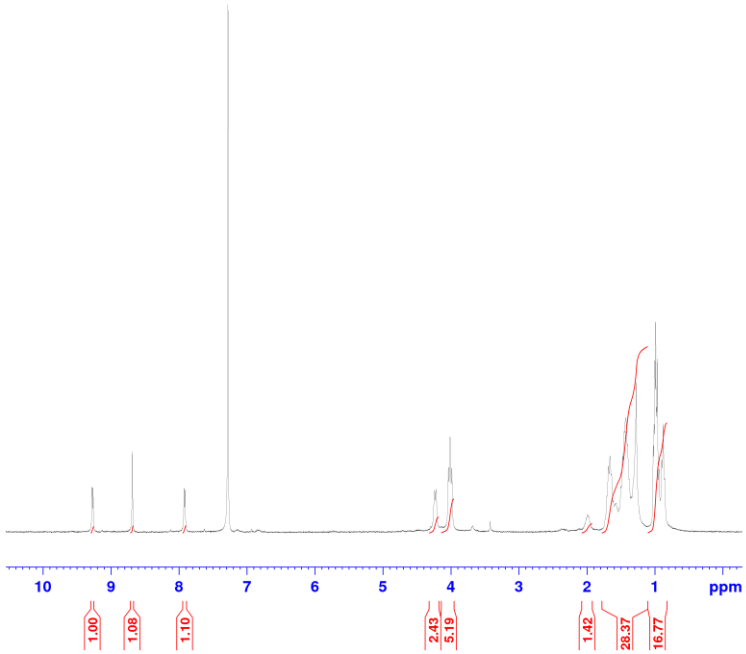

Figure 4. ^{1}H NMR of pure A3

Even thought the compounds were not overly soluble, the UV-Vis spectra (Figure 5) in solution were obtained. They showed decent absorption with typical onset of absorption around the 750 – 790 nm mark, corresponding to band-gaps of1.57 eV to 1.65 eV. This is inline with other DPP compounds that have seen use as acceptors in bulkheterojunction devices. These results offered some solace to the otherwise troublesome compounds.

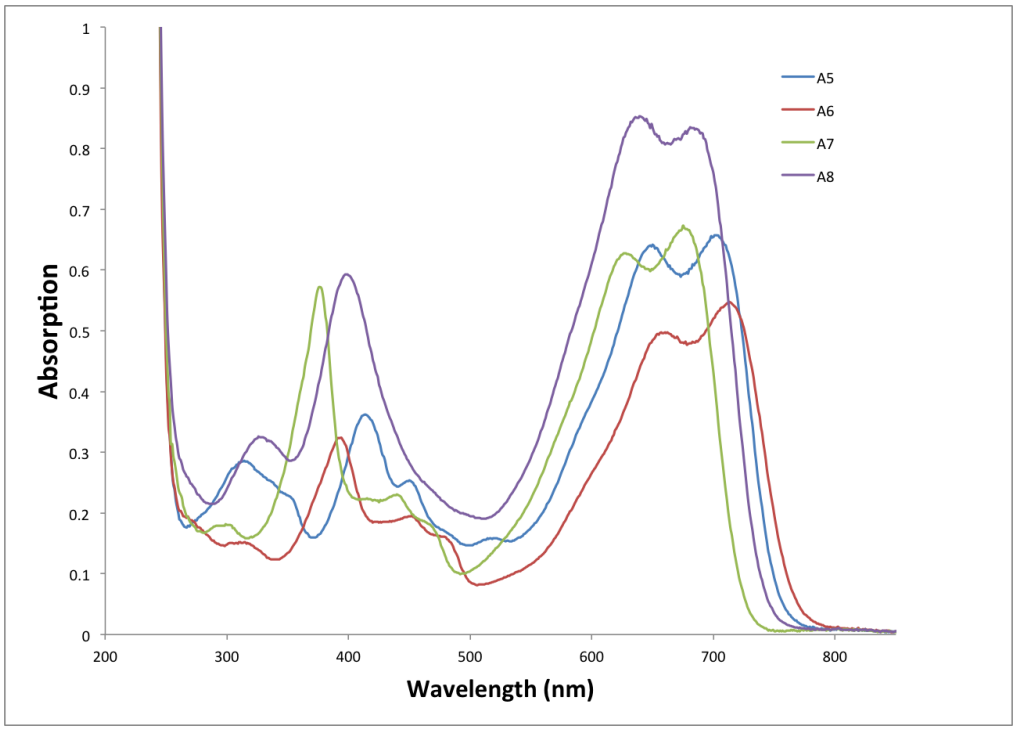

Figure 5. UV-Vis of class-A compounds in chloroform

It was hoped that, despite the poor solubility of the compounds, their optical properties may offer compensation when employed in a bulkheterojunction OPV device. A5 and A6 were chosen for initial testing, as they were the purest of the analogues, andtheir structures offered an interesting comparison due to their varying ring size. Unfortunately both compounds displayed little to no activity as electron acceptors. For this reason,together with cost and time constraints the Class-A compounds were not considered for further testing and analysis.

1. Popere, B. C.; Della Pelle, A. M.; Thayumanavan, S., BODIPY-Based Donor–Acceptor π-Conjugated Alternating Copolymers. *Macromolecules* **2011,***44* (12), 4767-4776.
2. Sonar, P.; Ng, G.-M.; Lin, T. T.; Dodabalapur, A.; Chen, Z.-K., Solution processable low bandgap diketopyrrolopyrrole (DPP) based derivatives: novel acceptors for organic solar cells. *J. Mater. Chem.* **2010,***20* (18), 3626.
3. (a) Patil, H.; Zu, W. X.; Gupta, A.; Chellappan, V.; Bilic, A.; Sonar, P.; Rananaware, A.; Bhosale, S. V.; Bhosale, S. V., A non-fullerene electron acceptor based on fluorene and diketopyrrolopyrrole building blocks for solution-processable organic solar cells with an impressive open-circuit voltage. *Phys. Chem. Chem. Phys.* **2014,***16* (43), 23837-23842; (b) Li, Y.; Sonar, P.; Singh, S. P.; Soh, M. S.; van Meurs, M.; Tan, J., Annealing-Free High-Mobility Diketopyrrolopyrrole−Quaterthiophene Copolymer for Solution-Processed Organic Thin Film Transistors. *J. Am. Chem. Soc.* **2011,***133* (7), 2198-2204.

6.0 Conclusion

6.1 Acceptor compounds

The use of organic compounds in photovoltaic cells has many challenges to overcome before they can see actual use in generating usable quantities of electricity at an affordable price. As was seen in the early years of inorganic solar cells their efficiencies and cost meant that they only saw use in specialized sectors, such as military and scientific experimentation. Nonetheless, once their power output was capable of doing so, they started supplying the energy needed to operate everyday devices such as radios. Over the course of years they are now in common use. Portable devices like calculators and watches use them to recharge batteries that allow them to see continuous use, and more recently there has been an explosion in their use to generate domestic power, thanks chiefly to the decreased costs of their production as well as generous government subsidies.

Although organic solar cells currently have relatively low efficiencies when compared to their inorganic counterparts they have the potential to be much cheaper due to the low cost of bulk synthesis of compounds and far more practical as a result of their light weight and flexible architecture. The cost savings not only come from the compounds themselves but also the way in which they are fabricated, as organic solar cells such as bulk heterojunction cells, can be manufactured using cheap methods like roll-to-roll, and inkjet printing. This also means that shapes and sizes can be easily customized to suit almost any specification, unlike traditional solar cells that usually come in standard sizes with little variation from the standards.

However there are still many barriers that need to be overcome in order to see these applications a reality. Chiefly is the issue with efficiency. This project attempted to achieve this by synthesising an array of small molecules for use as

both electron donors and electron acceptors for use in bulk heterojunction solar cells, in the hopes of achieving high efficiencies with simple compounds.

For the electron acceptors chosen for further investigation the use of di-DPP compounds, labeled N6 – N8.

DPP was chosen as it in itself is a simple compound that can be synthesized in gram – kilogram quantities. When used in either small molecules or polymeric materials, DPP analogues have been shown to be adequate non-fullerene electron acceptors. For polymeric DPP compounds, efficiencies as high as 5% have been observed when blended with P3HT as the donor material. Small molecules, however seldom see such gains with efficiencies typically ranging from 0.5 – 2.0%, usually with a low V_{oc} (less than 1 V), however some reports of these compounds reaching efficiencies as high as 3% with V_{oc} greater than 1 V do exist. These compounds (N6 & N7) were both synthesized in decent yields and were typically soluble in common solvents ensuring simple and effective purification as well as processing.

6.1.1 N6

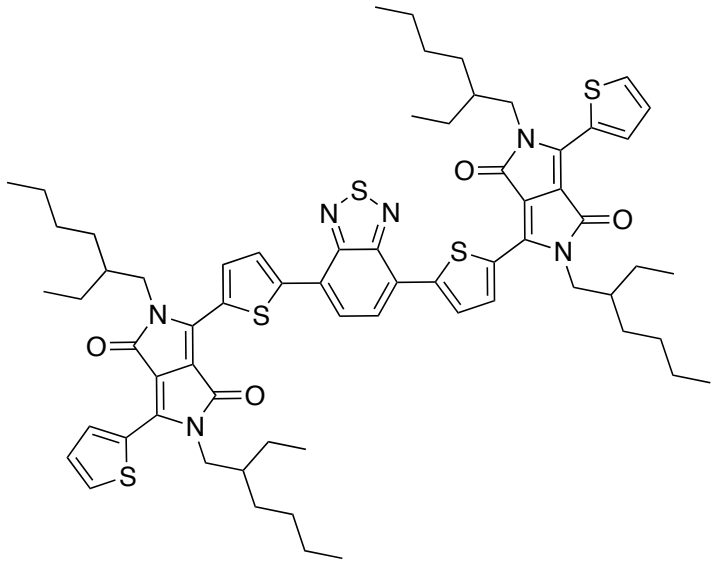

V_{OC} : 1.08 V
J_{SC} : 2.06 mA/cm^2
PCE : 1.16%

Figure 1. Structure and performance of N6

Fullerenes are the most commonly used acceptor component in bulk heterojunction cells. This is due to its excellent performance as well as its ease to work with. However at a cost of $1300 for 500 mg it is expensive. This is in part due to the manner in which C_{60} is isolated and purified. This led us to investigate the use of alternate compounds as acceptor materials within BHJ cells. Based on a simple A-D-A system, N6 uses DPP as a terminal acceptor unit and thiodiazone as its central donor. The material showed excellent solubility and was syntesised in a decent yield of 72%. The compound also showed moderate thermal stability with degradation occurring at 150°C. When tested for their photovoltaic performance the best device was shown to have a PCE of 1.18% and a high V_{oc} of 1.08 V with a J_{sc} of 2.06 mA/cm^2. Although the efficiency of the cell is moderate by todays standards it is still within the range of what is commonly seen for non fullerene acceptors and its open circuit voltage is still among the highest for this type of device.

6.1.2 N7

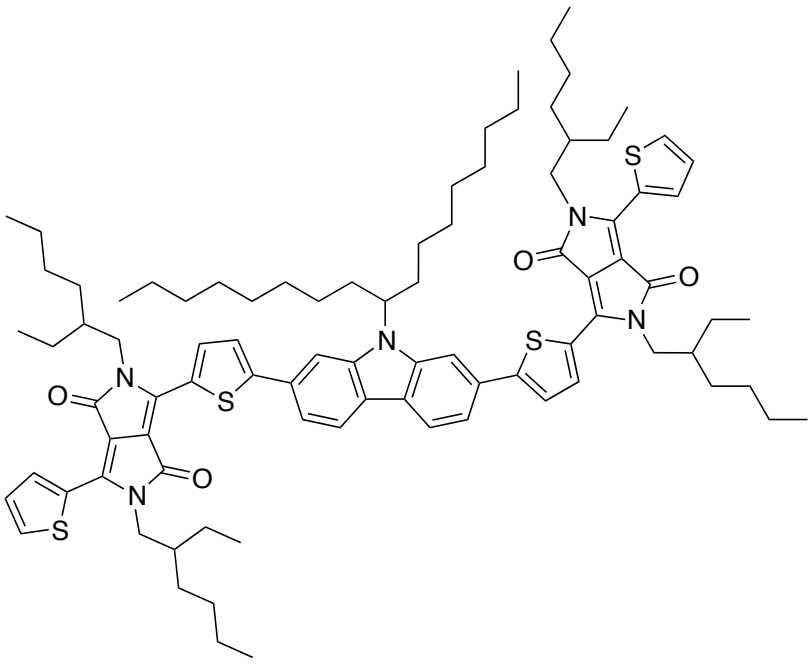

V_{OC} : 1.17 V
J_{SC} : 3.16 mA/cm^2
PCE : 2.3%

Figure 2. Structure and performance of N7

Building on the success that was had with the A-D-A system in which DPP was used as the terminal acceptor moiety, N7 was designed and synthesised. This

compound used a simple carbazole derivative as its core component. Synthesised in a similar fashion as to N6, N7 was also obtained in a decent yield. Despite their chemical and structural similarities however, N7 showed a much higher thermal stability than that of N6, with no sign of degradation until 380°C. Overall N7 out performed N6 in every measurable way and gave a PCE of 2.3%, a V_{oc} of 1.17 V and a J_{sc} of 3.16 mA/cm^2. These result are very encouraging considering recent results in the literature for similar non-fullerene DPP acceptor systems have efficiencies of about 3%, with similar V_{oc}.

6.1.3 A1 – A4 DPP Compounds

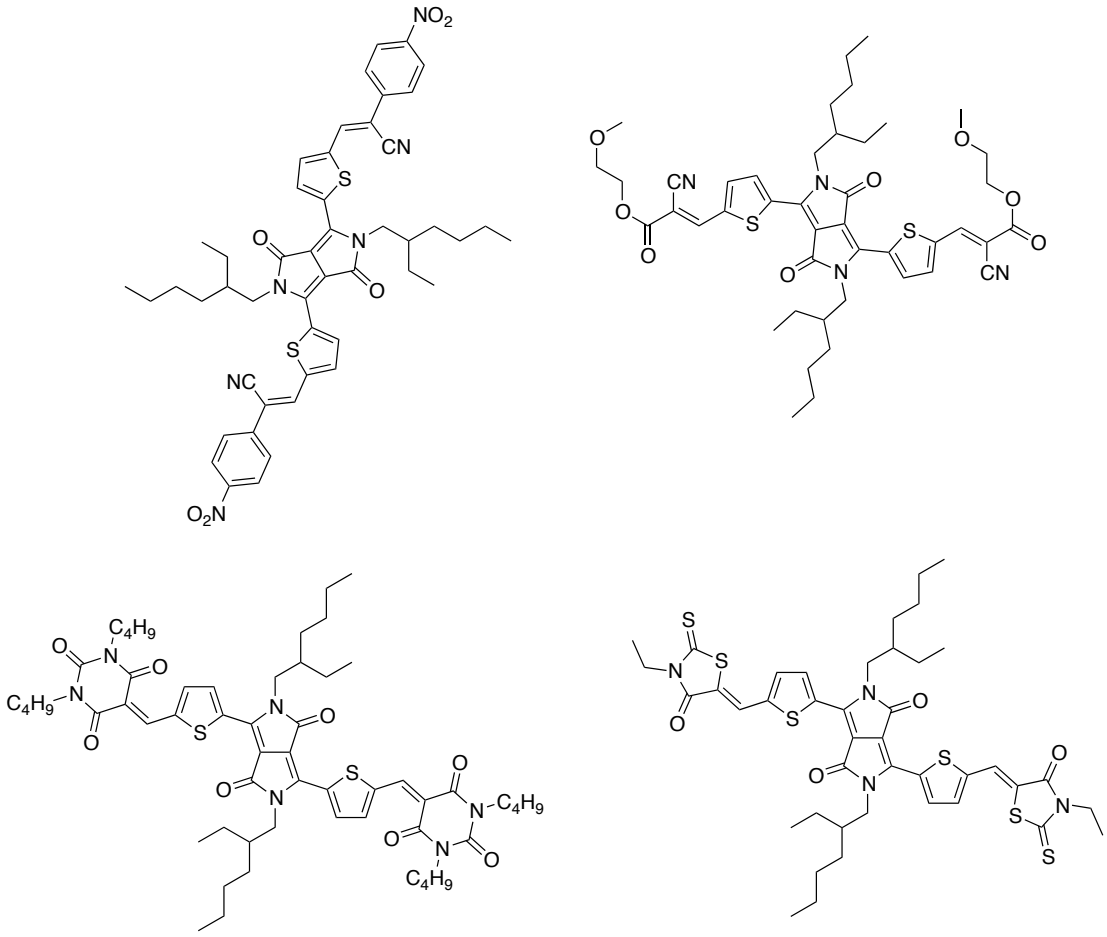

Figure 3. Structure of A-Class compounds

As previously discussed A1 – A4 were difficult to obtain as a pure product. The main impurity of these compounds was the mono-substituted derivative. This was observed in the ^{1}HNMR as a proton with a chemical shift corresponding to

that of a formyl-group proton (ppm approx. 10) being present. As it became evident that the mono-substituted compound was the main impurity in these DPP derivatives, attempts to drive the reaction to completion were undertaken. These attempts included the use of high boiling solvents and catalytic ammounts of base and acid but despite these modifications no change was observed in any of the reactions. The only manner in which to obtain the compounds in any form of purity sufficient for testing was to conduct purification after purification and in a sense "enrich" the sample towards a useable standard. This meant a high throughput of sample for minimal amount of pure compound.

As is often the way with compounds used in bulk heterojunction devices solubility is paramount in order for them to be processed. Compounds A1 – A4 all displayed the necessary optical and electronic characteristics needed in order to work within BHJ cells. However they presented poor solubility in common organic solvents (toluene, chloroform, dichloromethane) as well as other "exotic", less common solvents such as chloro-benzene, 1,2 and 1,4 dichlorobenzene and tetrachloroethylene. Consequently simple and efficient purification was near impossible and even when a moderately pure compound was obtained the devices from it suffered with poor performance and efficiency. Consequently they will likely never be used as compounds in bulk heterojunction solar cell devices in their current form.

The issue of compound solubility is a known one and studies into the affects of solubility on device performance for simple devices of P3HT blended with various derivatives of C_{60} and C_{70} and showed that there is a relationship between solubility and performance. This relationship most likely arises from the effect that the solubility of the acceptor material has on the morphology of the device. I this study Troshin *et. al* aim was to give insight into found that the optimal solubility for a P3HT:Fulerene blend was 30 – 80 mg/ml and it would be safe to assume that a similar relationship would exist for other donor-acceptor pairs, from their work Toshin *et. al* concluded that in order to have "correct material combinations" there must be a similarity in solubility, this unfortunetly was not the case for A1 – A4.[1]

Other research also suggests that solublising groups, usually long saturated alkyl chains, play a significant role in a compounds performance within a BHJ cell most likely due to the affect this has on its morphology. Within simple polymers Piliego *et. al* demonstrated that the length and shape of N-substituted alkyl chain played a significant role in manipulating device efficiency as well as morphology. Although the output voltage of these different materials changed negligibly device efficiency increased as a direct result of increased current density. This resulted in a range of efficiencies from 2.8 – 6.8%.[2]

Consequently the poor performance of the A1 – A4 is a direct result of its poor solubility. However it is worth note that the compounds displayed all the required optical and electronic charecteristics and warrant further investigation. With tuning of the solubility, these compounds may lead to a further understanding of DPP analogues and their use within solution processable cells.

6.2 Donor Materials:

6.2.1 AS1 and AS2

It was a desire to keep the methodologies and preparative techniques as simple as possible. This was achieved by keeping to simple synthetic methods from easily attainable starting materials. In keeping with the idea of simplicity the purification techniques used are also trivial.

It was found that the activity of a simple, yet efficient, compound (AS1) was significantly enhanced by the insertion of a π-spacer (thiophene) between the donor and acceptor regions of that molecule. AS1 and AS2 used an almost identical donor-acceptor-donor motif of design the only difference being that AS2 used a thiophene pi-spacer between the regions of donor and acceptor. This significantly enhanced the light absorption properties of AS2 as well as red-

shifting lambda max, indicative of a decrease in the optical bandgap. The power conversion efficiencies of AS1 and AS2 were 1.23% and 4.11% respectively – the presence of the theiophene spacer resulted in a greater than threefold increase in efficency AS2 was also a very simple molecule to purify and was attained in significant yield. The use of simple column chromatography and recrytalisation assured that AS2 was isolated in good quantities as well as high purity. AS2 also displayed fantastic solubility in common organic solvents such as toluene, chlorobenzene and chloroform, which is essential for p-type materials if they are to be incorporated into a bulk heterojunction device

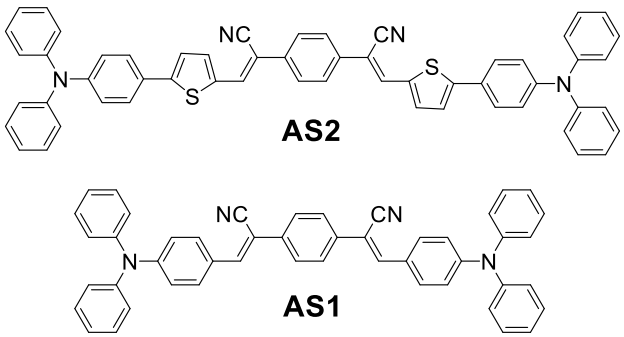

AS2
V_{OC} : 0.88 V
J_{SC} : 8.01 mA/cm^2
PCE : 4.1%

AS1
V_{OC} : 0.9 V
J_{SC} : 3.15 mA/cm^2
PCE : 1.23%

Figure 4. Structure and performance of AS1 & AS2

6.3 Future Direction:

As demonstrated by AS2, π-spacer selection can play a significant role in compound and device performance. Future work in this area would benefit greatly from further investigation as has been demonstrated here. Also, a more in depth and computational approach could be under taken in a similar manner to that seen in pharmaceutical research in which QSAR has aided researchers in finding optimal structures. This technique determines the efficacy of an array of compounds, all structurally similar but with minor variations. Some of the most common approaches to this method are simple substitutions on aromatic rings. This approach would be useful in not only determining how different electron donating or withdrawing groups affect the overall efficiency of a given structure.

Future work building on what has already been achieved with A1 – A4 would also offer better insight into the behavior of A-A-A molecules and their limits. It would be advantageous to investigate the possible use of better solubilizing agents such as poly-ethers or different types of alky chains. This would give insight into whether the poor performance of such materials is directly related to their processability or their actual electronic properties.

1. Troshin, P. A.; Hoppe, H.; Renz, J.; Egginger, M.; Mayorova, J. Y.; Goryachev, A. E.; Peregudov, A. S.; Lyubovskaya, R. N.; Gobsch, G.; Sariciftci, N. S.; Razumov, V. F., Material Solubility-Photovoltaic Performance Relationship in the Design of Novel Fullerene Derivatives for Bulk Heterojunction Solar Cells. *Adv. Funct. Mater.* **2009,** *19* (5), 779-788.
2. Piliego, C.; Holcombe, T. W.; Douglas, J. D.; Woo, C. H.; Beaujuge, P. M.; Fréchet, J. M. J., Synthetic Control of Structural Order inN-Alkylthieno[3,4-c]pyrrole-4,6-dione-Based Polymers for Efficient Solar Cells. *J. Am. Chem. Soc.* **2010,** *132* (22), 7595-7597.